

LATE QUATERNARY HISTORY OF FLEMISH PASS, SOUTHEAST CANADIAN  
CONTINENTAL MARGIN

by

Tammo Jan Huppertz

Submitted in partial fulfillment of the requirements  
for the degree of Master of Science

at

Dalhousie University  
Halifax, Nova Scotia  
December, 2007

© Copyright by Tammo Jan Huppertz, 2007

DALHOUSIE UNIVERSITY

Department of Earth Sciences

The undersigned hereby certify that they have read and recommend to the Faculty of Graduate Studies for acceptance a thesis entitled “Late Quaternary history of Flemish Pass, southeast Canadian continental margin” by Tammo Jan Huppertz in partial fulfillment of the requirements for the degree of Master of Science.

Dated: \_\_\_\_\_

Supervisor: \_\_\_\_\_

Readers: \_\_\_\_\_

\_\_\_\_\_

\_\_\_\_\_

DALHOUSIE UNIVERSITY

DATE: 20<sup>th</sup> December. 2007

AUTHOR: Tammo Jan Huppertz

TITLE: Late Quaternary history of Flemish Pass, southeast Canadian continental margin

DEPARTMENT OR SCHOOL: Department of Earth Sciences

DEGREE: M.Sc. CONVOCATION: May YEAR: 2008

Permission is herewith granted to Dalhousie University to circulate and to have copied for non-commercial purposes, at its discretion, the above title upon the request of individuals or institutions.

---

Signature of Author

The author reserves other publication rights, and neither the thesis nor extensive extracts from it may be printed or otherwise reproduced without the author's written permission.

The author attests that permission has been obtained for the use of any copyrighted material appearing in the thesis (other than the brief excerpts requiring only proper acknowledgement in scholarly writing), and that all such use is clearly acknowledged.

## Table of contents

Table of contents .....	iv
List of Tables .....	vii
List of Figures: .....	viii
Abstract .....	x
List of Abbreviations Used .....	xi
Acknowledgements .....	xii
Chapter 1. INTRODUCTION .....	1
1.1 Topographic and Tectonic Setting of Flemish Pass .....	2
1.2 Geological Setting of Flemish Pass .....	3
1.3 Scope of Study.....	5
1.4 Why was Flemish Pass a Prime Area to Try Answering these Questions?..	5
1.5 Glacial History of the Area .....	6
1.6 Styles of Sediment Transport and Deposition .....	7
1.7 Sediment Transfer to Deep Water .....	8
1.8 Climate and Oceanic Circulation.....	10
1.9 Data Availability and Quality .....	11
1.10 Objectives .....	11
1.11 Organization of the Thesis .....	12
Chapter 2. TEMPORAL AND SPATIAL DISTRIBUTION OF LATE QUATERNARY MASS TRANSPORT DEPOSITS (MTDS) IN FLEMISH PASS	14
2.0 Abstract.....	14
2.1 Introduction .....	15
2.2 Geological Setting .....	16
2.2.1 Bathymetry .....	16
2.2.2 Oceanography .....	20
2.2.3 Geology of Flemish Pass.....	20
2.2.4 Geology of the Areas Adjacent to Flemish Pass .....	22
2.2.5 Mass Transport Deposits in the Greater Area .....	23

2.2.6 Heinrich Layers .....	24
2.3 Materials and Methods.....	25
2.4 Results .....	27
2.4.1 Key Reflections .....	27
2.4.2 Seismic Stratigraphy of the Grand Banks Margin.....	29
2.4.3 Mass Transport Deposits.....	33
2.4.4 Core Control of MTDs.....	38
2.4.5 Chronological Control .....	40
2.4.6 Sedimentation Rates .....	43
2.5. Discussion.....	47
2.5.1 Glacial History of the Grand Banks Margin.....	47
2.5.2 Character and Distribution of MTDs .....	48
2.5.3 Initiating Processes .....	54
2.5.3.1 Earthquakes.....	55
2.5.3.2 Sea Level and Gas hydrates.....	55
2.5.3.3 Heinrich Events.....	56
2.5.3.4 Melt Water Influx.....	56
2.5.3.5 Relationship of Glaciation to MTDs.....	57
2.6 Conclusion .....	58
Chapter 3. TEMPORAL DISTRIBUTION OF LATE QUATERNARY TURBIDITES AND CONTOURITES IN FLEMISH PASS: A GLACIALLY INFLUENCED PERCHED SLOPE BASIN OFF SOUTHEAST CANADA .....	60
3.0 Abstract.....	60
3.1 Introduction .....	61
3.2 Regional Setting.....	63
3.2.1 Physiography.....	63
3.2.2 Geology of Flemish Pass.....	65
3.2.3 Oceanographic Setting .....	66
3.2.4 Late Quaternary Stratigraphic Framework for Flemish Pass .....	67
3.2.5 Distinction of Turbidites from Contourites.....	69
3.3 Materials and Methods.....	70

3.4 Results .....	71
3.4.1 Core Correlation .....	71
3.4.2 Sandy Facies in Flemish Pass .....	72
3.4.3 Sandy Units in High-Resolution Seismic Data .....	73
3.4.4 Correlated Sand Packets.....	83
3.4.5 Temporal Distribution of Facies .....	87
3.5. Discussion.....	89
3.5.1. Characterization of Facies.....	89
3.5.2 Facies Interpretation.....	91
3.5.3 Distribution of Sandy Facies in Flemish Pass.....	95
3.5.4 Initiation of Turbidity Currents in Flemish Pass .....	97
3.6 Conclusions .....	98
Chapter 4. CONCLUSIONS.....	100
References .....	108
Appendix .....	124

## List of Tables

Table 2. 1: Radiocarbon dates collected since 2005 in Flemish Pass.....	44
Table 3. 1: Counts of sand size grains from sands from Flemish Pass .....	77
Table 3. 2: different sedimentary facies.....	78

## List of Figures:

Figure 2.1: Overview map of Flemish Pass and adjacent areas along the eastern Canadian continental margin.....	18
Figure 2. 2: Map of central and northern Flemish Pass, showing the different lobes and channels .....	19
Figure 2. 3: (a) Type section on Kyle lobe for the reflections traced in Flemish Pass and (b) their relationship to the MD95-2026 core on Sackville Spur...	28
Figure 2. 4: Airgun seismic cross section upslope from Kyle Lobe, showing the till tongue (red line) above seismic reflection FP 75.....	30
Figure 2. 5: Till tongue above reflection FP 75 upslope from Gabriel Lobe. ....	31
Figure 2. 6: a) Airgun seismic section showing a till tongue (arrow) above reflection FP 75 and the overlying iceberg scouring; b) boomer seismic section showing till tongues above FP 75 and above FP 80 and their relationship to the iceberg scouring. ....	32
Figure 2. 7: Cross-section in the Kyle Lobe area showing lensoid MTDs.....	34
Figure 2. 8: Map of stratigraphic position of MTDs in Flemish Pass.....	35
Figure 2. 9: Stratigraphic relationship of MTDs from the Grand Banks and Flemish Cap slopes in central Flemish Pass. ....	36
Figure 2. 10: Cross-section of stacked MTDs in the channel system upslope from Kyle Lobe. ....	37
Figure 2. 11: Examples of MTD facies type A <sub>FP</sub> , B <sub>FP</sub> and C <sub>FP</sub> in Flemish Pass. .	39
Figure 2. 12: Core control used in this study. ....	41
Figure 2. 13: Re-interpretation of the $\delta^{18}\text{O}$ curve.....	45
Figure 2. 14: Sedimentation rates excluding MTDs for intervals between key reflections. ....	46
Figure 2. 15: Summary of key features of the three MTD types described from Flemish Pass.....	50



Figure 2. 16: Summary figure showing the timing of failure events (locations from Fig 2.8) of the different MTDs in Flemish Pass.....	52
Figure 3.1: Location map of Flemish Pass. ....	62
Figure 3.2: Map of central Flemish Pass showing the core control used for the sand beds.....	64
Figure 3.3: Correlation of key cores in Flemish Pass. ....	68
Figure 3.4: Sedimentological logs.....	75
Figure 3.5: Plots of grain size with depths (“grain size maps”) from selected intervals of cores in Flemish Pass.....	76
Figure 3.6: Plot of the facies in a ternary diagram. ....	79
Figure 3.7: Sparker seismic profile of sand sheet on Gabriel Lobe. ....	80
Figure 3.8: Sparker seismic profile from the eastern side of the basin showing large sediment waves along the sea bed. ....	82
Figure 3.9: Correlation of sands to Heinrich layers and Greenland ice core stadials, see Figure 3.12. ....	84
Figure 3.10: Spatial distribution and thickness of sand packets A through C on Kyle Lobe, X indicates no sands. ....	85
Figure 3.11: Stratigraphic position of sand bed in cores in Flemish Pass. The arrow indicates that the core is longer than displayed. ....	86
Figure 3.12: Summary figure showing the relationship of the sand beds .....	93
Figure 4.1: Ice sheet configuration on the easternmost Grand Banks margin adjacent to Flemish Pass .....	102
Figure 4.2: Initiating processes in Flemish Pass.....	106
Appendix.....	124

## **Abstract**

The shallow sedimentary sequence in Flemish Pass, a small perched basin along the north-eastern Grand Banks margin, was studied for improving the knowledge of timing of glaciation, and its influence on slope and basin sedimentation, using high-resolution seismic profiles and 10 m long piston cores. A new basin-wide seismic stratigraphy was defined and calibrated by multiple dating methods. The spatial and temporal extent of mass transport deposits (MTDs) was used to understand the impact of ice sheets on sedimentation in Flemish Pass. Grain size analyses from sandy beds indicate turbidite and contourite activity in the basin. More turbidites were deposited during Greenland stadials, more contourites during interstadials, which may link to the oceanic regime. From the temporal and spatial distribution of MTDs and turbidite sands, different initiating processes have been proposed.

## List of Abbreviations Used

AMS	Accelerator mass spectrometer
AZ	Ash zone
BIO	Bedford Institute of Oceanography
CCGS	Canadian Coast Guard Ship
CIE	Commission Internationale d'Eclairage
DMBC	Downing basin moraine complex
DTS	deep tow seismic (i.e. Hunttec DTS)
FP	Flemish Pass
GPS	global positioning system
H-	Heinrich event number
IRD	ice rafted detritus
L*, a, b	spectral qualities
MST	Multi-sensor track
MTD	mass transport deposit
OIS	oxygen isotope stage
pc	piston core
SEG	Society of exploration geologists
twc	trigger weight core

Position of seismic figures:

Example: 2006048 224/0600 = (year)-(cruise number)-(Julian day) (time of day in UTC)

## **Acknowledgements**

The completion of this thesis would not have been possible without the unlimited help of my supervisor David J. W. Piper, who accepted me two years ago as a German B.Sc. student to take on the challenge to do my thesis at Dalhousie University, Halifax in cooperation with the Bedford Institute of Oceanography in Dartmouth. Thank you so much for giving me guidance when I needed it, but also for showing me that I can do research independently, which was an amazing preparation for my future academic career.

I would also like to thank my supervisory committee, Martin Gibling from Earth Sciences at Dalhousie University and Paul Hill from Oceanography at Dalhousie University to help me throughout my thesis work for challenging the research ideas and guide me in the general direction.

Huge thanks to Edward King at the Geological Survey at the Bedford Institute of Oceanography for helping me so much improving and understanding the geological history in Flemish Pass and its relationship to the Grand Banks. You were always there for geological discussions and to challenge my research ideas for guiding them in the right direction. Also a great thank you to Gordon D. M. Cameron from the Geological Survey at the Bedford Institute of Oceanography for helping me out in understanding the geology in the area by asking challenging questions throughout the last two years. Without you two, Edward and Gordon, me and my thesis would not be where they are now.

My special thanks goes also to Owen Brown and Kate Jarrett in the lab facilities at BIO, you two were always helping me out when I processed my data

sets in the lab throughout the two years. I never had to wait for lab time but I could always squeeze in my sampling and run the machines for that. Therefore unlimited thanks.

I also want to thank all the other research scientists and staff at the Geological Survey at BIO for helping to make my thesis possible, it was great fun to work in the group and I am looking forward to future projects.

Thanks also to the cruise members from the 2006048 cruise on Hudson to Flemish Pass in September of 2006, when several cores and seismic data were collected, which were vital to this study.

My final thanks are to all my close friends here in Halifax who guided and introduced me to the “Experience Canada”. When my thesis and life gave me a hard time, you were always there for me. And of course to my family back in Germany.

This study has been funded by NSERC, the Geological Survey of Canada and through the Geological Society of America.

## Chapter 1. INTRODUCTION

The style of Quaternary continental margin sedimentation is quite variable along formerly glaciated continental margins in areas such as Canada, Norway and Alaska (Piper et al., 1973; Piper and Skene, 1998; Taylor et al., 2000). Major deep-sea fans have developed seaward of large traverse troughs, marking the site of former ice streams (Hesse et al., 1996; King et al., 1998; Andrews and MacLean, 2003). The style of sedimentation seaward of outer shelf banks is less well known, with minor downslope supply and more important along-slope supply of sediment in proglacial plumes (Taylor et al., 2000). In such settings, submarine canyons appear to be important conduits for sediment transport (Jenner et al., 2007).

This study investigates the style of Quaternary sedimentation on the continental margin of Flemish Pass over the past 200 ka in order to better understand how glacial processes and margin morphology control continental margin sedimentation. Flemish Pass is an 1100 m deep perched basin on the continental margin east of the Grand Banks of Newfoundland. It is unusual compared with adjacent parts of the southeast Canadian margin in several respects. Its shallow depth means that much of the downslope supply of sediment is trapped in the basin, rather than being spread widely over abyssal plains. In the last glacial maximum, ice extended only part of the way across the Grand Banks. Submarine canyons are very poorly developed in Flemish Pass.

For this reason, Flemish Pass is well suited to provide further insights into continental margin sedimentation processes.

## 1.1 Topographic and Tectonic Setting of Flemish Pass

Flemish Pass is a small, perched basin along the eastern Grand Banks margin. The topography of the area is characterized by the basement high of Flemish Cap to the east of Flemish Pass. Due to the presence of Flemish Cap, which is composed of basement grandiotite (King et al., 1985), the depths to basement increases in Flemish Pass from a few meters close to Flemish Cap to ~2 km in the west along the slope break of the Grand Banks (Grant and McAlpine, 1990).

The Grand Banks rift history started in the late Triassic and the pre-rift sequence is characterized by several unconformities created in a fluvial-coastal system by sea level fluctuations (Enachescu, 1987; Keen et al., 1987). The rifting history can be divided into three major stages. Flemish Pass is separated from the Jeanne d'Arc basin by the Central Ridge, and bound to the east by the basement high of Flemish Cap, which consists of unstretched continental crust (Foster and Robinson, 1993). Several pre-Tertiary faults create a complex basement surface. Some of these faults may be related to deep salt movement creating small salt related tectonics (Enachescu, 1987), but none of the salt diapirs were large enough to influence the Quaternary sedimentary sequence in Flemish Pass (Foster and Robinson, 1993). This tectonic setting created the small perched basin of Flemish Pass with up to 2 km of sediments.

## 1.2 Geological Setting of Flemish Pass

The Quaternary sedimentary sequence in Flemish Pass is characterized by thick gray colored muds with varying amounts of ice rafted debris (IRD) and sand beds at specific horizons. Associated with these horizons are light colored carbonate rich event layers (Piper, 2005; Piper and Campbell, 2005) which have been interpreted as Heinrich layers originating from Hudson Strait (Andrews et al., 1987). Several cores have sampled this sequence and provide age control in the shallow sequence. Throughout the basin, thick mass transport deposits (MTDs) have been described, which are Quaternary in age (Piper and Pereira, 1992). The deeper, pre-Quaternary seismic sequence is also characterized by large MTDs which cover the area. Most of these flows are thicker than the younger deposits (Campbell et al., 2002).

Sackville Spur marks the northern limit of Flemish Pass. This shallow sediment drift has been created since the Late Mesozoic and extends from the shelf break to the basin floor. This Spur is characterized by sediment failures along the northern and southern flanks and may still be active (Kennard et al., 1990).

To the north of this sediment drift is Orphan Basin. This is a large open basin up to 3000 m of water depth (Tripsanas and Piper, in press). Due to its proximity to Flemish Pass, it has a similar glacial history and the sedimentary processes within this basin may provide a useful comparison to Flemish Pass, even though there are important differences to Flemish Pass, e. g. the bathymetry and topography of the basin, the character of the slopes, and the position to ice



sheets during the last glaciation. The southern margin of the basin is characterized by several deep channels and steep slope topography. During the last glaciation, an important ice stream calved off Newfoundland along the western margin of the basin resulting in higher sedimentation rates throughout the basin. The earthquake record inferred from timing of widespread sediment failures may have also affected the sedimentary sequence in Flemish Pass (Tripsanas and Piper, 2007; Tripsanas and Piper, in press). Therefore, style and timing of sedimentation in Flemish Pass has been studied in context with Orphan Basin and the comparison and differences between the two basins has been used throughout the study to understand the glacial history of the greater area.

The two possible sediment sources for the sediments in Flemish Pass are the Grand Banks of Newfoundland and Flemish Cap, which have distinctly different petrology: the Grand Banks lithologies comprise Paleozoic plutonic and volcanic rocks (Slatt, 1977; Fader and Miller, 1986) which are also present in the sandy deposits on the shelf. The Flemish Cap petrology is characterized by far traveled lithologies transported to the area as IRD (Piper and DeWolfe, 2003). Different muds deposited during different times in Flemish Pass also show differences in origin, displayed in their color and foraminifera assemblages: reddish and olive gray colors have been correlated through Flemish Pass and along the margin regionally (Piper and DeWolfe, 2003). This petrology data could be used to understand the main sediment flux sources for the basin: most of the sediment along the floor of the pass has originated from the Grand Banks as turbidites or mass transport deposits (Piper and Pereira, 1992).

### 1.3 Scope of Study

On the eastern Grand Banks margin, oxygen isotope stage (OIS) 2 ice likely did not reach to the outer margin but terminated on the inner shelf area (King et al., 2001), which is in contrast to other slopes on the southeast Canadian continental margin, where ice terminated along the shelf break (King and Fader, 1986). The following major questions were addressed in this study:

- (1) When was the last time that ice reached the outer Grand Banks margin upslope of Flemish Pass?
- (2) How does the extent of ice on the shelf at glacial maximum influence the volume and style of sedimentation on the continental margin?

### 1.4 Why was Flemish Pass a Prime Area to Try Answering these Questions?

Flemish Pass is a comparatively shallow and confined basin, so it gives the unique possibility to study the temporal variability of MTDs and turbidity current deposits on a glaciated continental margin and may be used as a study area for answering the questions posed above. In this basin, previous studies have shown the presence of a deep sediment record spanning more than 200 ka (Piper and Campbell, 2005). Additionally, MTDs and turbidites are trapped in the basin (Piper and Pereira, 1992), creating an almost complete Quaternary sedimentary record in the basin, as the few unconformities identified in the

sequence are of Neogene age (Kennard et al., 1990). A clear contourite record (Piper and Campbell, 2005) and late Holocene oceanic circulation models in the basin (Colbourne and Foote, 2000) can further be used to understand reworking and erosion in the basin, giving the opportunity to understand the glacial history in the area.

## 1.5 Glacial History of the Area

The glacial history of the southeast Canadian continental margin, reaching as far back as OIS 12 (~450 ka), had been previously reconstructed from the thickness and extent of till tongues along the slope (Mosher et al., 1989; Piper and Brunt, 2006) and from transverse troughs eroded by major ice streams on the shelf (Shaw et al., 2006). The deposits of these erosive processes are found seaward of the transverse troughs in the basins along the margin, where they were deposited as glacial debris flows (Rashid and Piper, 2007; Tripsanas and Piper, submitted) or as hyperpycnal turbidite deposits (Hesse et al., 1997; Piper et al., 2007).

During OIS 2 (~ 22 ka), the Grand Banks ice sheet likely did not cross the outer shelf and terminated along the western Orphan Basin margin (Tripsanas and Piper, 2008, in revision) and southwards in Downing Basin (King et al., 2001). Proglacial sand on the outer shelf may have been transported to the Hibernia exploration area during discharge of meltwater (Fader and King, 1981).

On a higher temporal resolution, sediment supply may have fluctuated over stadial-interstadial time scales on the outer eastern Grand Banks as a result of

changes in sediment supply during Heinrich events (Veiga-Pires and Hillaire-Marcel, 1999; Benetti, 2006). Furthermore, the strength of the Labrador Current over the last glacial cycles has varied greatly (Hillaire-Marcel and Bilodeau, 2000), but detailed circulation models, including flow strength at different water depths through the water column, are not available. Generally it is accepted that the Labrador Current strengthened during glacial stages. Sediment supply may also have varied due to minor sea level variations of less than 30 m (Lambeck and Chappell, 2001). These sea level fluctuations on a small time scale are related to the Greenland climatic stadials and interstadials (Björck et al., 1998; Andersen et al., 2006), which are climatic anomalies with cooler and warmer climatic stadials with less change than on a glacial-interglacial cycle.

## 1.6 Styles of Sediment Transport and Deposition

Three major styles of sediment deposition can be differentiated along marine basins off glaciated margins. In ice-proximal settings, sediment deposition occurs mainly in till tongues from grounded ice (King et al., 1991; Piper and Brunt, 2006). Frequently, these deposits are interlayered with glaciomarine sediments (King, 1993). Till tongues represent the outer limit of grounded till along the shelf break and have been deposited directly by the ice sheet in a marine environment (King, 1993).

Ice streams are wide zones within a glacier wherein ice flows significantly faster than the surrounding ice (Shaw et al., 2006). These ice streams supply large amounts of poorly sorted sediment under and within the ice to the margin.

This sediment accumulates along the shelf break and the upper slope, creating high sedimentation rates in these meta-stable areas. When failure due to overloading occurs, glacial debris flows (GDFs) may evolve from the failed sediment (Tripsanas and Piper, 2008, in revision), which are directly connected to shelf-edge glaciation (King et al., 1998).

Glacial plumes supply the shelf break with large volumes of fine grained sediment, which is transported to the area by sediment-laden supraglacial and subglacial meltwater (Lemmen, 1990; Hesse et al., 1997). These plumes are especially important during deglaciation, when large amounts of rock flour are released from Hudson Strait creating carbonate-rich Heinrich events along the southeast Canadian continental margin (Andrews and MacLean, 2003; Piper, 2005). These fine grained sediments may precondition the continental slope for failures by overloading, local oversteepening and creation of excess pore pressures (Mosher et al., 2004).

## 1.7 Sediment Transfer to Deep Water

Three major types of sediment transfer to deep water have been recognized along the southeast Canadian continental margin: (I) retrogressive sediment failures are related to earthquakes, (II) creep and decollement eventually lead to failures, and (III) turbidity currents may be created by hyperpycnal flows, evolve from other sediment failures, or may be storm generated.

Retrogressive failures are widely recognized on the southeast Canadian continental margin (Mosher et al., 2004; Piper, 2005; Jenner et al., 2007) and

appear related to earthquakes along the margin, because they occur simultaneously in multiple drainage systems. These earthquakes appear to occur randomly along passive margins but show a more frequent occurrence in areas glaciated in the Pleistocene (Toews and Piper, 2002) and at times of ice maximum and retreat (Piper, 2005; Tripsanas and Piper, 2007), suggesting that some are related to glacial rebound (Husebyea and Mäntyniemi, 2005).

Creep, decollement, and eventual failures are frequently observed along the Scotian Slope and are important initiators for mass failures (Mosher et al., 2004). The failures may show a correlation to weak geotechnical horizons. There is no clear relationship to glaciation.

Turbidity currents transport large amounts of sediment into the deep ocean. Three types of processes may initiate turbidity currents on glacially influenced margins. Hyperpycnal flows transport sediment-laden meltwater to the outer shelf and slope, which may evolve into turbidity currents. The hyperpycnal flows may also lead to failures by oversteepening canyon walls, which may evolve into turbidity currents (Piper et al., 2007; Tripsanas and Piper, submitted). Sediment mass failures can initiate turbidity currents by transformation of slumps to debris flows, which further evolve to turbidity currents (Piper et al., 1999). Storm waves initiate rare turbidity currents in the marine Holocene record off southeast Canada (Piper, 2005) and may have been even more important during the Pleistocene glacial when more storms occurred in the North Atlantic (Stauffer, 2000).

Generally, various processes may initiate sediment failures along continental margins. Most of these processes do not show a clear relationship to glacial stages and few of the failures on the eastern Canadian continental margin have been linked to ice sheet processes. Nevertheless, ice sheets are important suppliers for large amounts of poorly sorted unlithified sediments to the outer shelf area, the shelf break and upper slope.

## 1.8 Climate and Oceanic Circulation

Sea level and climate variability has been widely recognized from ice cores in Greenland and coral studies in the tropical areas (Walker, 2005). Sea level varies greatly over the course of a glacial-interglacial cycle, and the average sea level was up to 110 m lower during the last glacial maximum (Lambeck and Chappell, 2001). The amount of sea level fluctuation is area-dependent and may be influenced by local factors (Lambeck et al., 2002b). On a higher resolution, sea level can also fluctuate between stadial and interstadial cycles, recognized, for example, in Greenland ice cores (Björck et al., 1998) within a climatic stage. These sea level fluctuations are generally a magnitude smaller and generally on a 10 to 30 m scale (Lambeck et al., 2002a; Sasaki et al., 2004), depending on local factors and climate variability.

## 1.9 Data Availability and Quality

Most of the data used during this study are old data sets (pre-1990) collected in the area on different cruises over the last 30 years. All the data are stored at the laboratory facilities at the Geological Survey of Canada at the Bedford Institute of Oceanography in Dartmouth, NS. The data sets available from Flemish Pass are mainly seismic Hunttec sparker and boomer and lower resolution airgun data. Additionally, up to 11 m long piston cores were collected for sampling the shallow Quaternary sequence in Flemish Pass. In the fall of 2006 additional core and seismic data were collected over three days during CCGS Hudson cruise 2006048 purposely for this study in Flemish Pass (Piper and King, 2008).

## 1.10 Objectives

The main objectives for this study were to improve the understanding of timing and distribution of mass transport deposits (MTDs) and turbidite and contourite sands in the basin over the last glacial cycles in order to understand sediment fluxes and processes associated with ice sheet fluctuations during different glacial stages since oxygen isotope stage (OIS) 6 in the area. Additionally, the improved understanding of Flemish Pass in comparison to Orphan Basin may improve the understanding of processes affecting the Grand Banks margin and the inner and outer shelf areas.



The motivation for this study was thus generally two-fold. The study addresses problems of a more local scope in Atlantic Canada, relevant to past ice sheet configuration on the outer Grand Banks and upper slope. Some aspects of the study will also have a wider audience, interested in mass transport processes and sediment fluxes along glaciated continental margins. The study highlights the potential to understand continental shelf processes by studying basin sedimentation.

### 1.11 Organization of the Thesis

This thesis was written as a paper-based thesis. A short introduction provides the setting and background for the two manuscripts, which will be submitted shortly. Paper 1 will be submitted to Marine Geology, Paper 2 was written for Sedimentary Geology. All the research, ideas and interpretation were carried out by the student, T. J. Huppertz, but the supervisor, D. J. W. Piper, helped to guide the research and improved the manuscript.

Following the two papers is a short conclusion, where the results of both papers are summarized and concluded. Following the conclusion are the cited references and a data appendix, which is a draft for a Geological Survey of Canada Open File Report including all the data sets this study was based on.

The objectives outlined in the thesis have been approached in two ways: the stratigraphic control used geophysical methods supported by piston core data,

whereas the sediment characterization was based on sedimentological and petrographic methods.

The central chapters of the thesis are manuscripts ready for publication, with minor layout changes to fit the thesis format. The references cited throughout the thesis are provided only once in a reference list at the end of the thesis.

The last chapter (Appendix) is a draft Geological Survey of Canada Open File Report which contains background information on methodology and all of the data sets used during this study. All the results from this study were based on these data sets.

## **Chapter 2. TEMPORAL AND SPATIAL DISTRIBUTION OF LATE QUATERNARY MASS TRANSPORT DEPOSITS (MTDS) IN FLEMISH PASS**

### **2.0 Abstract**

Flemish Pass is a small, perched basin on the northeastern Grand Banks slope along the eastern Canadian continental margin. Mid to Late Quaternary glaciations on the continental shelf strongly influenced sedimentation on the outer shelf and slope and deposited several thick-bedded mass transport deposits (MTDs), which are interlayered with hemipelagic muds and thin-bedded turbidite sands.

A regional seismic stratigraphy, based on 500 km of seismic airgun and sparker or boomer Hunttec controlled by 60 piston cores up to 11 m long, was dated using 30 radiocarbon dates, the presence of Ash Zone II and oxygen isotope stratigraphy in cores. This stratigraphy was used to determine continental margin sediment flux variations over several glacial-interglacial cycles for the last 170 ka. The seismic character of the different MTDs in Flemish Pass was used to define three MTD types in the study area.

Using the chronological control, it was demonstrated that all the mapped MTDs failed during glacial times. During the glacial advances till deposits in water depths < 600 m along the Grand Banks margin were dated from oxygen isotope stage (OIS) 6. Thick MTDs from both slopes of the basin characterize the

floor areas in Flemish Pass at this time: some of these OIS 6 flow deposits may be glacial MTDs whereas other deposits have a weaker climatic correlation. No outer shelf till is recognized correlating with OIS 2. Only minor MTDs and less extensive till advances are present in OIS 4. Three possible processes may have initiated the observed MTDs: earthquakes, sea level change, and Heinrich events with related meltwater fluxes.

## 2.1 Introduction

Mass transport deposits (MTDs) are widely recognized in basins along continental margins around the world and have been deposited under various climatic settings. Several studies have used seismic and core data to map their temporal and spatial distribution along slopes for improving the understanding of volumes of sediment fluxes over time in these areas (Laberg and Vorren, 1995; King et al., 1996; Piper et al., 1997; Domack et al., 1999; Piper, 2005) and how these flows were initiated (Mulder and Cochonat, 1996; Mosher et al., 2004; Tripsanas and Piper, submitted).

Mass transport deposits were studied in central and northern Flemish Pass, a small perched 1100 m deep basin along the eastern Canadian continental margin (Fig. 2.1), which has been influenced by Late Quaternary glaciations. The MTDs are interbedded with thick muds and thinner sandy beds.

Due to its morphological setting, sediment from failures on the flanks of Flemish Pass is trapped on the floor. In contrast, elsewhere on the eastern

Canadian margin sediment failures run out onto the abyssal plain, where it is more difficult to sample and study these flow deposits.

A high-resolution seismic stratigraphy is outlined for the basin. Chronology is controlled by radiocarbon dating, tephra stratigraphy, Heinrich layer stratigraphy and oxygen isotope stratigraphy from piston cores. The shallowness of the MTDs in the sequence and related sediments and their stratigraphic distribution was used to study these deposits and determine (1) their spatial distribution over the basin and (2) variations in sediment budgets and fluxes over time. This information is used to better understand the glacial history of the area for the last 170 ka.

## 2.2 Geological Setting

### 2.2.1 Bathymetry

Two bathymetric basins bound the eastern slope of the Grand Banks: Flemish Pass to the east and the deeper Orphan Basin to the northeast. Flemish Pass is a perched basin confined by the basement high of Flemish Cap to the east (Fig. 2.1), created structurally during initial rifting of the North Atlantic in the Cretaceous (Grant, 1972).

The floor of Flemish Pass is generally flat with very low-relief lobes termed Kyle and Gabriel Lobes on the western edge (Piper and Pereira, 1992) and East Central and Southern Baccalieu lobes in the east (Fig. 2.2). Flemish Pass is 1100 m deep and 50 km wide at its narrowest section just south of Kyle Lobe and

widens northwards to 80 km east of Sackville Spur: it is up to 100 km wide in the south, before dropping steeply to the Newfoundland Basin.

The depth of the shelf break on the northeastern Grand Banks slope increases northwards from 250 m upslope from Kyle Lobe to more than 400 m at Sackville Spur (Fig. 2.2), probably due to variation in subsidence rate on the Grand Banks (King and Sonnichsen, 1999). Flemish Cap is a 150 by 200 km plateau above a poorly defined slope break at about 350 m. This plateau is 139 m deep at its shallowest point (Monahan and Macnab, 1974).

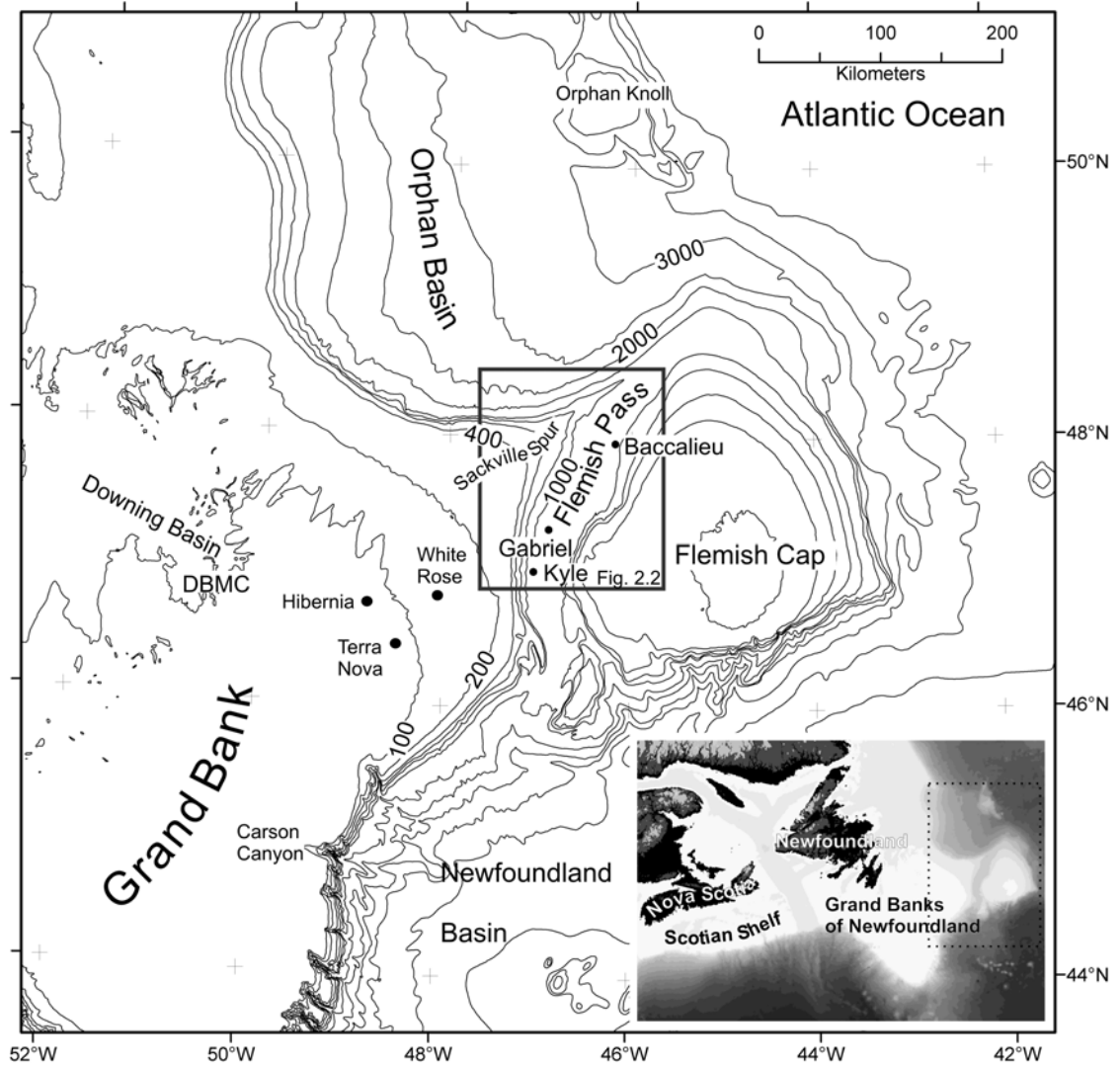


Figure 2.1: Overview map of Flemish Pass and adjacent areas along the eastern Canadian continental margin; the black circles are oil exploration wells, DMBC= Downing Basin Moraine Complex formed during Wisconsin deglaciation at 15 ka ago (King et al., 2001), 200 m isobaths down to 1000 m water depth, below 1000 m at 500 m spacing.

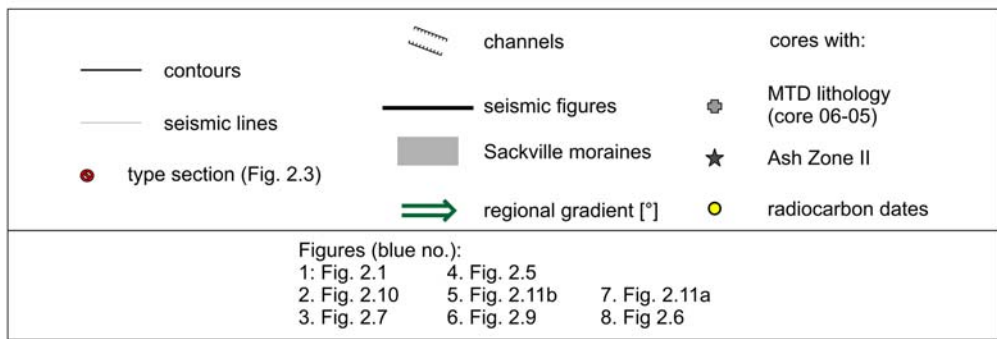
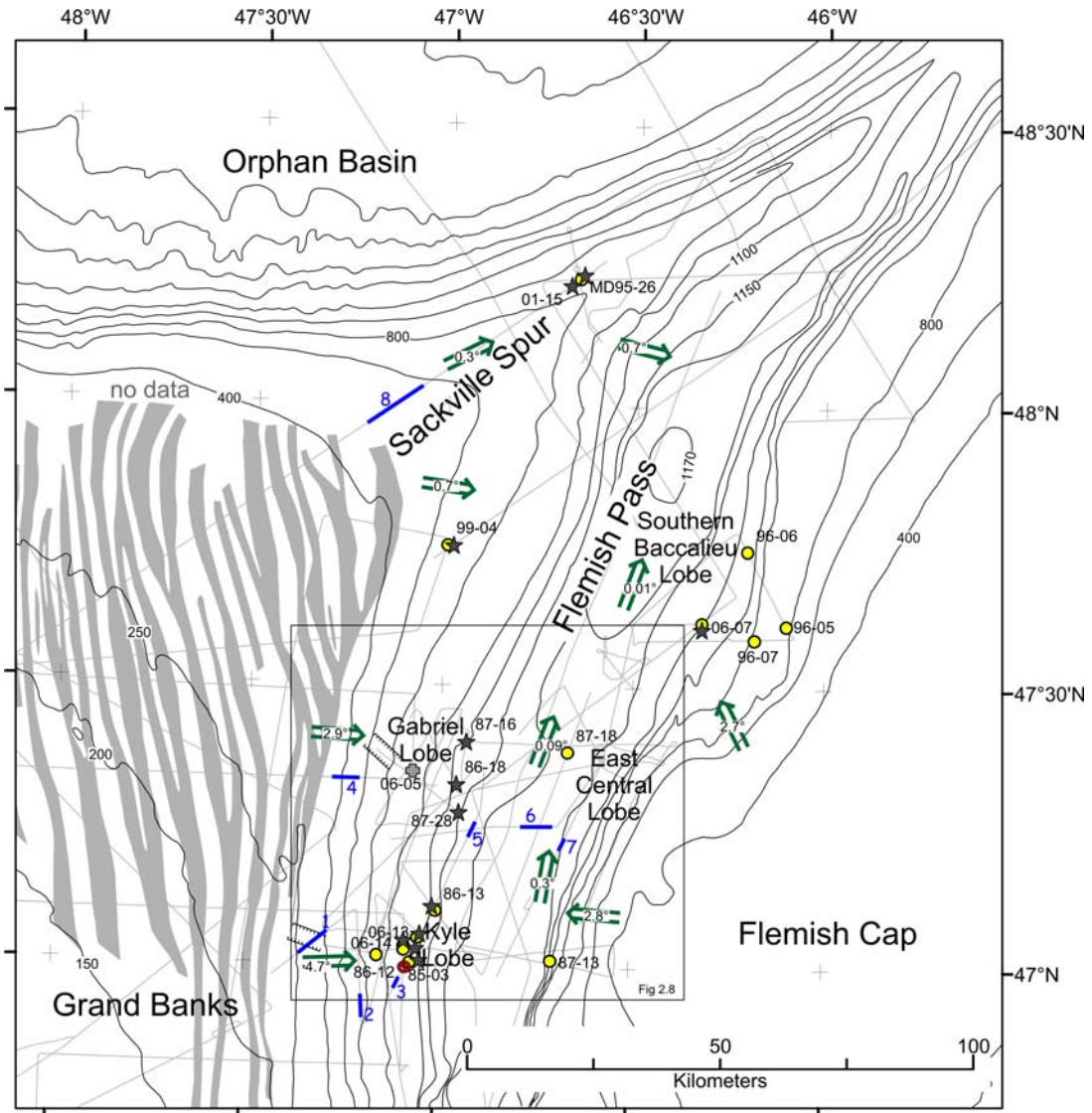


Figure 2. 2: Map of central and northern Flemish Pass, showing the different lobes (named after nearby wells) and channels, core control and age control. The green arrows indicate the regional slope gradient [°].



### **2.2.2 Oceanography**

Morphology strongly influences the oceanic setting in Flemish Pass. The southward-flowing shallow branch of the cold Labrador Current splits in Orphan Basin. The flow speed of this surficial current is generally less than 15 cm/sec, reducing to 3 cm/sec at 185 m water depths (Ross, 1981; Colbourne and Foote, 2000). The majority of the current flows along the outer margin east of Flemish Cap, but a minor branch flows southwards through Flemish Pass along the Grand Banks slope. The northward flowing warm Atlantic Current mixes with the Labrador Current in central Flemish Pass and creates an eddy system on Flemish Cap (Colbourne and Foote, 2000). The Labrador Current transports icebergs from Greenland and the Canadian Arctic to the area. These create large iceberg pits and smaller, related scours on the shelf and upper slope. Recent scours are generally 20-30 m wide and less than a meter deep and up to 15 km long (Lewis and Parrott, 1987; Parrott et al., 1990). Relict Pleistocene scours are 2-3 m deep and can be more than 50 m wide; some are more than 100 m across and strongly differ in size from the recent furrows (King, 1976; Piper and Pereira, 1992).

### **2.2.3 Geology of Flemish Pass**

Flemish Pass has gradually been infilled by prograding sequences from the Grand Banks; this progradation started in the Mesozoic and reflects sea-level variations in the area (Piper and Normark, 1989; Foster and Robinson, 1993).

These sea-level fluctuations created several unconformities in the sequence, e. g. at the base of the Miocene and the base of the Pliocene (Kennard et al., 1990), recognized in several exploration wells.

The shallow Quaternary sedimentary sequence in Flemish Pass has been investigated using airgun seismic data for the deeper sedimentary sequence and high resolution boomer (Huntec) seismic and core control for the shallower subsurface section (Piper and Pereira, 1992). The sedimentary sequence in Flemish Pass is characterized by thick uniform muds. Some sandy horizons have been interpreted as turbidite deposits; these turbidites originated from the Grand Banks slope (Piper and Pereira, 1992). Along the base of the Flemish Cap slope some thick-bedded sandy sequences indicate contourite activity (Piper and Campbell, 2005).

Sidescan data from the area show a few channels along the slope of the Grand Banks and iceberg scouring along the slope down to 600 m water depths (Piper and Pereira, 1992). Two main channels are found in the central and northern part of Flemish Pass on the Grand Banks slope: the Kyle channel zone and Gabriel channel (Fig. 2.2). The channels have changed little over the Mid to Late Quaternary (Piper and Normark, 1989) and were pathways for MTDs and turbidity currents (Piper and Pereira, 1992). In contrast, seismic profiles upslope from the North Central Lobe and Southern Baccalieu Lobe do not show any indication of channelized flows across the Flemish Cap slope.

#### **2.2.4 Geology of the Areas Adjacent to Flemish Pass**

The Grand Banks of Newfoundland is a collective term for an area in excess of 100 000 km<sup>2</sup> comprising several banks and channel systems with a maximum water depths of 300 m. Relict deposits of earlier more extensive ice advances are found near the shelf break and are mostly reworked, whereas glacial deposits of the oxygen isotope stage (OIS) 2 are best developed on the inner and middle shelf (King and Sonnichsen, 1999; Sonnichsen et al., 1999).

Tills extend to the shelf break on the northern and eastern Grand Banks (Piper and Brunt, 2006), creating subtle features underlain by overconsolidated muds on the northeast Grand Banks, including the Sackville Moraine complex (Figure 2.2). This moraine complex extends as prominent ridges down to at least 400 m water depth (King et al., 2001). In contrast to till elsewhere on the Grand Banks margin, the moraines on Sackville Spur have not been truncated by upper slope failure and erosion, except in the extreme northwest (Sonnichsen et al., 1999; King et al., 2001).

The inner- and mid-northeastern Grand Banks shelf is covered by low-stand sands formed in a proglacial setting in the Hibernia and Terra Nova area, which filled in tunnel valleys. To the northwest of this area, the Downing Basin Moraine Complex (DBMC, Figure 2.2), represents an ice lobe complex with various moraines and open tunnel valleys. King et al. (2001) interpreted this area as glaciated during the last glaciation and inferred that ice receded from the area after 15 ka.

The glacial history along the eastern Grand Banks shelf break adjacent to Flemish Pass is poorly constrained. The Sackville Moraines suggest the presence of ice along the shelf break at some time before OIS 2 (King et al., 2001). The maximum ice extent during OIS 2 is less well understood because the deposits of this ice sheet may have been eroded since deposition or may be too thin to be recognized, even though some sandy deposits from a proglacial setting in the Hibernia area have been assumed to be Wisconsin in age (Fader and King, 1981).

Flemish Cap was likely never glaciated but its shallow crest may have been just subaerially exposed during extreme glacial low-stands (Lambeck and Chappell, 2001) when taking regional subsidence (King and Sonnichsen, 1999) and rebound into account; unpublished seismic profiles show no evidence of tills or seismic facies deposited in an ice-margin setting.

Sackville Spur is a sediment drift which extends from the easternmost Grand Banks slope down onto the basin floor of Flemish Pass. It was created in the later Cenozoic by the interaction of the Labrador Current and the North Atlantic current in the area. Several scarps have been identified along its slopes which created large muddy buried mass transport deposits in northern Flemish Pass (Kennard et al., 1990; Piper and Campbell, 2005).

### **2.2.5 Mass Transport Deposits in the Greater Area**

In Orphan Basin, to the northwest of Flemish Pass, glacial MTDs derived from the Trinity Trough ice stream have been interpreted as being

deposited between 14.5 and 30 ka (Hiscott et al., 2001; Tripsanas and Piper, submitted). Slides occurring on the southern margin of Orphan Basin at specific horizons have been interpreted as earthquake-induced failures (Tripsanas and Piper, 2007; Tripsanas and Piper, 2008, in revision).

Likewise, on the northeastern Grand Banks margin, north of Carson Canyon (Fig. 2.1), correlative MTDs were found at discrete horizons based on high resolution seismic data (Toews, 2003) and indicate synchronous failure at specific time intervals. Similar failures have been observed along most of the south eastern Canadian continental margin, where every few tens of thousand years a failure occurs, creating a MTD (Piper, 2005).

### **2.2.6 Heinrich Layers**

Heinrich layers (Heinrich, 1988) are widely recognized in the North Atlantic and were deposited by melting icebergs originating from Hudson Strait and other major ice outlets. In the Labrador Sea and adjacent areas these layers are rich in detrital carbonate (Andrews, 1998) and are important lithostratigraphic markers. The corresponding Heinrich events can be linked to deglaciation events (Andrews, 1998; Andrews and MacLean, 2003). Up to 12 of these events are described from the region (Tripsanas and Piper, 2008, in revision), but only the upper six are widely recognized along the eastern Canadian margin (Rashid et al., 2003a).

## 2.3 Materials and Methods

The shallow mass-transport deposits in Flemish Pass have been surveyed using seismic airgun and high resolution Hunttec boomer or sparker seismic systems on several cruises over the last two decades. The high resolution airgun data imaged the upper few hundreds of meters below the seabed. The Hunttec boomer system images up to 50 m below seabed at a 1 m vertical resolution. The Hunttec sparker system is more energetic and allows penetration of up to 120 m in sediments (Mosher and Simpkin, 1999). Track lines of available data are shown in Fig 2.2.

A new seismic stratigraphy was outlined for the basin by tracing reflections digitally. Older paper records were scanned and converted into jpeg2000 (\*.jp2) and imported into ArcGIS 9.1 (ESRI software), where seismic reflections were traced by creating shape files. These seismic records were not georeferenced. Data collected in 2006 was digitally recorded as SEG Y files, which were exported as tiffs (\*.tif) and imported into ArcGIS.

Piston core data were used to ground truth the shallow seismic data. Sixty cores have been used in this study. Cores were taken using either the 6 cm diameter Benthos Corer or the Atlantic Geoscience Centre long piston corer with a diameter of 12 cm. The cores were split in a shore-based laboratory, where digital color (CIELab), physical property data (GEOTEK MST) and digital photography were collected. Additionally, the cores were visually described and summary core plots created.

Radiocarbon dates were determined using accelerator mass spectrometry (AMS) on foraminifer tests of *N. pachyderma* sinistral. Dates were calibrated using the CALIB radiocarbon calibration program (CALIB REV 5.0.1) by M. Stuiver and P. J. Reimer (<http://calib.qub.ac.uk>), with a reservoir correction of 450 years following the methodology from Tripsanas et al. (2007 (in press)) in Orphan Basin. Radiocarbon dates older than 24 ka were calibrated following the Marine04 database, which reaches back to 50 ka (Hughen et al., 2004).

Petrology was used to identify the North Atlantic Ash Zone II (AZ II) in several cores in Flemish Pass. Channel samples 1x0.5x5 cm were used to determine the location and extent of this ash zone in the cores. These samples were washed at 53  $\mu\text{m}$  and studied using light microscopy. Volcanic tuff, lava particles and obsidian were found in these layers, which showed the same zonal pattern as described for Ash Zone II (Haflidason et al., 2000).

The correlation between the piston and trigger weight core is especially difficult in older cores (pre-1996), where up to 2 m may be missing at the top of the piston cores. Where trigger weight and piston cores overlapped, they were correlated using variation in the CIELab L\* and a\* color plots. In cases where there was no overlap between trigger weight and piston core, it was assumed that the gap between the base of the trigger weight core and the top of the piston core was 5 cm. Cores were correlated with the seismic data using an assumed velocity of 1500  $\text{ms}^{-1}$ . Where the piston and trigger weight core correlate, the error in the core-seismic correlation is estimated to be  $\pm 0.5$  m. Where no core correlation was possible, this error could be as much as several meters.

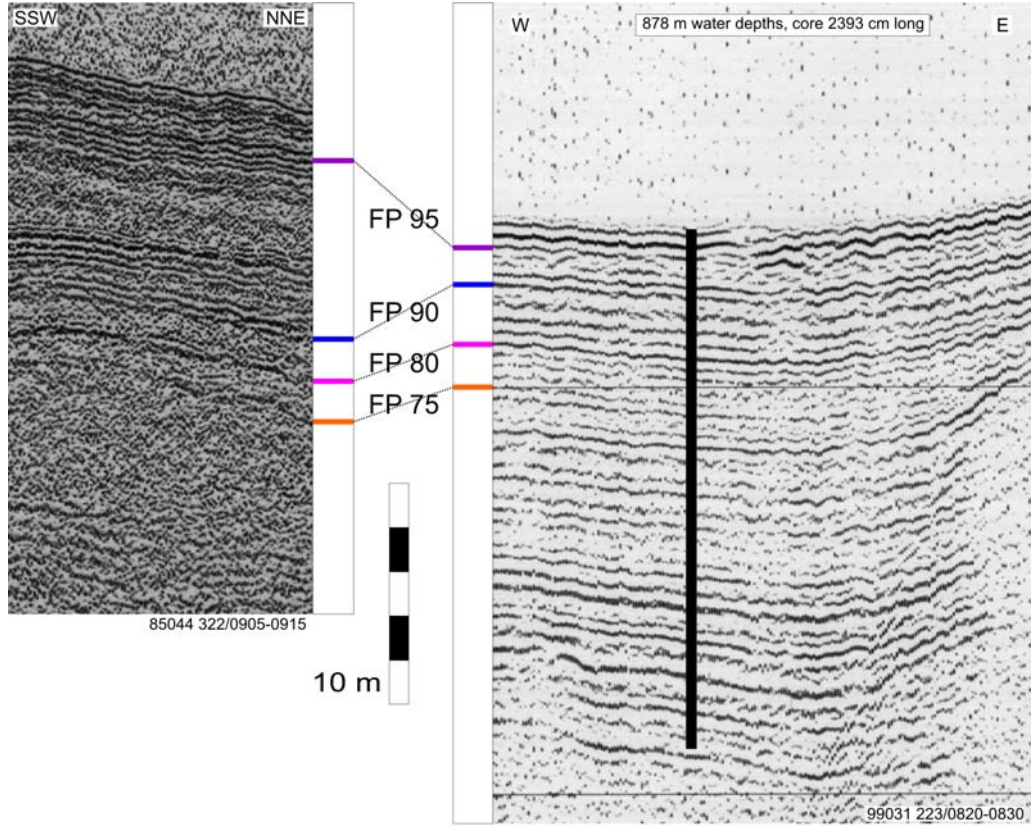
## 2.4 Results

### 2.4.1 Key Reflections

Four high-amplitude reflections were defined at a type section on Kyle Lobe: FP 95, FP 90, FP 80 and FP 75 (from youngest to oldest, Fig. 2.3a). An older reflection, FP 70, was locally distinguished below the depths of acoustic penetration, including at the type section.

Reflections were traced throughout Flemish Pass from south of Kyle Lobe to Sackville Spur. Upslope, tracing was possible into the zone of iceberg scouring at about 600 m water depth. On Sackville Spur, the key reflections were correlated to the core MD 95-2026 (Piper and Campbell, 2005) (Figure 2.3b). Repetitive tracing shows that the error in tracing the reflections is generally one seismic cycle or approximately 0.5 m. Reliability of seismic correlation was checked by comparing the results to an independent correlation of older seismic profiles by Campbell et al. (2002).





(a) type section

(b) correlation to MD95-2026 core

Figure 2. 3: (a) Type section on Kyle lobe for the reflections traced in Flemish Pass and (b) their relationship to the MD95-2026 core on Sackville Spur

#### **2.4.2 Seismic Stratigraphy of the Grand Banks Margin**

Seismic traverses onto the Grand Banks from Flemish Pass show in both airgun and Hunttec data that several poorly stratified incoherent deposits extend to ~ 650 m water depth (Figs. 2.4, 2.5). The features are underlain by the seismic reflection FP 75. These features appear to originate from the Grand Banks. A similar pinch-out of incoherent facies occurs between FP 80 and FP 90 (Fig. 2.6). In other areas along the eastern Canadian continental margin such structures have been termed till tongues (Mosher et al., 1989). The sedimentary sequence below these till tongues, imaged on the airgun data, indicates poorly stratified sediments with few continuous reflections deeper in the section.

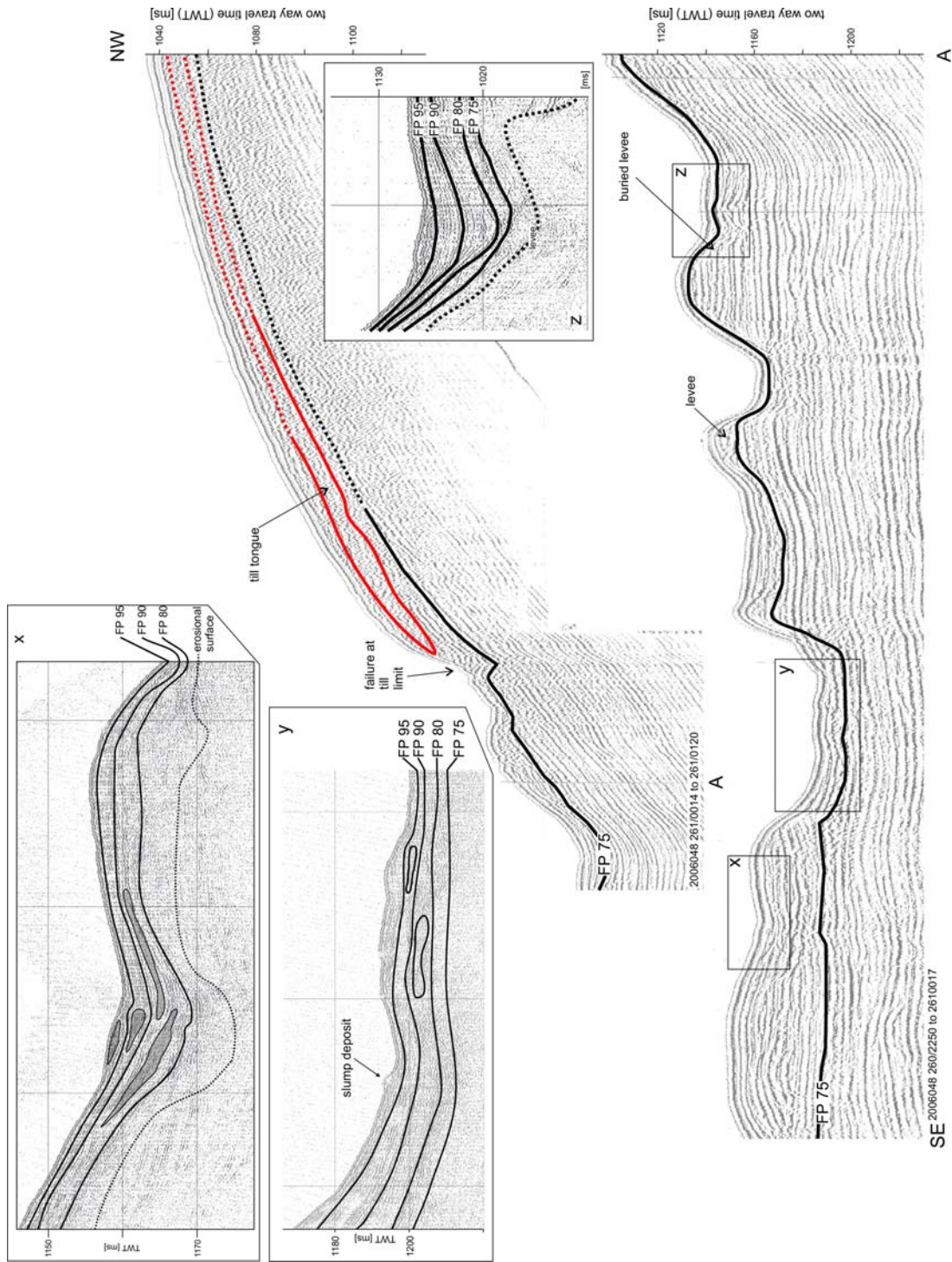


Figure 2. 4: Airgun seismic cross section upslope from Kyle Lobe, showing the till tongue (red line) above seismic reflection FP 75 and its relationship to channels and MTDs downslope: x) seismic boomer cross section of stacked MTDs in a channel; y) seismic boomer cross section of overbank area adjacent to channel showing complex fill by MTDs and sandy units; z) seismic boomer section through a levee and its relationship to the reflections

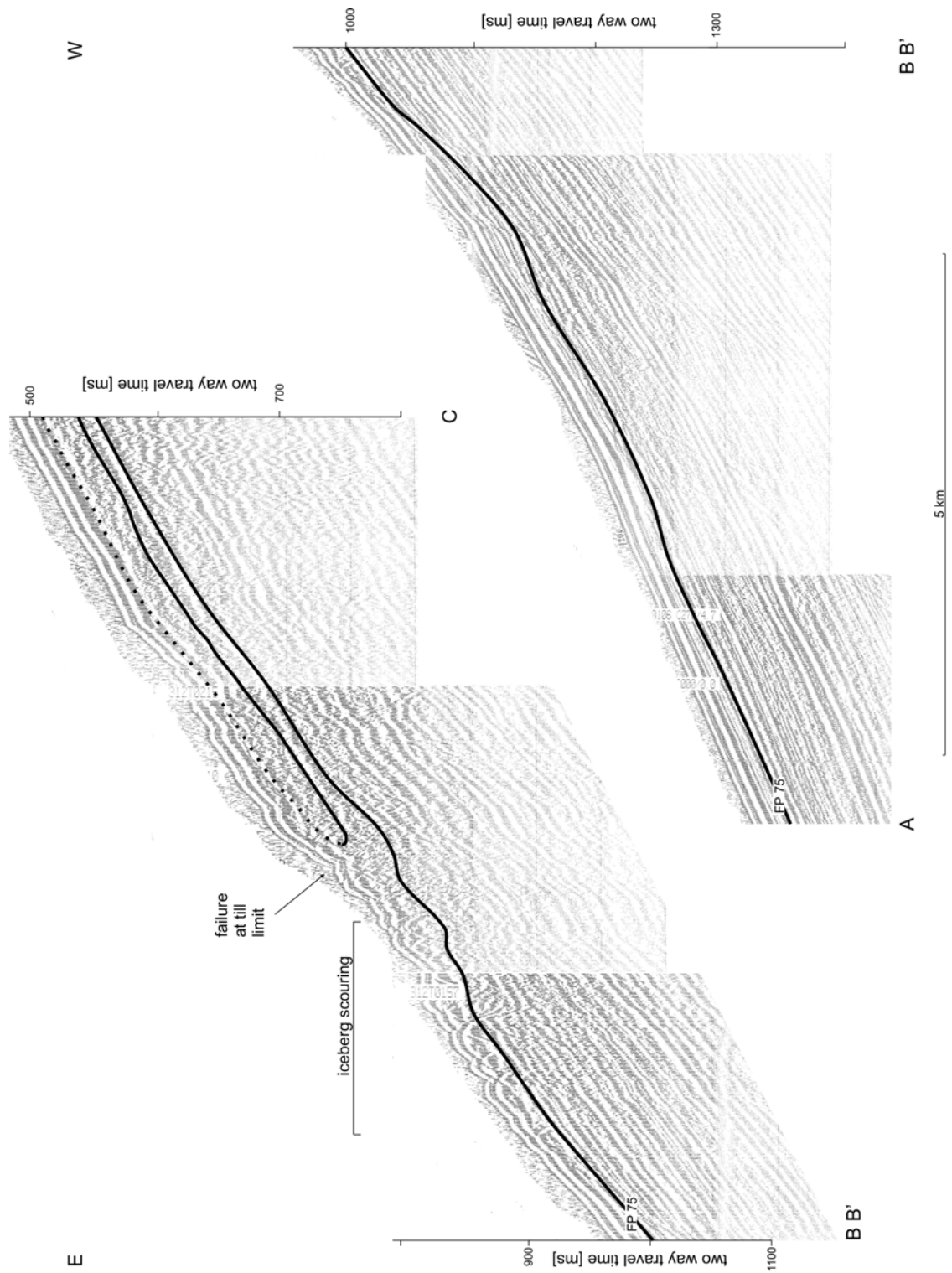


Figure 2. 5: Till tongue above reflection FP 75 upslope from Gabriel Lobe and its relationship to surficial iceberg scouring and the Grand Banks shelf break.

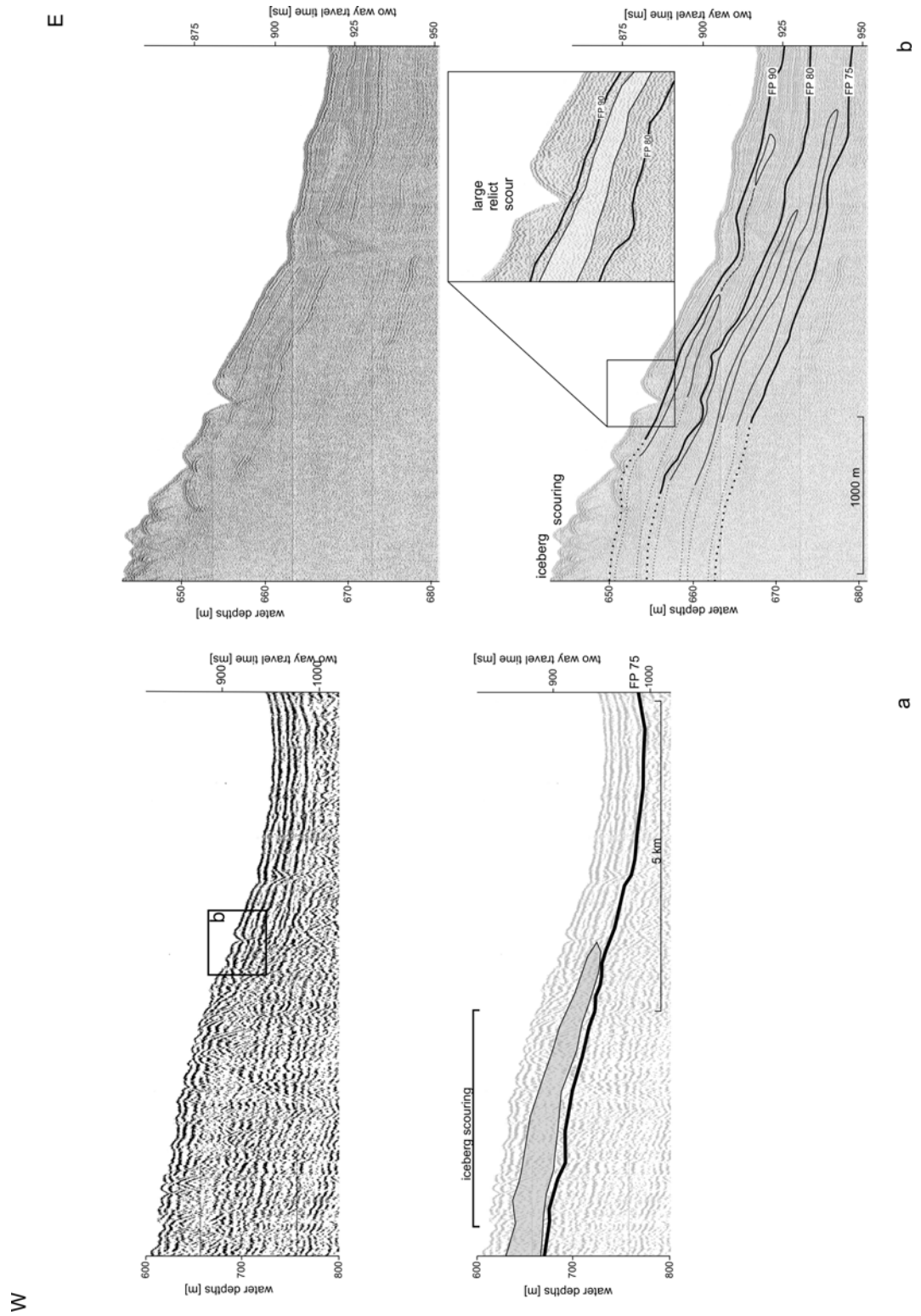


Figure 2: 6: a) Airgun seismic section showing a till tongue (arrow) above reflection FP 75 and the overlying iceberg scouring; b) boomer seismic section showing till tongues above FP 75 and above FP 80 and their relationship to the iceberg scouring.

### 2.4.3 Mass Transport Deposits

Mass transport deposits in seismic data show a highly incoherent return. This seismic character has previously been described from mass transport deposits using Huntco seismic data from other slopes along the eastern Canadian margin, where these features were ground truthed by core-seismic correlation (Piper, 2005; Piper et al., 2005; Tripsanas and Piper, submitted).

The basal boundaries of the MTDs are mostly sharp with few erosional structures. The upper boundaries are less well defined due to hyperbolic refractions, particularly in the Gabriel Lobe where rough MTD surfaces create highly scattered returns. Most of the mass transport deposits are lensoid in cross section with well-developed pinch-outs when thinning. The deposits usually follow the local topography and fill channels (Fig. 2.7). The MTD thickness in Flemish Pass varies from 1 to 25 m with an average of 7 m.

On the western side of the basin, all of the mapped MTDs appear to have originated from flows across the Kyle and Gabriel lobes (Figs. 2.2, 2.8). The MTDs from the Eastern Central Lobe were not channelized but appear to have originated as widespread failures from the Flemish Cap slope (Fig. 2.9), which is locally characterized by small depressions. Seismic reflection profiles show that the Kyle and Gabriel channels were active over long time spans and are sources of different mass transport flows (Fig. 2.10). The stacked MTDs result in morphological lobes in the basin which have a very low regional gradient of less than  $0.3^\circ$ , creating very flat floor morphology in the basin. The only elevated areas are the constructional features created by MTD lobes.

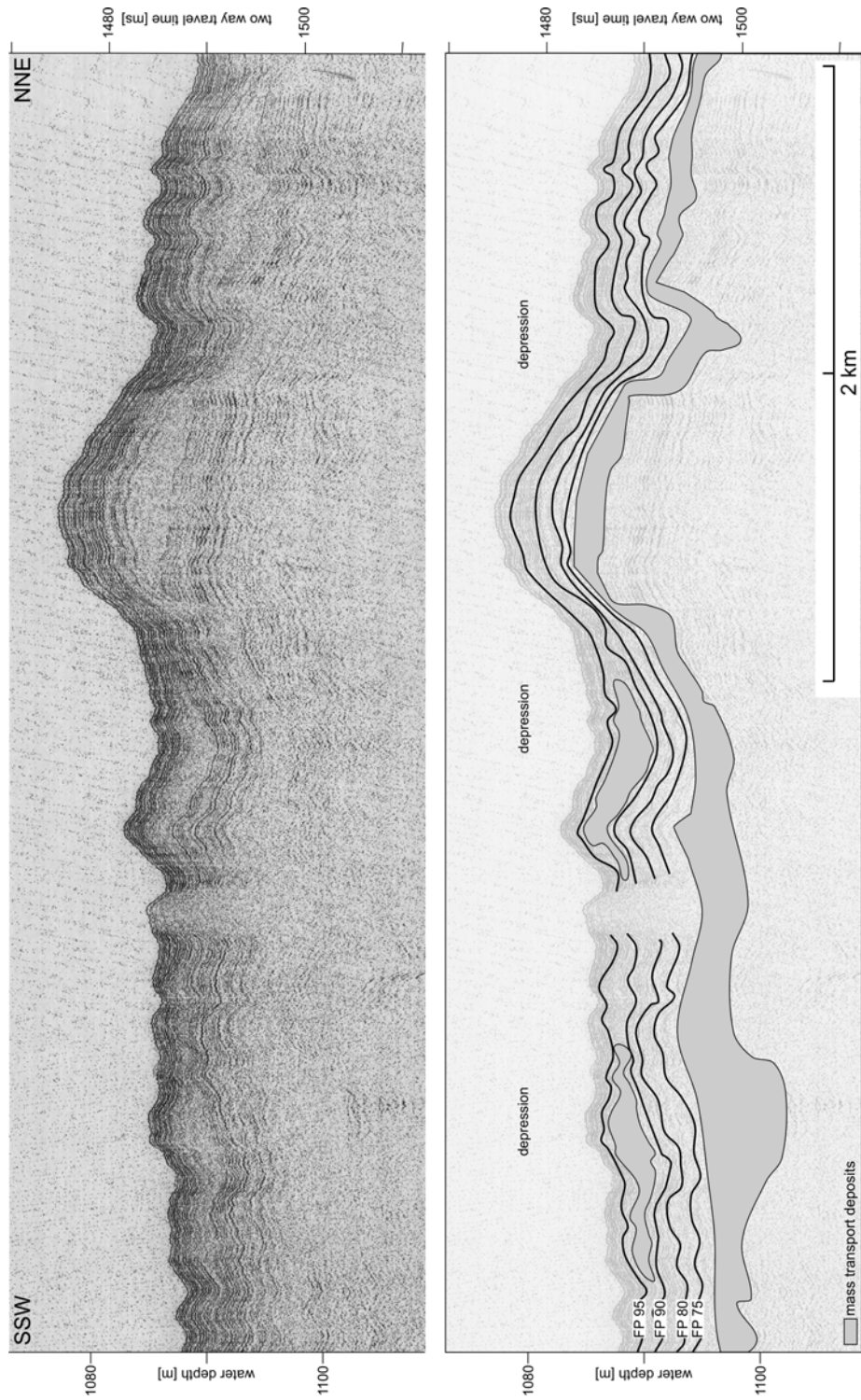


Figure 2. 7: Cross-section in the Kyle Lobe area showing lensoid MTDs; they fill in small depressions and generally follow the local topography; locally they may construct morphological features.

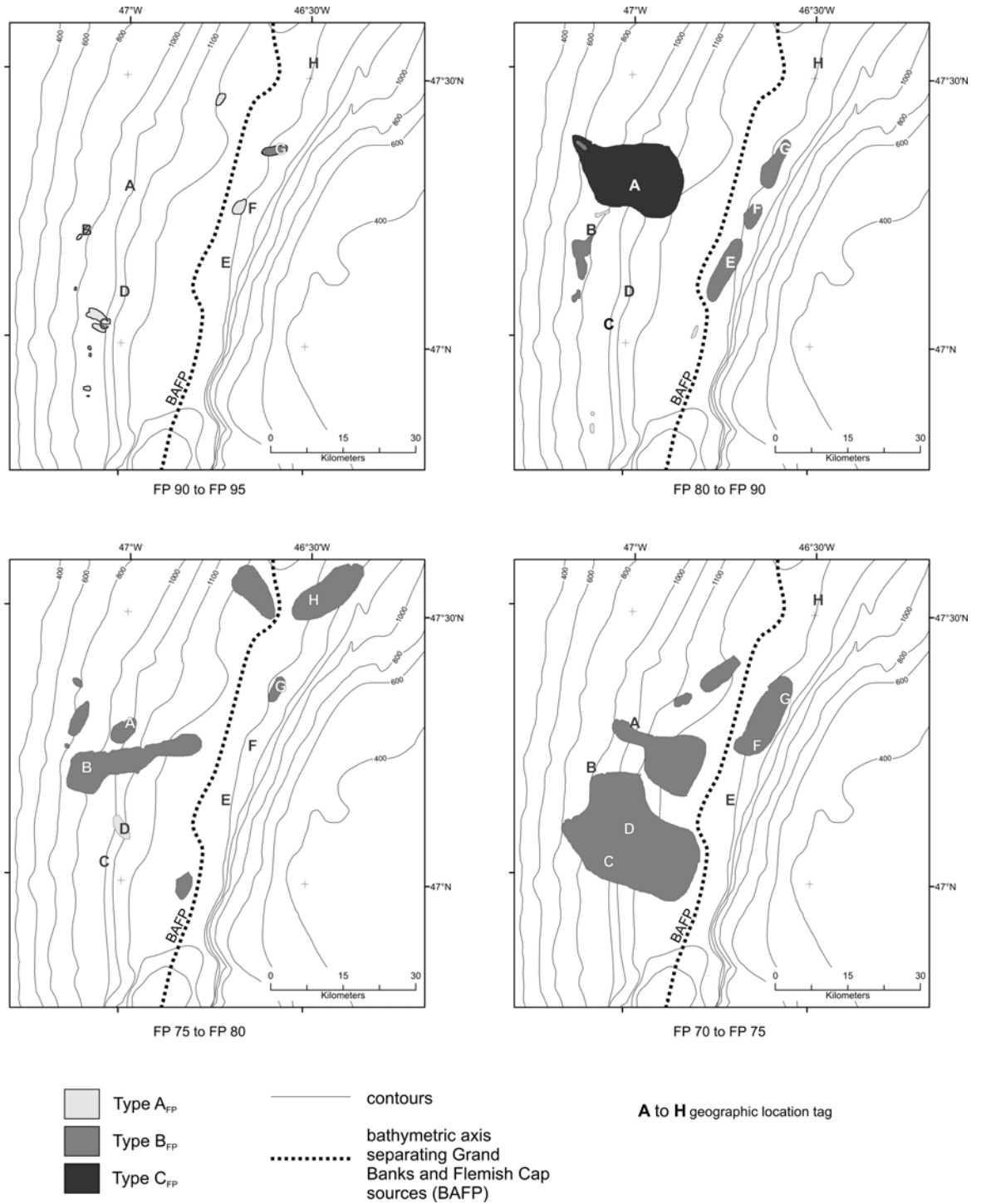


Figure 2. 8: Map of stratigraphic position of MTDs in Flemish Pass and their relationship to the traced reflections; the main channels on the Grand Banks are indicated; Letters A to H indicate virtual boreholes.



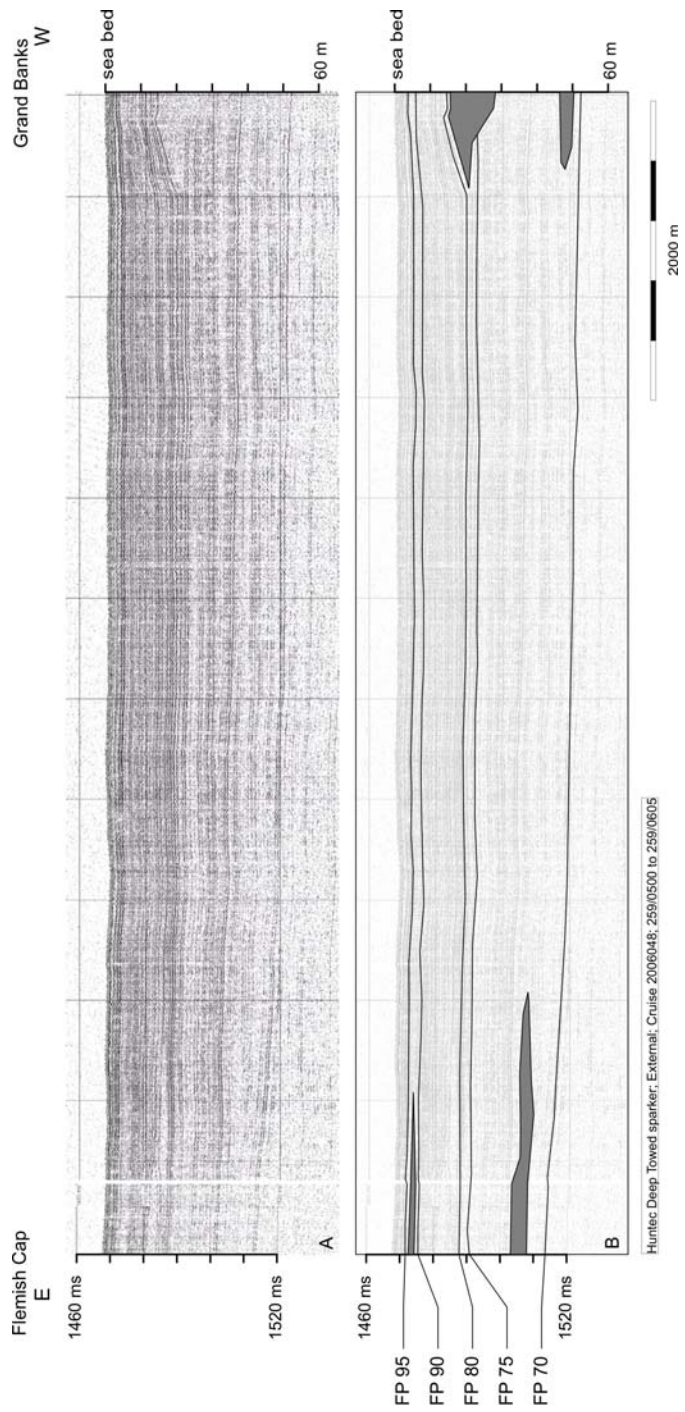


Figure 2. 9: Stratigraphic relationship of MTDs from the Grand Banks and Flemish Cap slopes in central Flemish Pass.

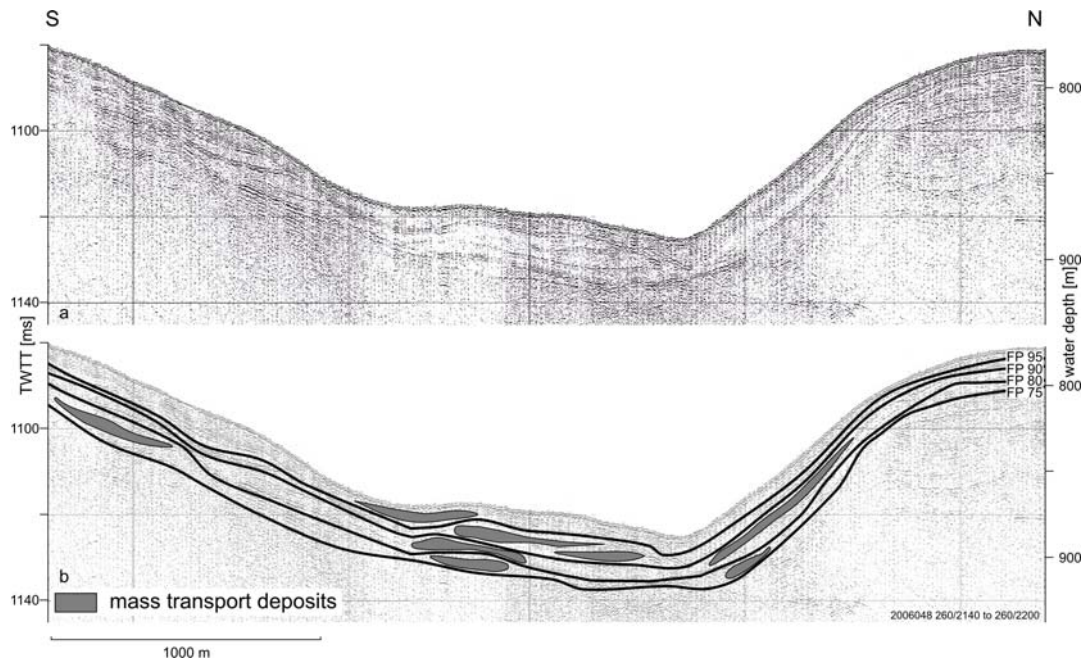


Figure 2. 10: Cross-section of stacked MTDs in the channel system upslope from Kyle Lobe.

Volumes of mass transport deposits were calculated using the approximate area and thickness of the MTDs. Generally, older deposits deeper in the section are more abundant, show larger spatial extent and are thicker than younger deposits.

The characteristic acoustic signature of the MTDs was used to classify the flows into three different types (Fig. 2.11). Type A<sub>FP</sub> is characterized as an incoherent poorly stratified sequence. These deposits show a limited run out distance and follow the local topography with no basal erosion, the distal pinch-out is gradual. Type B<sub>FP</sub> is a thick incoherent deposit that has a long run out distance spreading along the basin floor, with erosive structures at the base; the pinch-out resembles that from Type A<sub>FP</sub>. These deposits were only recognized from the sequence below FP 80. Type C<sub>FP</sub> are very thick deposits with more than 20 ms thickness, which have a very rough surface and an erosive base. These flows have a short run out distance and come to an abrupt termination in the basin creating a strong relief on the basin floor; diapir-like structures, perhaps elevated blocks, are common (Fig 2.11b). Not every MTD can be confidently assigned to one of these three types.

#### **2.4.4 Core Control of MTDs**

Core control is available for MTDs less than 10 m subbottom. Only one recent core sampled an MTD (core 06-05, Fig. 2.2). Several older (pre-1990) cores on Gabriel Lobe also sampled the shallowest MTDs, and even though the cores are dried out, they show similar lithologies as the 06-05 core.

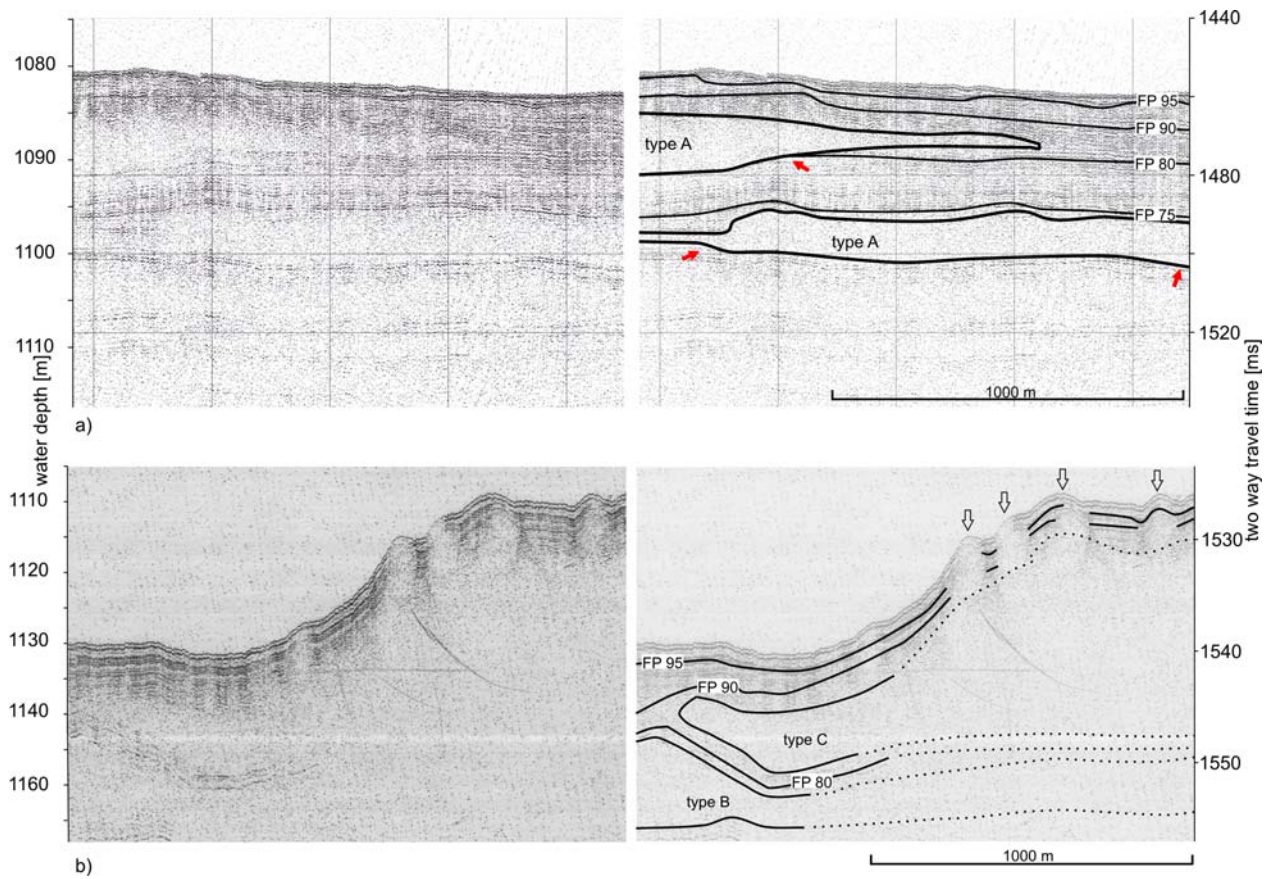


Figure 2. 11: Examples of MTD facies type  $A_{FP}$ ,  $B_{FP}$  and  $C_{FP}$  in Flemish Pass, a) central Flemish Pass, the arrows indicate basal erosion, a feature of the type A MTD; b) Gabriel Lobe, the arrows indicate areas showing the rough surface of the flow, which is typical for this MTD type.

The MTD in core 06-05 consists of blocks of different muddy lithologies with sharp sub-horizontal contacts. Towards the base of the MTD the blocks are larger and contain less sand. Several blocks still show the pre-failure bedding of the sediments.

#### **2.4.5 Chronological Control**

The traced reflections were indirectly dated by correlating the reflections to cores with age control. Four different approaches were used: (1) radiocarbon dates on shells or foraminifera (Table 2.1, Fig. 2.2), (2) Heinrich layers (Fig. 2.12), (3) the North Atlantic Ash Zone II below Heinrich bed H5a (Figs. 2.2, 2.12) and (4) an oxygen isotope curve from core 2026 on Sackville Spur (Fig. 2.13).

Radiocarbon dates are available from several cores distributed over the basin and are summarized in Table 2.1. All of the finite ages are consistent with results of other dating methods established independently. A few dates older than 50 ka are interpreted as infinite ages: they are bracketed in figures.

Heinrich layers were identified in Flemish Pass using comparison of downcore CIELab color plots with published color data from the Labrador Sea (Andrews and Barber, 2002) and Orphan Basin (Tripsanas et al., 2007). Identification of specific Heinrich layers was confirmed by radiocarbon dates (Fig 2.13). Interpretation of the color plots was confirmed by carbonate data from cores MD95-26, 99-04 and 96-06, and by comparison with cores from the Labrador Sea (Veiga-Pires and Hillaire-Marcel, 1999). Heinrich Layers H1 and

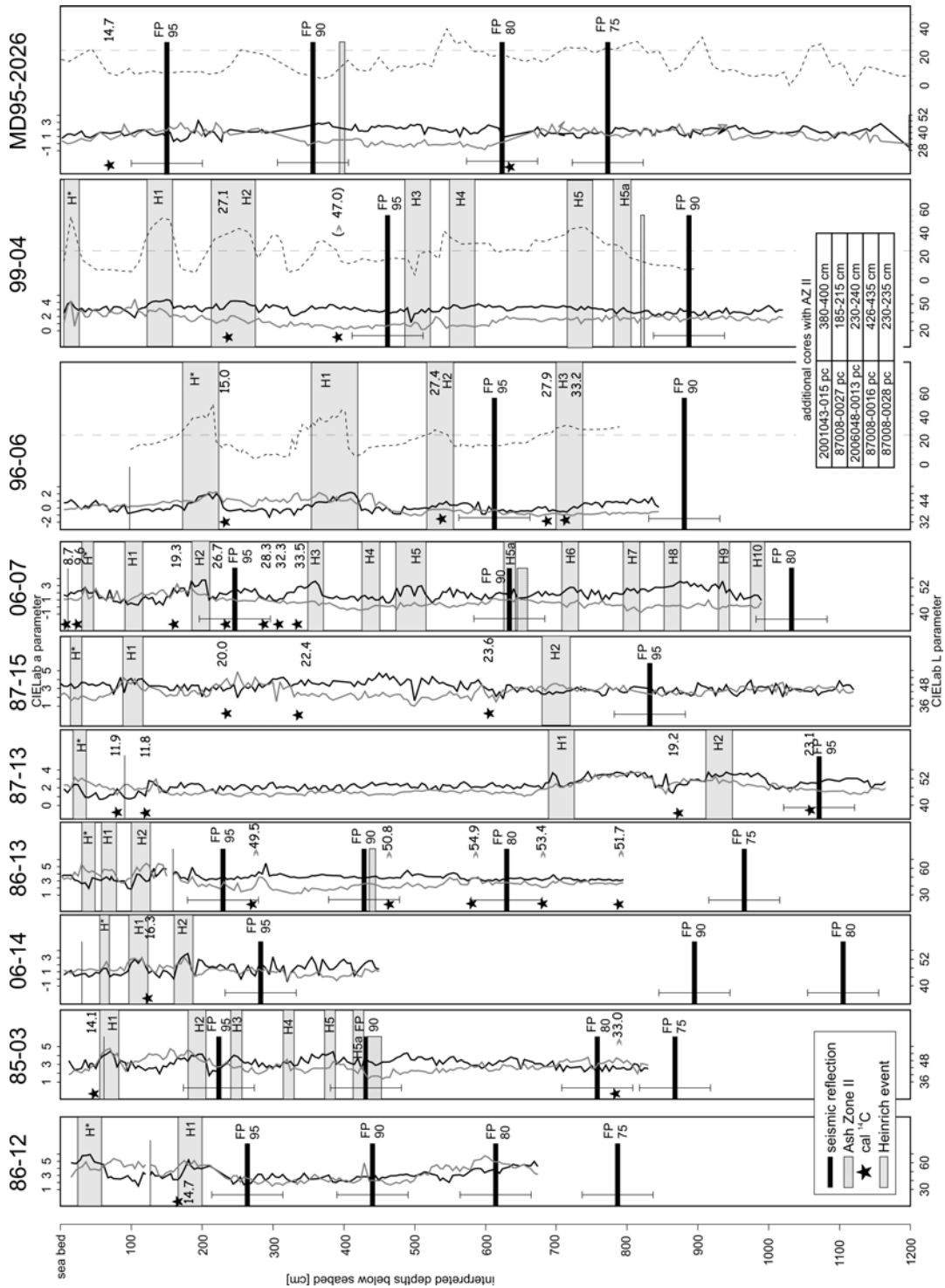


Figure 2. 12: Core control used in this study: the black solid core plot line is the CIE Lab L\* value, the gray solid line the a\*, carbonate plots are in dashed lines; the thin black line at about 1 m depths represents the correlation between the trigger weight core (TWC) and the piston core (PC); the stars indicate  $^{14}\text{C}$  dates, the gray box is the position of the AZ II; a small table indicates the position of the AZ II in other cores from Flemish Pass.

H2 were usually easily recognizable, but older layers were generally less clearly developed.

The North Atlantic Ash Zone II, with an age of  $54.5 \pm 2$  ka (Austin et al., 2004), was found in 12 cores in Flemish Pass and occurred between 200 and 400 cm depth in cores (Fig. 2.12).

The oxygen isotope curve from core MD95-2026 was interpreted by Piper and Campbell (2005) on the basis of a radiocarbon date of  $52.5^{14}\text{C}$  ka at 632 cm depth. The presence of Ash Zone II at 380 to 400 cm is inconsistent with this interpretation and shows that the radiocarbon date is infinite. Reinterpretation of the oxygen isotope curve places the heavy isotope peak at 620 cm at the top of MIS 6 (Fig. 2.13). The lower part of the curve between OIS 6 and 8 shows a good match to the deep-marine global oxygen isotope record (Walker, 2005).

Stretching of long Marion Dufresne cores has been widely reported from muddy sequences (Hiscott et al., 2001; Toews and Piper, 2002; Skene and Piper, 2003). However, the North Atlantic Ash Zone II was also found in core 01-15, 3 km to the east of MD95-2026, where it occurs at 380 to 400 cm depth. This suggests that stretching was not a problem in the MD95-2026 core (Fig. 2.13). Little or no stretching was described from tuff-rich sequences (Anastasakis and Pe-Piper, 2006) which are comparable to sandy sequences found in MD 2026 on Sackville Spur.

From these datasets, approximate ages were assigned to the different reflections giving stratigraphic control to the sedimentary section in Flemish Pass (Figs 2.12, 2.13): reflection FP 75 was dated to OIS 6.4 or approximately 170 ka,

FP 80 was deposited during OIS 5.5 with an age of 125 ka, FP 90 was deposited during OIS 3.3 at about 45 ka and FP 95 formed during OIS 2 about 25 ka ago.

#### **2.4.6 Sedimentation Rates**

Sedimentation rates for sediments excluding the MTDs were calculated for the intervals between the key reflections (FP 75 to seabed, Fig. 2.14) at 14 locations in Flemish Pass. The average sedimentation rates have been relatively constant since OIS 5.5 with values typically in the range 0.1-0.2 mm/yr. Between OIS 5.5 and 6.4 (FP 75-FP 80) the sedimentation rate doubled to 0.4 mm/yr. The largest spatial variability of sedimentation was found during this interval, where generally the Flemish Cap side showed higher sedimentation rates compared to the Grand Banks side of the basin. This trend decreased since this time and during the youngest interval since deposition of FP 95 the sedimentation rate has been relatively constant over the basin. When including the thickness of the MTDs in the sedimentation calculations, the highest sedimentation rates were along the Grand Banks slope and the adjacent western area of Flemish Pass.



Radiocarbon dates in Flemish Pass							
core	<sup>14</sup> C age	calibrated age		depths [cm]		lab no.	material
86018-013	49500 ±2000	x	x	51	I	UCIAMS 32988	foraminifera
86018-013	>50800	x	x	244	I	UCIAMS 32989	foraminifera
86018-013	54300 ±3600	x	x	363	I	UCIAMS 32990	foraminifera
86018-013	>53400	x	x	467	I	UCIAMS 32991	foraminifera
86018-013	>51700	x	x	565	I	UCIAMS 32992	foraminifera
87008-013TWC	11900 ± 110	11029	86	80		TO-4487	foraminifera
87008-013TWC	11810 ± 90	10953	61	125		TO-2041	foraminifera
87008-013	13120 ± 100	12219	191	597		TO-7924	foraminifera
87008-013	19200 ±450	19805	561	737		Beta 22232, ETH 3209	foraminifera
87008-013	23130 ±190	27244	252	920		TO-7925	foraminifera
87008-015	23600 ±380	27777	451	645		Beta 22233, ETH 3210	foraminifera
87008-015	20095 ±50	20793	138	220		UCIAMS 38077	foraminifera
87008-015	22450 ±70	26469	128	310		UCIAMS 38078	foraminifera
MD95-2026	14710 ±100	14554	226	86		TO-8962	foraminifera
MD95-2026	52570 ± 2220	x	x	632	I	TO-6356	foraminifera
2006048-007TWC	19365 ±45	22485	77	130		UCIAMS 38074	foraminifera
2006048-007	8718 ±20	8007	72	10		UCIAMS 38068	foraminifera
2006048-007	9605 ±20	6878	70	40		UCIAMS 38069	foraminifera
2006048-007	26700 ±100	31502	178	235		UCIAMS 38070	foraminifera
2006048-007	28360 ±120	33271	200	276		UCIAMS 38071	foraminifera
2006048-007	32350 ±200	37285	248	310		UCIAMS 38072	foraminifera
2006048-007	33540 ±230	38487	273	360		UCIAMS 38073	foraminifera

Table 2. 1: Radiocarbon dates collected since 2005 in Flemish Pass, the I indicates infinite dates.

Core MD95-2026

Core 2001043-015

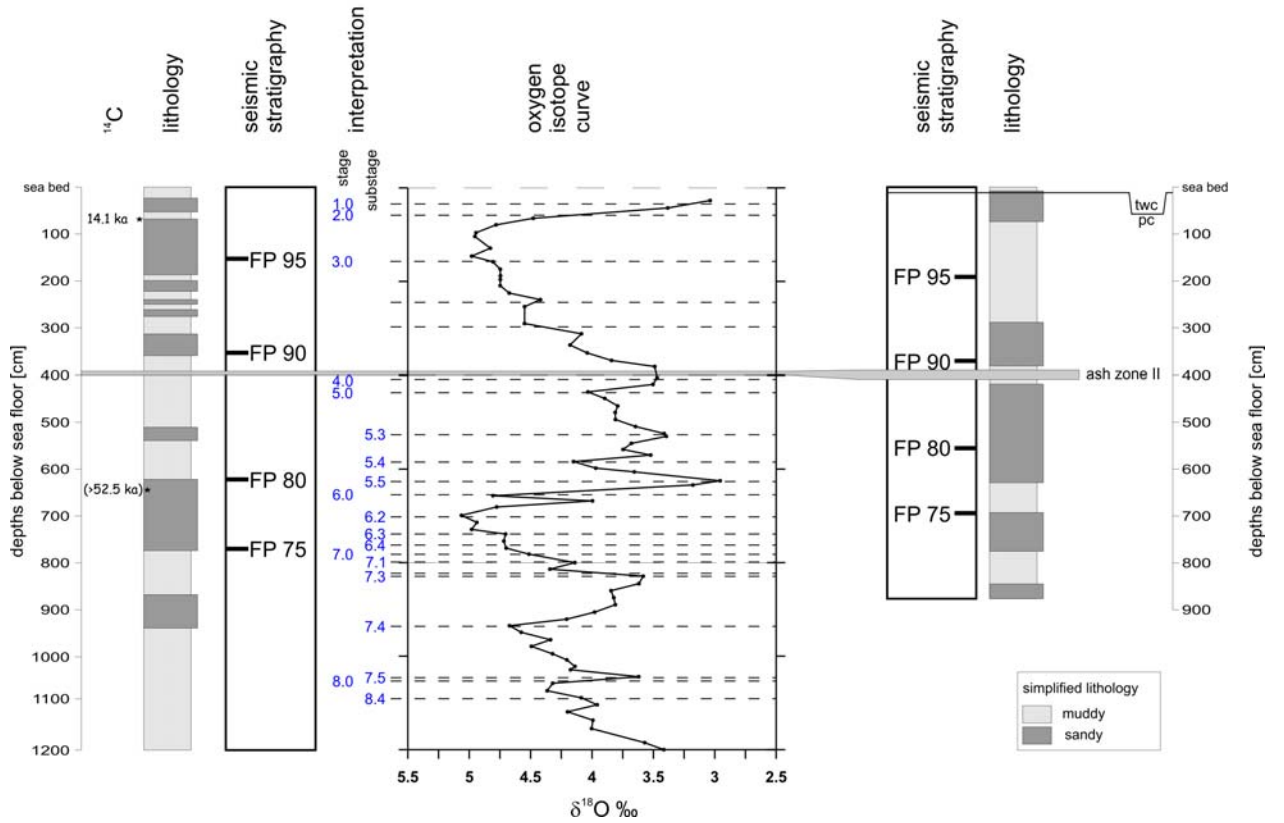


Figure 2. 13: Re-interpretation of the  $\delta^{18}\text{O}$  curve from core MD95 2026 on Sackville Spur and the correlation of AZ II to core 01-15; core lithology simplified.

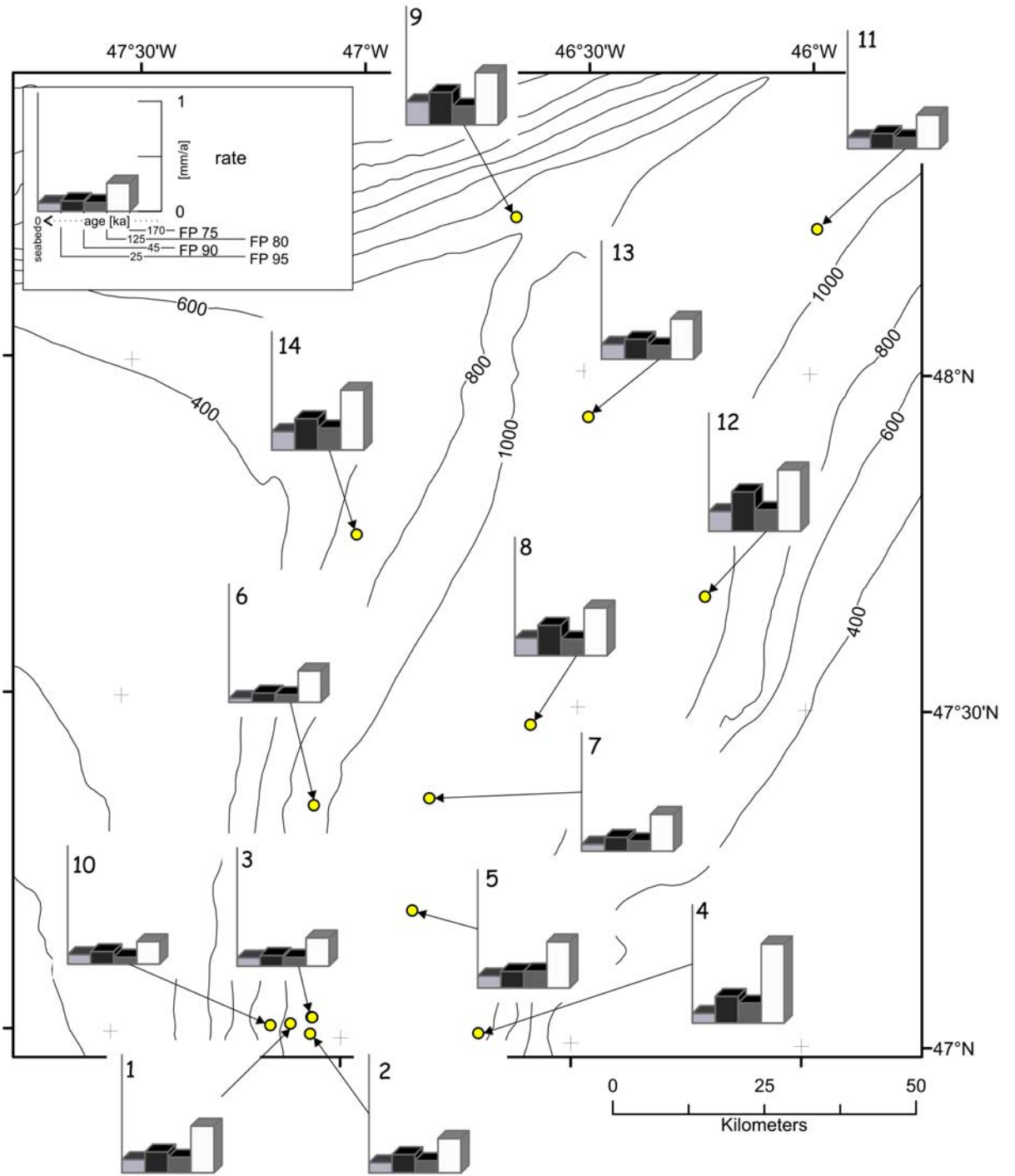


Figure 2. 14: Sedimentation rates excluding MTDs for intervals between key reflections.

## 2.5. Discussion

### 2.5.1 Glacial History of the Grand Banks Margin

The upper part of the eastern Grand Banks slope is characterized by seismically defined till tongues, which reach down to 650 m current water depths. This is a similar water depth to the pinch-out of till tongue reported elsewhere on the southeastern Canadian margin (Piper et al., 2002; Piper et al., 2005). Although the till tongues have not been directly sampled on the eastern Grand Banks, they pass upslope into a low relief moraine complex, the Sackville moraines (King et al., 2001). Elsewhere on the southeastern Canadian margin, till tongues exposed in slump scars comprise poorly sorted diamicton with petrography consistent with local ice supply (Piper and MacDonald, 2001) and show strong overcompaction with shear strengths up to 100 kPa (Piper and Brunt, 2006). They commonly terminate at slump scars. Only on low gradients seaward of major ice streams do till tongues pass seawards into glacial debris flows, such as in Orphan Basin (Tripsanas and Piper, submitted) and seaward of Hudson Strait (Rashid and Piper, 2007), where there is widespread evidence for associated hyperpycnal discharge of melt water. The till tongues on the margin of the eastern Grand Banks resemble those off other shallow banks and appear to represent the grounding limit of relatively dry ice (Piper and Brunt, 2006).

The prominent till tongues all pinch out in the interval between FP 75 and FP 80, corresponding to OIS 6. They imply that thick glacial ice completely crossed the Grand Banks at one or more times (cf. Fig. 2.6) during OIS 6. The

global isotopic record indicates that OIS 6 had greater ice extent than younger glaciations and the paleo-environmental conditions in the Labrador Sea were particularly cold in OIS 6 (Aksu et al., 1992). It seems likely that the morphologically distinct Sackville moraines (King et al., 2001) formed during this last major ice advance.

A possible younger till tongue was recognized on Sackville Spur (cf. Fig. 2.6b) just below FP 90 and therefore likely dating from OIS 4. The identification of the till tongue remains tentative, as it is not recognized farther south on the eastern Grand Banks margin. The till tongue may provide evidence for shelf crossing ice during OIS 4 but it is much thinner than that from OIS 6 suggesting a much shorter glaciation, consistent with oceanic paleo-environmental data. An OIS 4 shelf-crossing glaciation is recognized off Nova Scotia (Stea et al., 1998; Piper et al., 2002).

During OIS 2 no evidence for tills is found on the eastern Grand Banks slope, indicating that during OIS 2 the Newfoundland ice sheet did not reach this area. Rather, it most likely terminated in the DBMC area 200 km from the shelf break (King et al., 2001) with proglacial sands deposited in the Hibernia area (Fader and King, 1981).

### **2.5.2 Character and Distribution of MTDs**

Three different MTD types were described from Flemish Pass (Figs 2.15, 2.16); only Type A<sub>FP</sub> was sufficiently shallow in the sequence to be sampled by piston cores. This facies shows mud clast conglomerates and sub-horizontal

lithological contacts. Recent studies have classified different MTDs on the basis of lithology and sedimentary structures on the eastern Canadian continental margin (Mosher et al., 2004). Type A<sub>FP</sub> corresponds to Facies IIIb from Tripsanas et al. (2007 in press), which was created by failure and breakup of sediment clasts (Fig. 2.15).

Facies type B<sub>FP</sub> is a very thick MTD with a comparably long runout distance. Locally, basal erosion is observable, but generally it follows the local topography. This MTD facies type was only found during very low relative sea level in OIS 6 and possibly OIS 4 in Flemish Pass. MTDs with a similar seismic character have been described from the southeastern Canadian continental margin (Piper, 2005; Tripsanas and Piper, submitted) and other glaciated margins (e. g. Stein and Syvitski, 1997; Baltzer et al., 1998; Taylor et al., 2000). These deposits have been interpreted as glacigenic debris flows (King et al., 1998) when watery till fails off a paleo-ice stream, or as sandy debris flows when glacigenic sediment accumulated along the shelf break failed. Both possibilities may explain the temporal and spatial distribution of this facies in Flemish Pass; an ultimate answer will require sampling these flows.

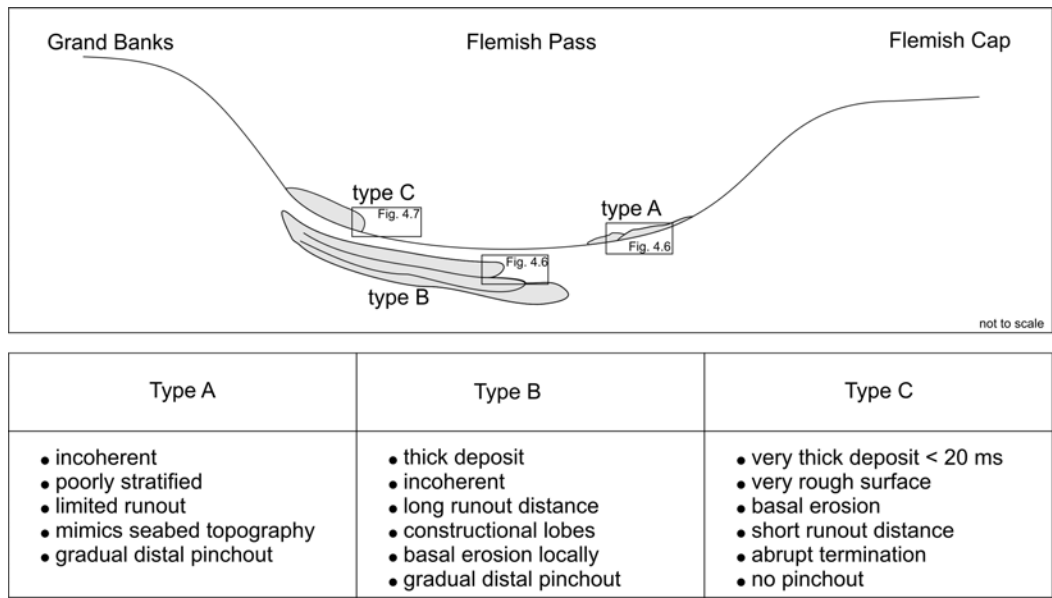


Figure 2. 15: Summary of key features of the three MTD types described from Flemish Pass.

MTD failures

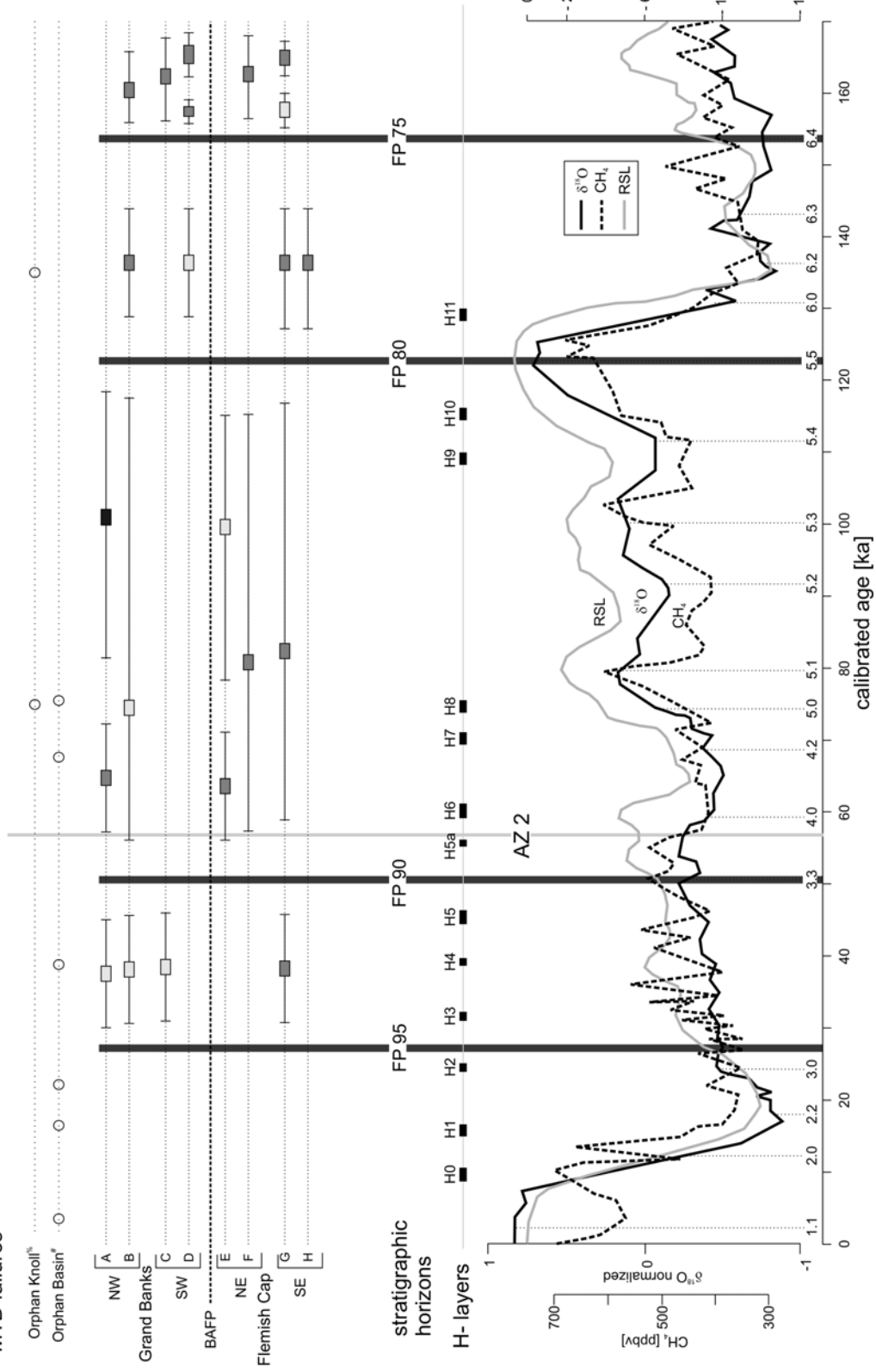




Figure 2. 16: Summary figure showing the timing of failure events (locations from Fig 2.8) of the different MTDs in Flemish Pass over time and their relationship to other slopes along the eastern Canadian continental margin (Piper and Gould, 2004; Tripsanas and Piper, 2007; Tripsanas et al., 2007 (in press)) in the context of Heinrich events, the global sea level curve (Waelbroeck et al., 2002), the marine oxygen isotope curve (Walker, 2005) and the global atmospheric CH<sub>4</sub> concentration from Antarctica ice cores (Spahni et al., 2005).

Facies type C<sub>FP</sub> is a very thick deposit with a rough surface. This type of MTD has been described from other parts on the eastern Canadian margin (Jenner et al., 2007) and was imaged with SEAMarc 1 and GLORIA in Flemish Pass (Pereira et al., 1985; Jacobs, 1988), where the typical hyperbolic structures (Figure 2.11b) were interpreted as actively rising diapiric features which modify the local seabed topography (Piper and Sparkes, 1986; Piper and Pereira, 1992). The available core data and new seismic data from this area suggest that this interpretation must be reconsidered: such refraction patterns have been found on other flow deposits (Prior et al., 1984; Armishaw et al., 1998) and result from the rough surface of these flows. Core control from a MTD similar in seismic appearance on the Scotian margin shows large sediment blocks on different angles, and geotechnical data indicates several tens of meters of burial compaction (Shor and Piper, 1989). This indicates that these blocky MTDs result from failure of material which is more consolidated than the type A<sub>FP</sub>, which will not disintegrate during transport.

Most of the MTDs along the Grand Banks margin appear to have been confined to channels before creating lobes along the basin floor. This observation differs strongly from the flows from the Flemish Cap slope, other parts of the eastern Canadian margin (Gauley, 2001; Mosher et al., 2004) and other continental margins (Cronin et al., 1998; Canals et al., 2000), where the flows resulting in MTDs are usually unconfined and follow the local gradient independent from the local topography; the channels are usually considered to have been formed by turbidity current activity (Cronin et al., 1998). These

unconfined flows are either retrogressive (Jenner et al., 2007), and related to salt tectonics (Mosher et al., 2004) or have developed from widespread failures along decollement horizons (Bryn et al., 2005a).

Several hypotheses may account for the observation of channelized flows on the Grand Banks slope in Flemish Pass: (1) MTDs may have been initiated only in canyon heads: this observation is supported by the lack of lower slope scarps and failure planes, at which retrogressive failures may have been initiated. Continuous till tongues to 650 m water depths and a maximum water depth of 1100 m does not allow for much scope for retrogressive failures. (2) The MTDs involved low viscosity flows, either with a high sandy component to them, which may have similarities to high density turbidity currents (Shanmugam, 1996), or similar to glacial debris flows. Such flows could be confined to channels and even create overbank deposits when overspilling the channel (Fig. 2.4). (3) The flows were originally widespread, but in areas with no channels present these deposits have been eroded by younger processes. No evidence for such erosion is seen in seismic reflection profiles.

### **2.5.3 Initiating Processes**

Initiating processes of several MTDs in Flemish Pass can be inferred based on their spatial distribution and stratigraphic position in the sedimentary record. The stratigraphic framework in Flemish Pass allows accuracy within  $\pm 5$  ka (Fig. 2.16). Therefore, minor changes in sea level and the methane record can not be considered in the interpretation, whereas long-term (more than 5 ka)

climatic changes can be used to infer possible mechanisms for sediment failure in Flemish Pass. Other failures less strongly related to climatic control may also have caused slope failures along the margin.

#### 2.5.3.1 Earthquakes

Earthquakes during glacial stages have been interpreted as frequent on the eastern Canadian margin (Mosher et al., 1994; Piper and Gould, 2004) and some are related to seismicity from glacial rebound with a reoccurrence interval of a few thousand to thousands of years (Piper, 2005). The earthquake record in the area has been instrumentally recorded for the last 150 years and was reconstructed based on failure frequency back to OIS 3 (Tripsanas and Piper, 2007). At this time no failures occurred in central Flemish Pass (Fig. 2.16), but the older failures in Flemish Pass during OIS 4 and especially OIS 6 may also be linked to earthquake activity along the margin.

#### 2.5.3.2 Sea Level and Gas hydrates

The question of timing of sediment failure during sea level change remains unanswered and studies have related failure to falling sea level (Summerhayes et al., 1979), rising sea level (Trincardi et al., 2003) and during glacial low stands (Maslin et al., 2004). A possible cause of failures during glacial time is the dissociation of gas hydrates (Nisbet, 1990) by increasing temperature or decreasing pressure or both. Dissociation of gas hydrates may initiate failures

(Kennett et al., 2003). Currently, the water temperature in Flemish Pass is 4°C (Colbourne and Foote, 2000) and has therefore not changed greatly since the glacial ocean circulation. Falling sea level will lead to reduction in pressure (P) and thus has potential to cause rapid release of gas hydrates. This could be an explanation for some of the failures identified in Fig. 2.16.

#### 2.5.3.3 Heinrich Events

It has been suggested that scouring by large icebergs during Heinrich events may have created failure by overloading and slumping (Clark and Landva, 1988; Piper and Hundert, 2002). None of the H-events appear to correspond to dated sediment failure in Flemish Pass.

#### 2.5.3.4 Melt Water Influx

Dense melt water from glacial runoff creates highly sediment-laden plumes, which transport poorly sorted sediment onto the slope (Lønne, 1997; Mulder et al., 2003), where it destabilizes the sea bed by overloading large areas along the slope break or by undercutting of canyon heads by hyperpycnal flows (Mosher et al., 2004; Piper and Gould, 2004).

The sedimentary record from Orphan Basin (Tripsanas and Piper, 2008, in revision) indicates the presence of meltwater in OIS 2 in the outer shelf area (King et al., 2007). Similar ice-margin discharge during OIS 4 and especially OIS 6 may have been an important agent for initiating MTDs. Evidence for such melt-

water discharge is seen in erosional channels and levee growth above FP 75 on the Grand Banks margin (Fig. 2.4)

#### 2.5.3.5 Relationship of Glaciation to MTDs

The MTDs in Flemish Pass correlate within the resolution of dating to stadial climatic stages. The last major shelf crossing glaciation occurred during OIS 6, with perhaps a minor shorter advance during OIS 4, but ice did not reach the study area in OIS 2. This glacial extent differs strongly from other parts of the eastern Canadian margin where the OIS 2 ice sheet terminated at the upper slope (King and Fader, 1986; Stea et al., 1998). This last glacial advance overprinted most of the previous ice sheet configurations and the ice sheet configuration during OIS 4 remains mostly unclear.

Therefore, the different distribution of the MTDs in Flemish Pass compared to other slope areas along the margin (Piper, 2005; Jenner et al., 2007; Tripsanas et al., 2007 (in press)) may be related to the difference in glacial history and therefore the different ice sheet configurations in the areas.

This is supported by comparison of sedimentation rates from Flemish Pass to the Scotian Shelf (Piper and Sparkes, 1987; Piper and MacDonald, 2001) and the Labrador slope (Stoner et al., 1998), which are an order of magnitude larger than the values from Flemish Pass. The lower rates may indicate more stable sediments along the slopes in Flemish Pass. Additionally, fewer glacially related earthquakes, triggered by ice sheet loading and unloading of sediments (Husebye and Mäntyniemi, 2005), may have occurred along the

northeastern Grand Banks slope due to fewer shelf-crossing glaciations influencing the area.

The frequency of sediment failures during OIS 6 is similar to failures in other areas along the eastern Canadian continental margin (Piper, 2005) suggesting that similar agents were the cause of these failures along the margin: most likely the presence of shelf-crossing ice. It is difficult to link specific failures to failing mechanisms as the resulting MTDs show few failure-typical structures. The higher sedimentation rates in Flemish Pass during OIS 6 may be due to plumes along the margin, which would explain a similar increase of sedimentation rates throughout the basin. Additionally, the stratigraphy allows a resolution of 5 ka on the MTDs. This resolution does not allow a distinction of MTDs initiated during ice sheet build-up and ice sheet recession during different stadial/interstadial cycles within a glaciation.

MTD facies B<sub>FP</sub> shows the strongest relationship to sea level low stands and is interpreted as glacigenic debris flows. These flows may have only been initiated during glaciations when sufficient under-consolidated muddy debris was transported to the outer shelf by the calving ice sheet for failure.

## 2.6 Conclusion

A new Late Quaternary high resolution seismic stratigraphy, tuned by different dating methods, was established for Flemish Pass on the eastern Grand Banks margin. The sedimentary sequence in the basin is dominated by

hemipelagic muds, which are interlayered with thick MTDs that cover large areas of central and northern Flemish Pass along the eastern Grand Banks slope.

Three different MTD types have been mapped from seismic and core data in Flemish Pass. The MTDs were deposited in glacial settings with different ice sheet configurations on the Grand Banks. The changing ice sheet configurations had a strong impact on the sedimentation rates in Flemish Pass. During OIS 6 the Grand Banks Ice Sheet terminated along the margin and supplied sediment, resulting in relatively high sedimentation rates in the basin. Since then, the sedimentation rates decreased significantly due to less extensive ice sheet extent and therefore less sediment supply to the outer margin.



# **Chapter 3. TEMPORAL DISTRIBUTION OF LATE QUATERNARY TURBIDITES AND CONTOURITES IN FLEMISH PASS: A GLACIALLY INFLUENCED PERCHED SLOPE BASIN OFF SOUTHEAST CANADA**

## **3.0 Abstract**

Flemish Pass is a small, perched, 1100 m deep basin along the southeast Canadian continental margin was created during initial rifting of the North Atlantic in the Mesozoic. Late Quaternary sediments include thin sand layers interbedded with hemipelagic muds. The distribution, age, grain size, sedimentary structures and petrology of these sands were used to distinguish between turbidite and contourite deposits and to understand the conditions leading to deposition of each type.

Sand packets comprised of several stacked sand beds, some with erosive contacts, are correlated across Kyle Lobe into the basin, where they show clear distal fining and create a poorly developed morphological lobe.

Six sediment facies were identified. Each facies shows a distinctive grain size distribution. They are: I contourites, II possible jökulhlaup deposits, III winnowed sequences, IV sandy turbidites, V muddy turbidites and VI hemipelagic sediment. The temporal distribution of the sand beds shows a strong correlation of turbidites to stadial climatic stages, whereas contourites are restricted to

interstadial times. This linkage may be related to variation in oceanographic circulation in Flemish Pass.

### 3.1 Introduction

Turbidity currents are important agents for transporting sands of a wide grain size range into the deep water. Sediments deposited by turbidity currents may be subject to bottom current reworking forming contourite deposits or winnowed sequences. Thin-bedded sandy beds were studied in central Flemish Pass, a small perched slope basin along the eastern Canadian continental margin (Fig. 3.1). Due to its bathymetric setting, the sandy beds are trapped at ~1100 m water depth and can therefore be sampled more easily by piston cores than if these beds were deposited in the abyssal plains to the north and south of Flemish Pass.

Sand beds from Flemish Pass were studied within cores and correlated between cores. The sedimentological and petrographic character and the distribution of the different sand beds in time and space were used to distinguish between turbidite and contourite deposits. Their age and distribution was used to understand processes leading to the formation of each sediment type.

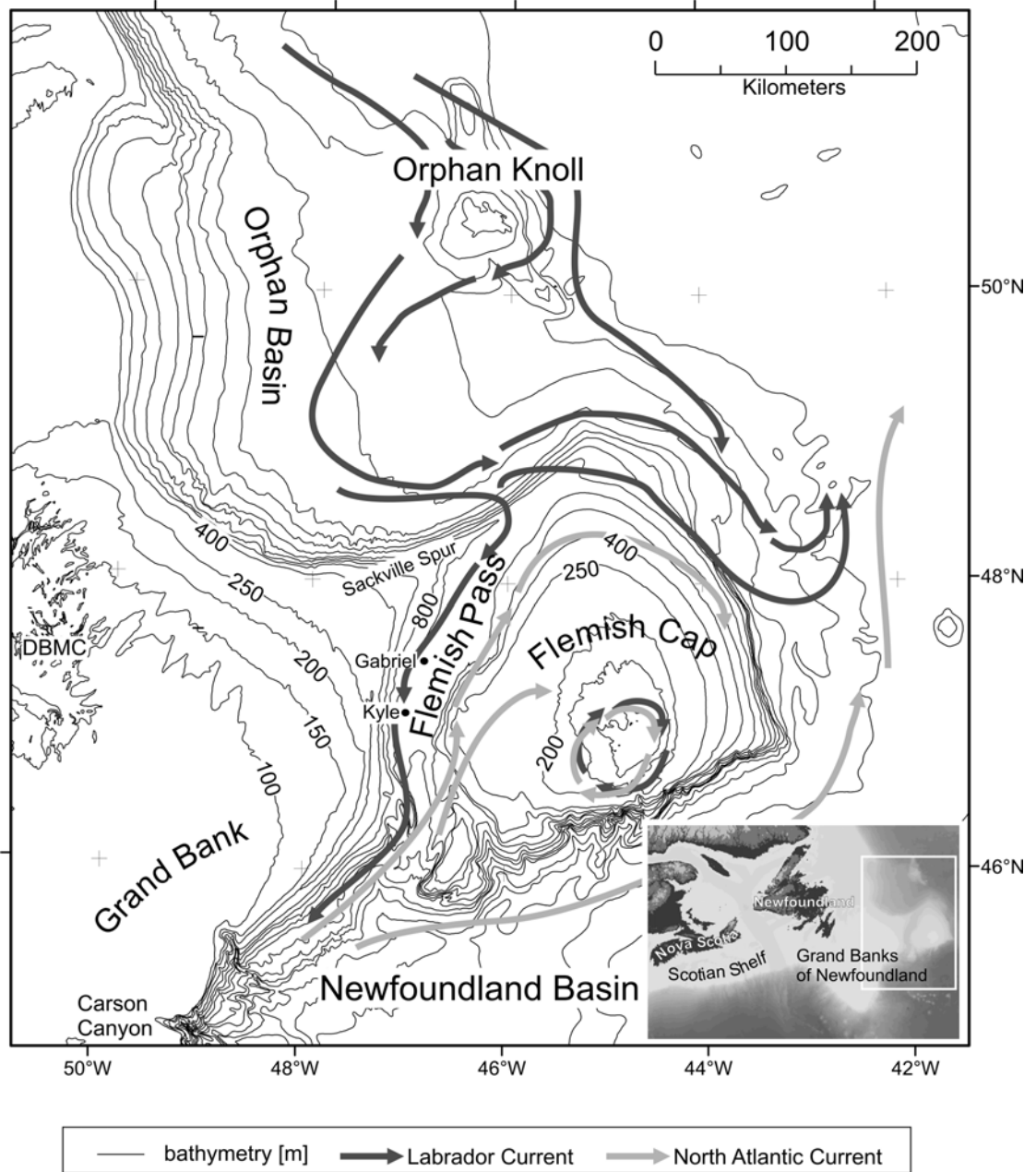


Figure 3.1: Location map of Flemish Pass, black circles are exploration wells, DBMC = Downing Basin Moraine Complex, the arrows indicate the oceanic circulation in the Flemish Cap area: gray arrows indicate the warm northwards flowing North Atlantic current and black arrows show the cold southwards flowing Labrador Current (after Colbourne and Foote, 2000).

## 3.2 Regional Setting

### 3.2.1 Physiography

The southeastern Canadian continental margin includes three small basins seaward of the Grand Banks: Flemish Pass to the east, Orphan Basin to the northeast and the Newfoundland Basin to the southeast (Fig. 3.1). This margin was created during initial rifting of the North Atlantic in Cretaceous times and Flemish Pass is considered to be a failed rift (Grant, 1972; Foster and Robinson, 1993).

Flemish Pass is 1100 m deep and 50 km wide in its central part near the Kyle well. Northwards and southwards the basin opens up significantly: in the north off Sackville Spur the basin is 80 km wide and in the south the basin reaches widths of more than 100 km before it drops off steeply into the Newfoundland Basin (Fig. 3.1). The depth of the shelf break on the Grand Banks deepens northwards, from 200 m near the Kyle well to 450 m along Sackville Spur (Fig. 3.2). This trend is due to differential subsidence (King and Sonnichsen, 1999). Flemish Cap is a basement high east of Flemish Pass with a poorly defined slope break at about 350 m bounding a 150 by 200 km plateau which is 139 m deep at its shallowest point (Monahan and Macnab, 1974; King et al., 1985).

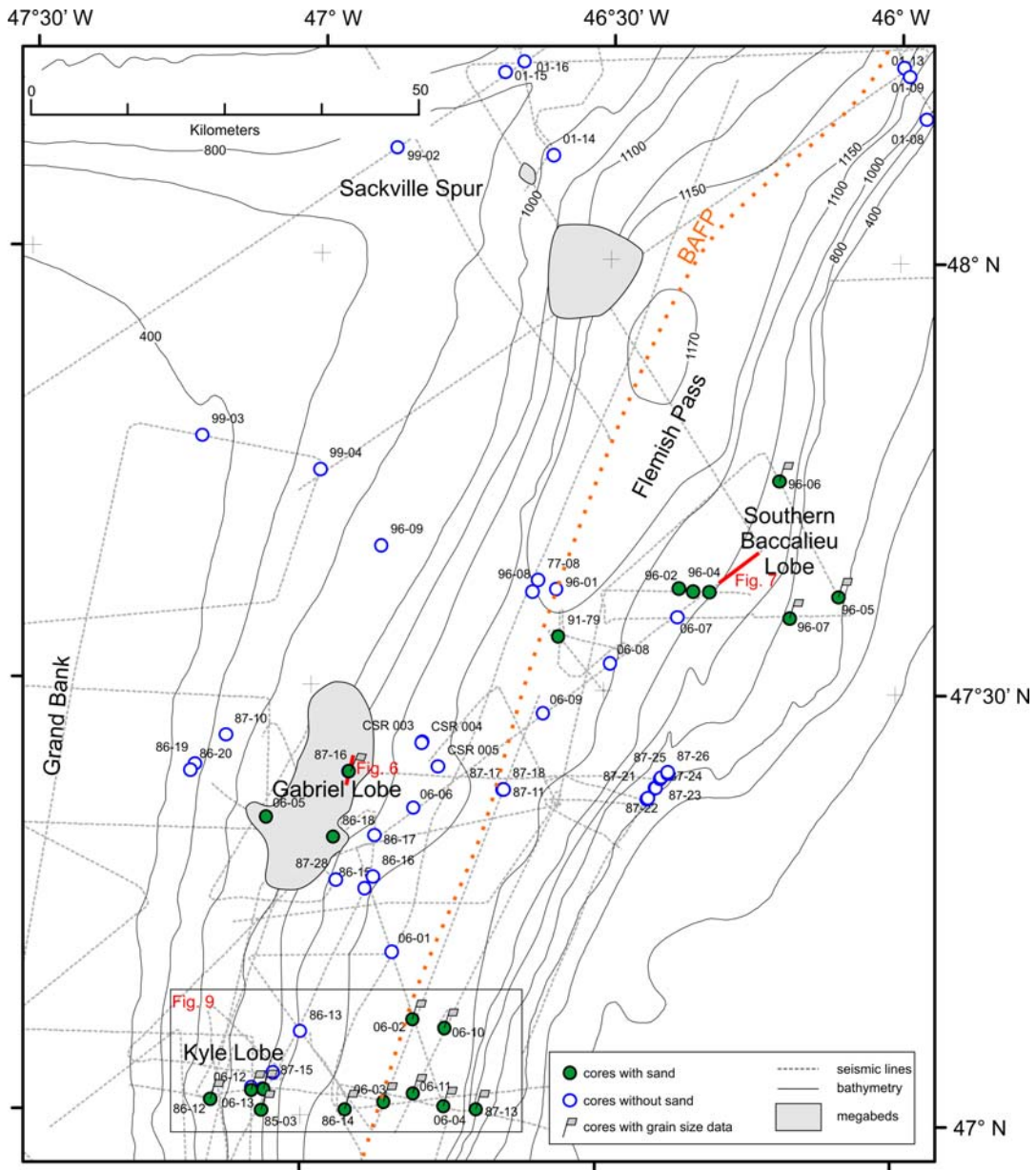


Figure 3.2: Map of central Flemish Pass showing the core control used for the sand beds, the position of the Figures. BAFP: bathymetric axis Flemish Pass, the bathymetry from Monahan and Macnab (1974).

### 3.2.2 Geology of Flemish Pass

Flemish Pass has been gradually infilled from the Grand Banks slope with fluvial-deltaic sequences prograding eastwards. This progradation was initiated in the Mesozoic and has been controlled by variations in sea level and basinward sediment flux (Piper and Normark, 1989; Foster and Robinson, 1993). Sea level variations have created several unconformities in the deeper sequence in Flemish Pass, e. g. during the Miocene and Pliocene (Kennard et al., 1990). Glacial ice crossed the Grand Banks at times in the Quaternary. During oxygen isotope stage (OIS) 2, ice covered only parts of the Grand Banks and likely terminated near Downing Basin on the inner shelf (King et al., 2001). Some of the thick sand deposits in the Hibernia area have been interpreted as proglacial deposits (Fader and King, 1981).

The shallow Quaternary sedimentary sequence in Flemish Pass is dominated by hemipelagic and turbidite muds with few sedimentary structures (Piper and Pereira, 1992). Predominantly silty muds were deposited from mass transport deposits (MTDs) and cover large areas in central Flemish Pass, and originated from both slopes of the basin (see Chapter 4 for more details).

Some sandy beds on a decimeter to meter scale are interbedded with the muds and have been interpreted as turbidites transported across the Grand Banks slope (Piper and Pereira, 1992). No turbidites have been reported from the Flemish Cap slope. Several thick-bedded sandy beds along this slope have been interpreted as contourite deposits formed by currents flowing along the western slope of Flemish Cap (Piper and Campbell, 2005).

Sidescan data show several channels and scarps on the Grand Banks slope. On the upper slope, iceberg scouring was observed to a water depth of 650 m (Piper and Pereira, 1992). Seismic data indicate activity over several glacial-interglacial cycles within channels (Piper and Normark, 1989), which have been conduits for MTDs (see Chapter 4 for more details).

Sediment waves have been imaged using high resolution and airgun seismic in the eastern part of Flemish Pass. These waves have been related to contourite processes in the area (Piper and Campbell, 2005).

### **3.2.3 Oceanographic Setting**

The Holocene oceanographic setting in Flemish Pass is dominated by two oceanic current systems (Fig. 3.1) which flow through the basin in opposite directions: the cold southwards flowing Labrador Current and the warm northward flowing North Atlantic Current (Stein, 1996). The Labrador Current, centered at 1000 m, originates in the northern Labrador Sea adjacent to Greenland, and has average annual flow speeds of  $20 \text{ cm s}^{-1}$  (Cuny et al., 2002).

South of Orphan Knoll and north of Flemish Pass, the Labrador Current branches into a near-shore current and an offshore branch. The near-shore branch follows the Grand Banks slope through Flemish Pass; the outer branch circles around Flemish Cap forming a gyre system with mean velocities of  $3.5 \text{ ms}^{-1}$ , which is centered on Flemish Cap. This gyre system forces the northward flowing North Atlantic current to branch south of Flemish Cap and thereby form a near-shore branch flowing through the eastern side of Flemish Pass and an outer

branch circling Flemish Cap on the Atlantic-facing slope (Colbourne and Foote, 2000). This oceanographic setting creates two currents flowing in opposite direction through Flemish Pass (Fig. 3.1).

### **3.2.4 Late Quaternary Stratigraphic Framework for Flemish Pass**

The stratigraphic framework for the Late Quaternary sedimentary sequence of Flemish Pass was established using seismic stratigraphy linked to an oxygen isotope record on Sackville Spur, radiocarbon dating on foraminifera and shells, and Heinrich layer stratigraphy. The Heinrich layers, rich in carbonate, were correlated using CIELab L\* and a\* values and total carbonate plots. Details of the stratigraphic control are presented in Chapter 4, and are summarized in Figure 3.3.

The glacial-interglacial environmental changes affecting Flemish Pass include both sea level changes and probable changes in the current system. Stadial-interstadial changes have only a small impact on sea level (Lambeck and Chappell, 2001) and their impact on currents is unknown. Heinrich events, which supply large amounts of ice rafted debris (IRD) and plume sediment transported from the north by the Labrador Current, occur at the end of stadials (Hemming, 2004).



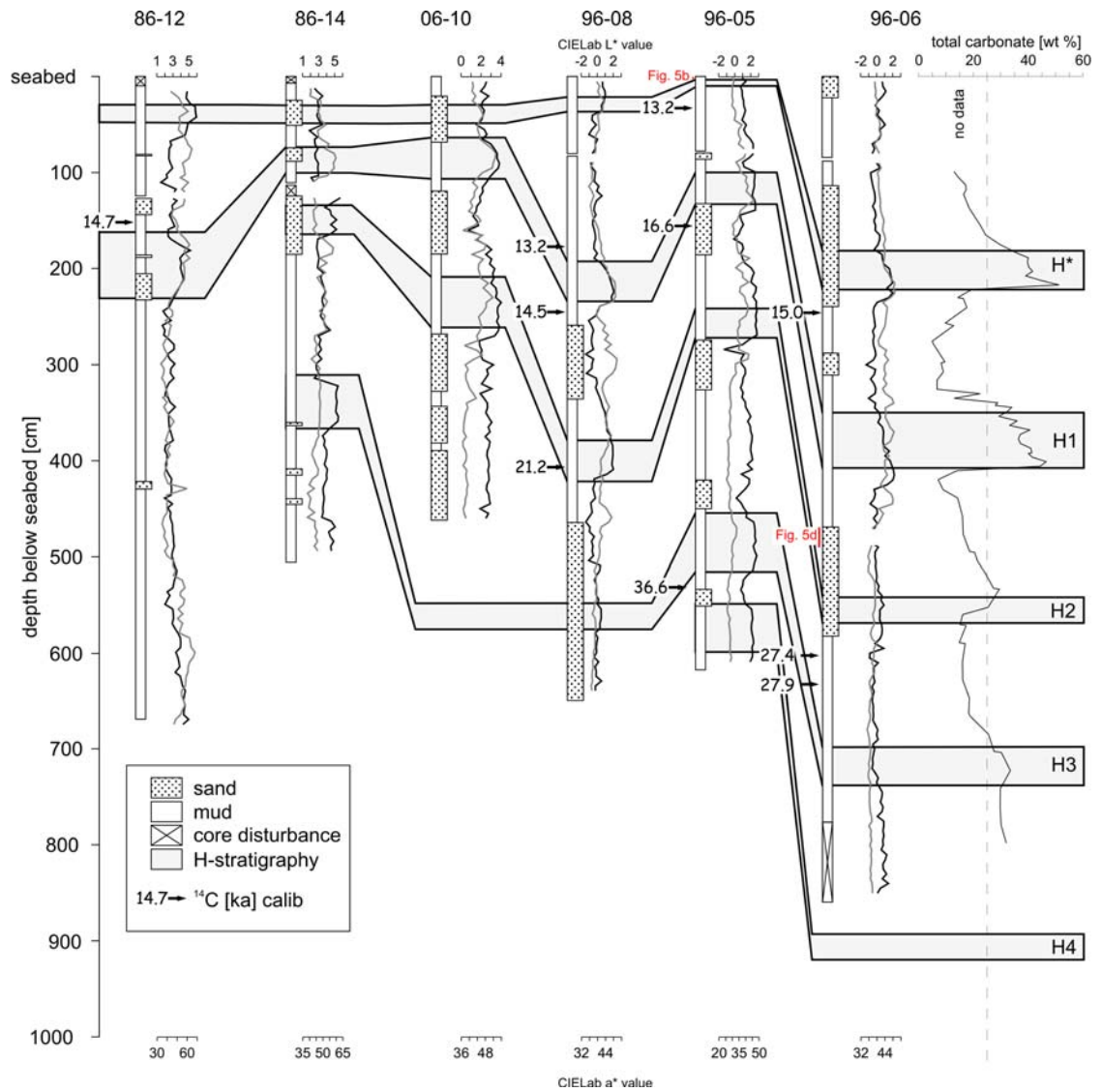


Figure 3.3: Correlation of key cores in Flemish Pass based on Heinrich Events, radiocarbon dates, spectrophotometer data and total carbonate plots from core 96-06: the black plot is the L\* value, the gray is the a\* value.

### **3.2.5 Distinction of Turbidites from Contourites**

Several study groups have proposed different seismic and sedimentary characteristics for distinguishing turbidite and contourite. Seismic characteristics of contourite drifts include semi-transparent intervals with migrating waves on scales dependent on current strength. Cyclicity between more transparent and more continuous facies may be evident (Stow et al., 2002; Bryn et al., 2005b). Additionally, the trend direction of sediment wave crests on seismic data can also indicate the depositional mode: crests trending perpendicular to the slope commonly indicate turbidity current processes, whereas slope parallel crests were more likely formed by contourite drifts. Levees also characterize turbidite channels along the slopes where the turbidity currents overspill (Rasmussen et al., 2003).

Sedimentological characteristics are further important indicators for distinguishing between turbidite and contourite deposits. Contourites are generally very well sorted and may have a coarser lag throughout the bed; few primary sedimentary structures such as cross bedding are preserved in the sands (Lovell and Stow, 1981). The overall sequence may have a negatively (inverse) and positively (normal) graded sequence (Gonthier et al., 1984) with no regular sequence of sedimentary structures (Stow and Piper, 1984). Petrographic studies may further help to distinguish between contourites and turbidites, as heavy minerals can be used to infer the source areas of the sands (Lovell and Stow, 1981).

Turbidites are characterized by a variable grain size distribution, in some cases with basal inverse graded beds. The sequence is characterized by normal graded beds within a regular sequence of sedimentary structures (Bouma, 1962; Stow and Piper, 1984). The overall sequence shows downslope fining and deposits large scale sand sheets or turbidite lobes in the basin (Walker, 1976; Galloway, 1998). The more distal areas are characterized by muddy turbidites (Piper, 1978) which reflect a similar fining sequence as their sandy counterparts (Stow and Piper, 1984).

### 3.3 Materials and Methods

Piston cores, either 6 or 12 cm in diameter, were collected throughout Flemish Pass, split and described. Digital spectrophotometer data (CIELab color) were collected on all cores. In specific cores, samples were taken for carbonate, grain size and petrography analysis. Sandy beds on a cm to m scale were correlated throughout the basin based on the existing high resolution stratigraphy from Flemish Pass (see Chapter 4). Grain size analysis, typically at 2 cm spacing, was used to characterize sand beds in 11 piston cores using the Beckmann Laser Coulter LS 230 with the Fraunhofer module. In coarser beds (including grains >2mm in diameter) the gravel, sand and mud fractions were separated by hand sieving, and the sand and mud fractions were analyzed separately using the Laser Coulter system. Muds interbedded with the sand beds were also sampled.

All the grain size analyses were plotted as a series of frequency curves downcore. Golden Software Surfer software was also used for visualization. 'Grain size maps' from the different beds in the different cores were created displaying the grain size variation downcore. The data were gridded in Surfer using triangulation. The bin size of 0.04  $\mu\text{m}$  on the Laser Coulter was plotted on the x-axis, the sample spacing was plotted on the y-axis and the percentage of grain size in each grain size class was plotted on the z-axis.

High resolution seismic Hunttec sparker and boomer profiles collected over the last two decades in Flemish Pass were used to image the upper few hundred meters below the sea bed. The boomer system images features up to 50 m deep in the sequence on a 1 m vertical resolution. The sparker profile allows, due to its higher energy output, penetration up to 120 m (Mosher and Simpkin, 1999).

## 3.4 Results

### 3.4.1 Core Correlation

CIELab  $L^*$  and  $a^*$  color values were used to correlate different Heinrich (H-) layers, which are characterized in the Labrador Sea by a positive peak in both the  $L^*$  and  $a^*$  plots (Andrews and Barber, 2002; Rashid et al., 2003b; Tripsanas and Piper, 2008, in revision). These H-layers are also high in detrital carbonate which could be used to correlate total carbonate curves in Flemish Pass (Fig. 3.3). Correlations were constrained by radiocarbon dates reported in Chapter 4

from Flemish Pass. These datasets were used to define a basin-wide Heinrich layer stratigraphy for Flemish Pass back to H3 (~30 ka).

The position of H1 at ~0.5 m below seabed commonly allowed the correlation between the trigger weight core and the corresponding piston core. Not all cores could be correlated as up to 1 m of sediment may be missing at the top of some piston cores. In such cases an arbitrary gap of 5 cm is shown in the core plot figures.

### **3.4.2 Sandy Facies in Flemish Pass**

Most sand beds in Flemish Pass have low matrix content. Several beds contain shell fragments and mud intraclasts. Beds are generally 10 - 100 cm thick. Generally, no visible sedimentary structures were detected during core description, but a few beds show poorly developed cross bedding on a cm-scale (Fig. 3.4). Previously unpublished counts of sand grain petrology from several cores were used to further characterize the different sand beds in some of the cores (Table 3.1). Characteristic features of the grain size plots were used to define six distinctive facies (Fig. 3.5, Table 3.2) following the notation of Folk (1966) (Fig 3.6):

The uniform sorted sand facies (Facies F I, Fig. 3.5a) is characterized by very well sorted (within a 0.5 phi range), 5-30 cm thick sand beds with no mud. A small granule component throughout the bed is characteristic for this facies.

The uniform sorted silt facies (Facies II, Fig. 3.5c) is similar to the uniform sorted sand facies in being very well sorted, but is predominantly silty and locally clayey with a low percentage of sand (2% sand fraction).

The poorly sorted sand facies (Facies F III, Fig. 3.5a) is a well sorted sand-dominated facies in beds typically less than 5 cm thick. Locally it may contain silty sequences. The thinner bedding and less well sorted character was used to differentiate the facies from the uniform sorted sand facies (FI).

The graded sand facies (Facies F IV, Fig. 3.5a and e) consists of sands with a basal inversely graded set overlain by several normally graded sets. The mud content is less than 2%. This facies usually occurs as a series of stacked beds. Rarely, cross laminations and basal erosion are seen in these beds.

The graded silty mud facies (Facies F V, Fig. 3.5d) is a silty, poorly sorted facies with more than 80% mud. Individual beds are generally 2-5 cm in thickness.

The muddy facies (Facies F VI, Fig. 3.5a) is characterized by thick bedded units with less than 1 % sand and a silty component that varies between 1 and 4%. Locally ice rafted debris (IRD) can be found in this facies. Bed thickness is highly variable.

### **3.4.3 Sandy Units in High-Resolution Seismic Data**

High resolution seismic data could not image most of the sand beds in Flemish Pass, as their thickness was below seismic resolution. Therefore, they do not show a specific seismic character, but occur within well stratified

sequences. Two large bodies were sufficiently thick to be imaged on sparker profiles (Fig. 3.7). They cover several km<sup>2</sup> in the Gabriel Lobe area and the area off the slope to the east of Sackville Spur (Fig. 3.2). The acoustic character is transparent with a poorly stratified incoherent return and no internal reflections. The basal contact is locally erosive (Fig. 3.8).

Two cores sampled the body on Gabriel Lobe: 87-16 and 86-18. In core 87-16, 80 cm of uniform sorted silt of facies F II was recovered. There are no sedimentary structures visible in the cores. This was the only bed in which facies F II was found. The silt bed was deposited above the regional reflection FP 95, dated to about 25 ka (see Chapter 4) and Fig. 3.8.

Large scale sediment waves have been imaged by Hunttec data on the eastern floor of Flemish Pass in the Southern Baccaieu area and were also ground-truthed by grain size data from cores 96-03 through 96-07 (Fig. 3.5b and d), which consists of the uniform sorted sand (F I) and the poorly sorted sand facies (F III). These sediment waves are several hundreds of meters in length and have an amplitude of 2-5 m. Generally, these sediment waves overlie well stratified muddy hemipelagic sequences (muddy facies F VI and thin sand beds of the uniform sorted sand and the poorly sorted sand facies (F I/F III)) (core 96-05 on Figs. 3.5b and 3.9, seismic profile 15 km to the west of core 96-05 in Fig. 3.8).

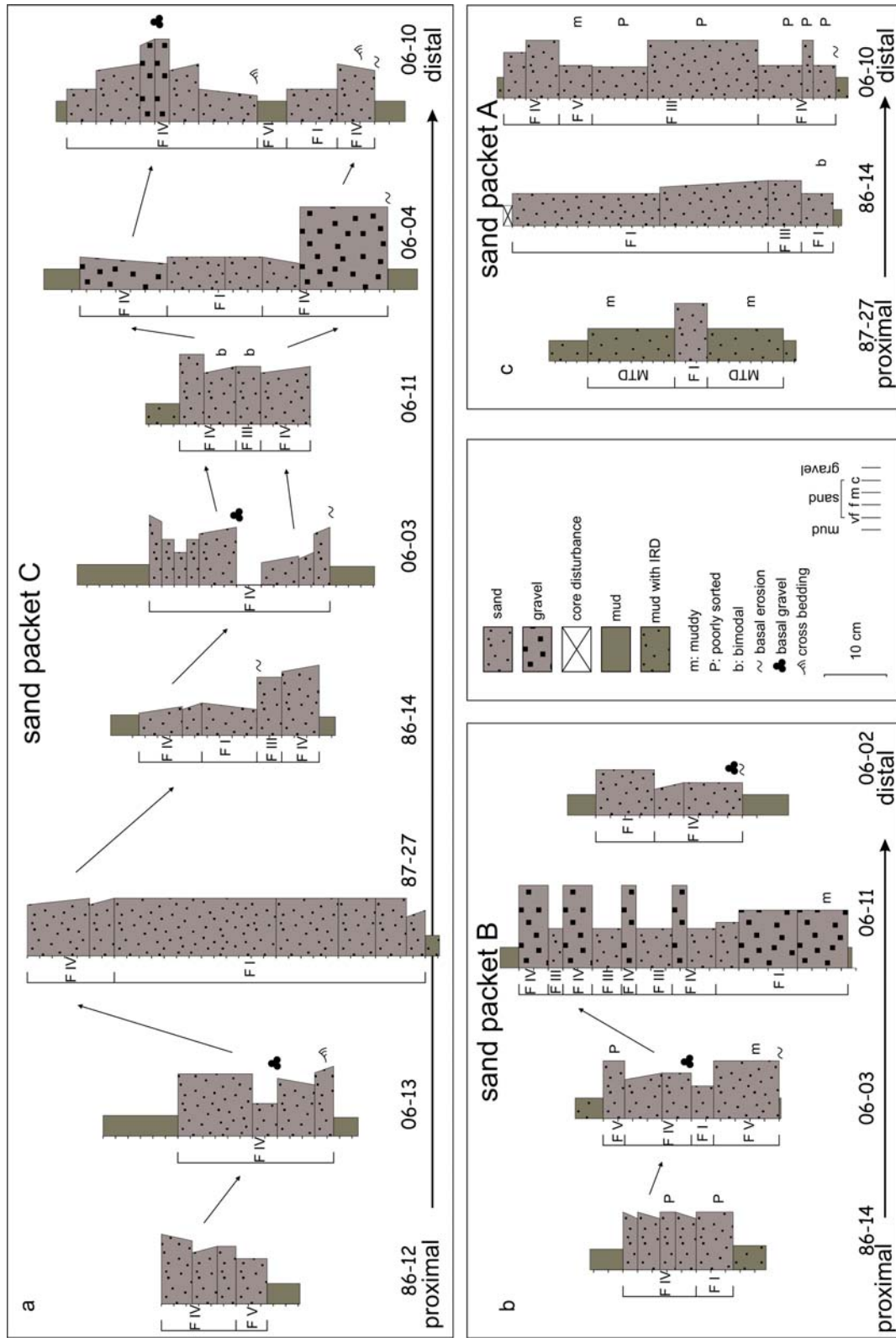


Figure 3.4: Sedimentological logs showing distribution of facies within sand packets from Kyle Lobe



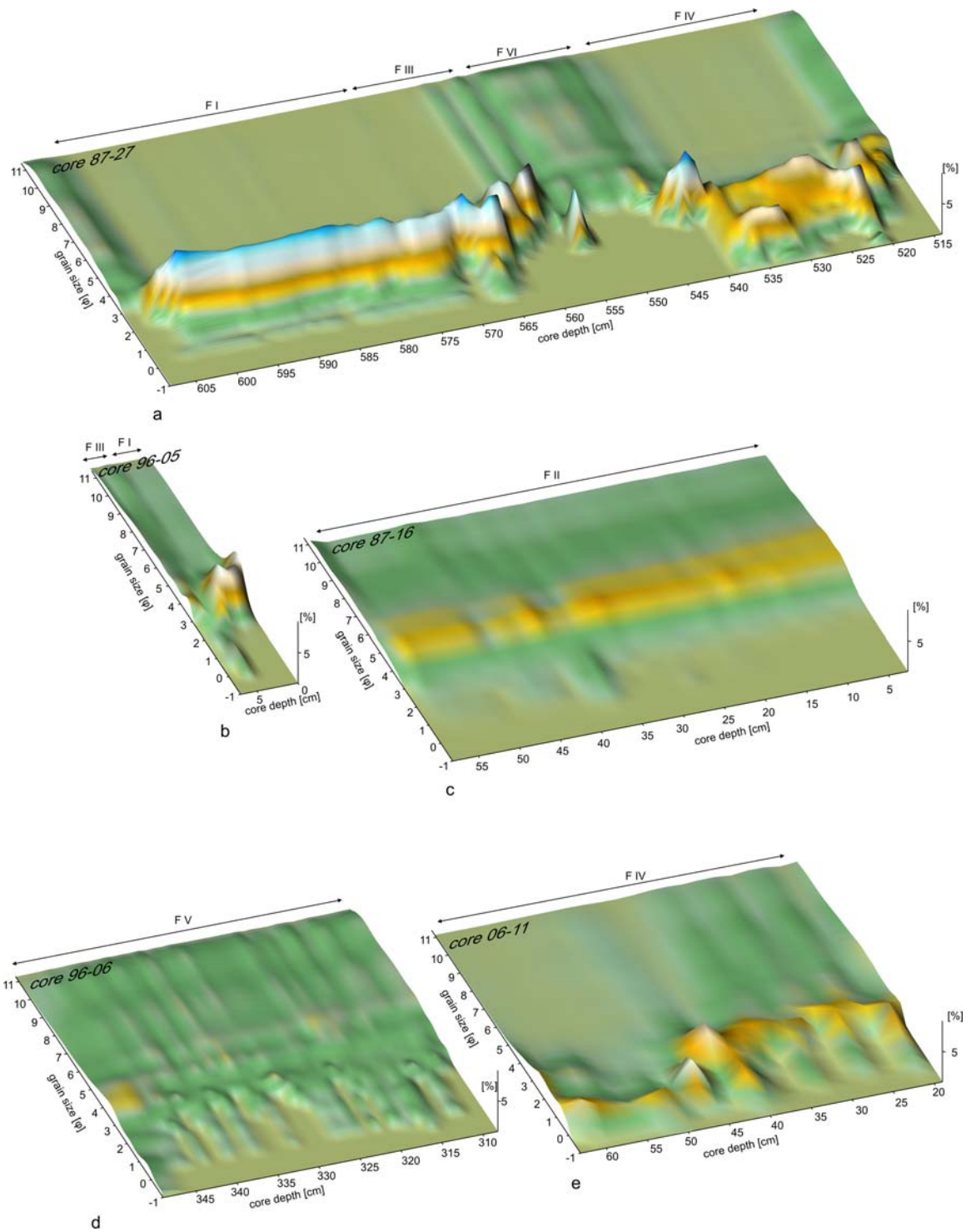


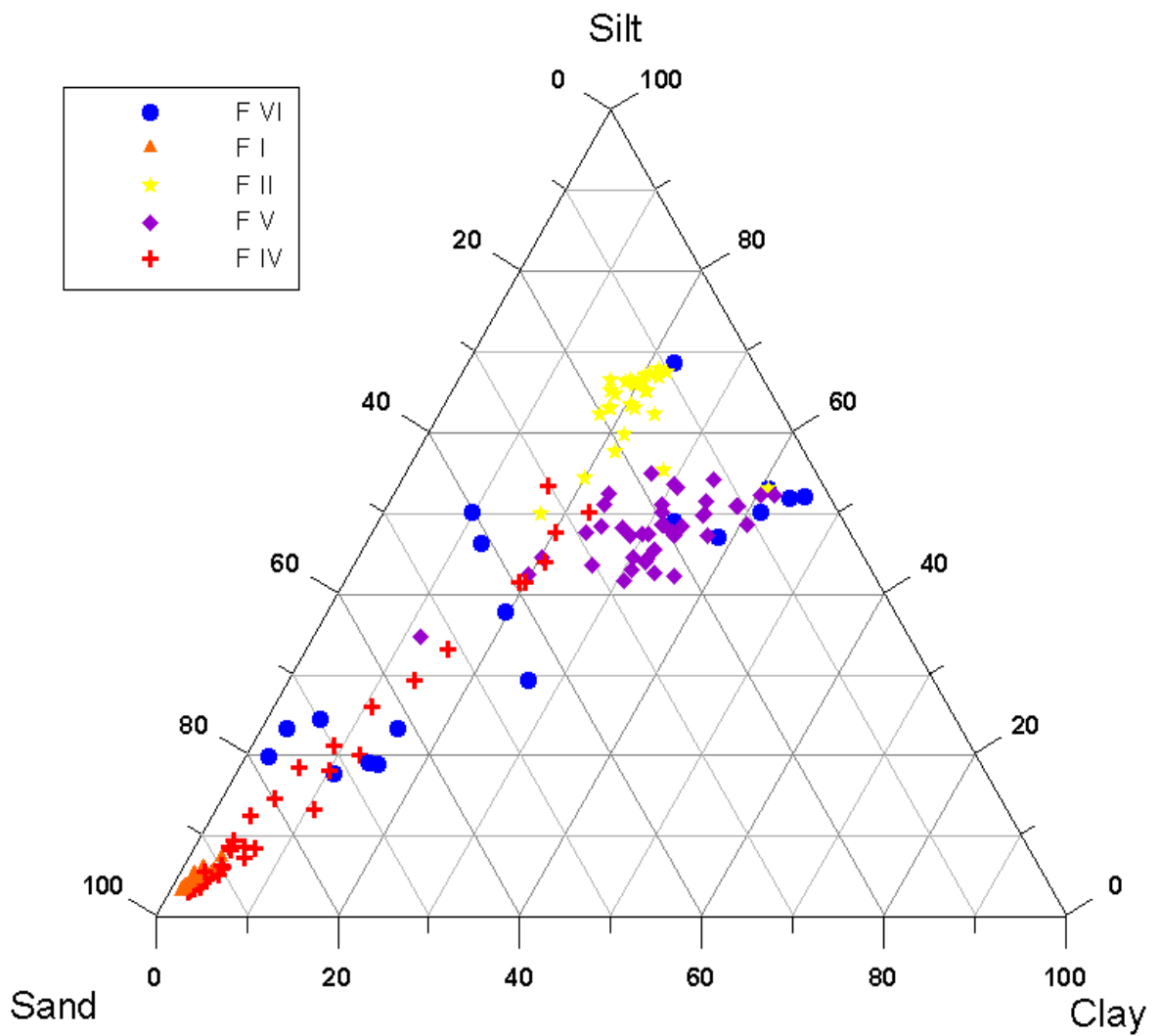
Figure 3.5: Plots of grain size with depths (“grain size maps”) from selected intervals of cores in Flemish Pass showing characteristics of different facies, grain size determined with the Beckmann Laser Coulter.

Cruise #	Core #	Water Depth (cm)	Depth (cm)	total grains counted	total non-biogenic, non-aggregate	percentage of total grains																	Interpretation of the petrology data		
						quartz	rounded quartz	feldspar	metamorphic rock fragments	carbonate rock fragments	siliclastic rock fragments	hornblende (amph)	dark basaltic glass + palagonite	light coloured heavy minerals	mica + chlorite	chert	pyrite covered quartz	pyrite cemented siliclastic rx.	dirty quartz	benthic foram.	planktonic foram.	siliceous spines		siliceous fossils (radio, diatoms)	other fossils
77014	008	2107	500	438	404	73.5	1	2.7	0.7	7.2	6.7	1.7	0.2	1.0	0.2	0.2	4.7	1.6	3.2	0.2	1.6	0	0	1.1	Turbidite
85044	003	1012	225	557	527	80.1	2.3	2.7	0.4	6.3	4.6	1.9	0.2	0.9	0	0	0.8	0.2	2.7	0.2	0.9	0	0	1.4	T. winnowed
85044	003	1012	350	414	404	60.5	4.9	3.7	0.7	15.3	7.4	5.2	1	0	0	0	1.2	1	1.2	0	0	0	0	0	T
91020	079	1143	40	542	526	64.6	1	3	0	11.4	13	1	0.2	1.3	0.4	0	3.8	3	3.1	0	0	0	0	0	no grain size data
91020	079	1143	166	495	475	80.2	1.3	3.6	1.1	6.7	4.2	1.3	0	0.6	0.2	0	0.8	1	1.8	0.2	1	0	0	0.2	no grain size data
96018	003	1088	80	424	403	71.5	2	2.5	0.7	9.9	6.2	2.2	1.2	1	0	0	2.7	0.7	2.8	0	0.7	0	0	0.7	T
96018	003	1088	450	439	428	73.4	2.3	2.6	0.5	8.4	5.6	1.4	0.9	2.1	0	0	2.8	0.5	1.6	0.2	0	0.2	0	0	T
96018	003	1088	500	435	403	70	3.5	1.7	0.5	12.9	6.2	2	0.2	0.7	0	0	2.2	1.8	0.9	0.2	0.2	2.1	0	2.1	C
96018	005	827	70	456	409	68.2	1	3.9	0.7	10.5	10.8	2.7	0.2	0.2	0	0	1.7	2.6	3.7	0.7	0.7	0	0	2.6	C
96018	006	1050	330	444	436	75.2	1.4	4.4	0.5	11.7	3.9	1.6	0	0.9	0	0	0.5	0.5	1.4	0	0	0	0	0	T?
96018	006	1050	490	443	414	72.2	1	4.1	1.4	12.1	3.6	2.2	0	0.7	0	0	2.7	2.7	2	0.2	0	0	0	1.6	T
96018	007	984	222	450	404	71	2.7	2.7	0.7	8.9	8.7	1.2	1.2	0	0	0	2.7	2.9	4.2	1.3	1.1	0	0	0.7	no grain size data
96018	007	984	330	508	434	66.6	1.4	2.5	0.9	16.8	7.6	2.1	1.2	0.2	0	0	0.7	1.2	5.3	2.8	0.8	1.2	0.6	2.8	C
96018	007	984	360	466	432	69.2	3.2	2.3	0.2	12.9	7.6	0.5	1	1	0	0	2.1	2.1	2.6	1.9	0.2	0	0	0.4	C
96018	007	984	380	465	438	66.9	1.8	2.5	0.7	11.2	7.9	1.8	1.4	0.7	0.5	0	4.6	0.2	1.9	1.9	0	0.4	0	1.3	C
96018	007	984	482	439	414	72	1.4	3.4	0.5	8.5	9.7	1.7	0	0.2	0.2	0	2.4	1.8	3.6	0.2	0	0	0	0	C
96018	008	933	160	490	444	64.4	4.5	3.2	0.9	9.9	12	1.6	0.5	1.4	0	0	2.3	1.2	3.5	1.6	1	0	0	2	C
96018	008	933	530	598	496	69	1.2	4.4	0.6	10.3	11	0.4	0.2	0.4	0	0	2.6	3.3	1.8	3.7	0.3	0.5	0	7.4	C
96018	012	1187	160	506	477	71.5	0.4	1.7	0.2	17.2	3.8	1.9	0.2	0.4	0	0	2.7	1.2	4.5	0	0	0	0	0.2	T
96018	012	1187	450	486	420	72.1	0	6.2	1.2	3.1	6.7	3.1	0.2	2.4	0.2	0	4.8	0.6	2.7	3.1	2.9	0	0	4.3	T
total sum				9495	8788																				
gray sum				5730	5252																				

Table 3. 1: Counts of sand size grains from sands from Flemish Pass, location of samples in Fig. 3.2 and 3.7, the gray shaded cores were key core to this study, samples counted by S. Weir-Murphy in 2004.

<b>sedimentary characteristics</b>	<b>facies</b>	<b>most valuable criteria for interpretation</b>	<b>interpretation</b>
well sorted sand (within a 0.5 phi range), beds 5 to 30 cm thick, no mud, granule lag throughout bed	uniform sorted sand facies (F I)	temporal and spatial distribution, petrology, grain size character	contourite deposit
very well sorted silt, locally clayey, low sand percentage (less than 2%)	uniform sorted silt facies (F II)	temporal and spatial distribution, grain size character, geometry, seismic character	? jökulhaup deposit
well sorted thin bedded sand (less than 5 cm thick), locally silty	poorly sorted sand facies (F III)	grain size character, temporal distribution	winnowed sequence
poorly sorted sand with varying percent of silt, locally basal inverse graded, mud content less than 2%, stacked normal graded sets	graded sand facies (F IV)	temporal and spatial distribution, petrology, grain size character	turbidity current deposit
silty, poorly sorted mud (more than 80% mud), 2 to 5 cm beds	graded silty mud facies (F V)	grain size character, spatial distribution	muddy turbidites
thick bedded mud, 1 to 4% silt and less than 2% sand, locally IRD present	muddy facies (F VI)	grain size character, presence of IRD, sediment color, lack of sedimentary structures	hemipelagic sedimentation

Table 3. 2: different sedimentary facies described from the grain size data in Flemish Pass and its interpretation



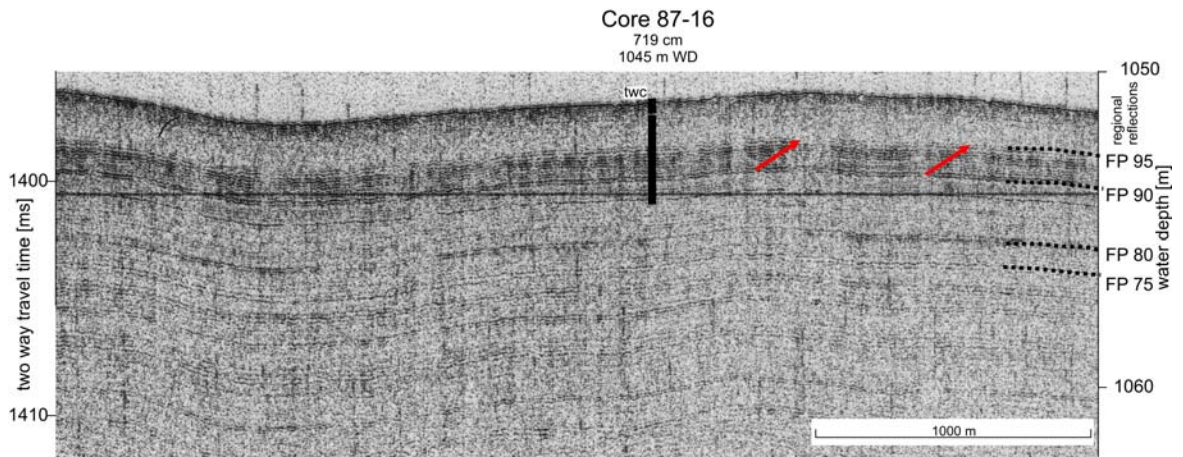


Figure 3.7: Sparker seismic profile of sand sheet on Gabriel Lobe showing location of core 87-16 and regional reflector FP 70 through 95 (see chapter 4 for more information), the red arrows indicate basal erosion of the sand bed.

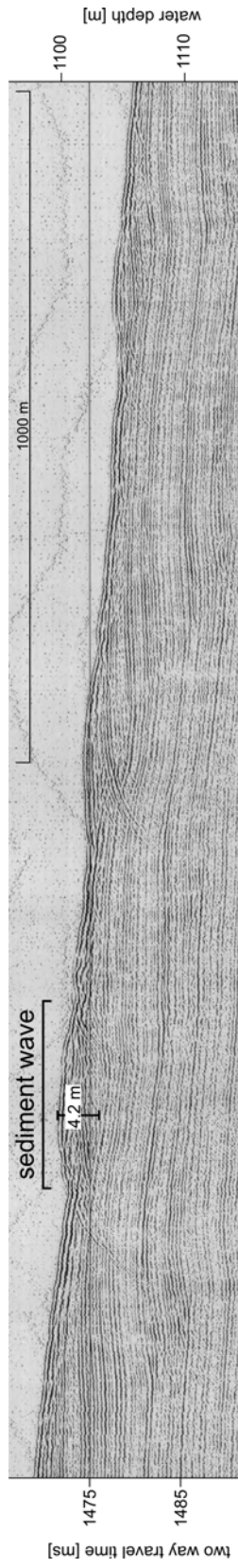


Figure 3.8: Sparker seismic profile from the eastern side of the basin showing large sediment waves along the sea bed.

#### 3.4.4 Correlated Sand Packets

Three different sand packets could be correlated within the basin near the Kyle well (Fig. 3.1) and show typical basinward fining (Fig. 3.4). The packets were termed A, B and C, with C being the youngest (Figs. 3.9, 3.10 and 5.11).

Sand packet A (Figs. 3.9 and 3.10) is recognized in 6 cores with grain size data available from 3 cores (Fig 3.4c). In core 87-27 this packet is 8 cm thick and is represented by the graded sand facies (F IV). In core 06-04 downslope, the sand packet occurs at the top of the piston core. In this core the sand packet thickens up to ~70 cm and the uniform sorted sand facies (F I) and the poorly sorted sand facies (F III) are present in the core. The third core (06-10) where grain size is available from this sand packet, it is represented by the poorly sorted sand facies (F III), the graded sand facies (F IV) and the graded silty mud facies (F V). The packet fines overall basinwards.

Sand packet B (Figs. 3.10 and 3.11) was described from 9 cores in the areas downslope from Kyle Lobe. Grain size data is available from 4 cores (Fig 3.4b). On the edge of the basin floor (Fig. 3.10 core 86-14) the packet is 15 cm thick and represented by the graded sand facies (F IV) underlain by the uniform sorted sand facies (F I). Basinwards, the packet is characterized by the graded sand facies (F IV) and the poorly sorted sand facies (F III) and has overall fined slightly basinwards (Fig 3.4b). Northwards, the packet is characterized by uniform sorted sand facies (F I), underlain by the graded sand facies (F IV).



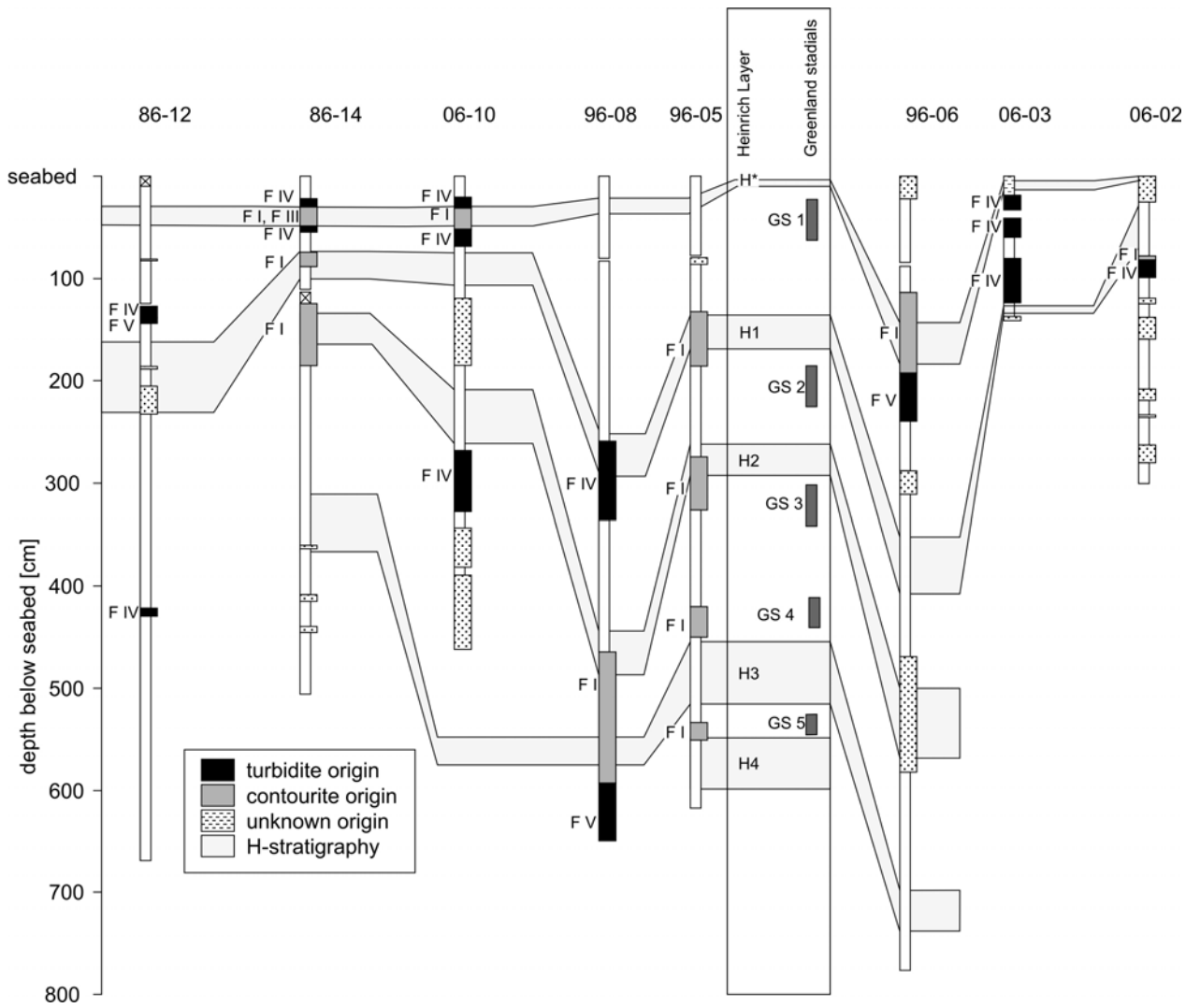


Figure 3.9: Correlation of sands to Heinrich layers and Greenland ice core stadials, see Figure 3.12.

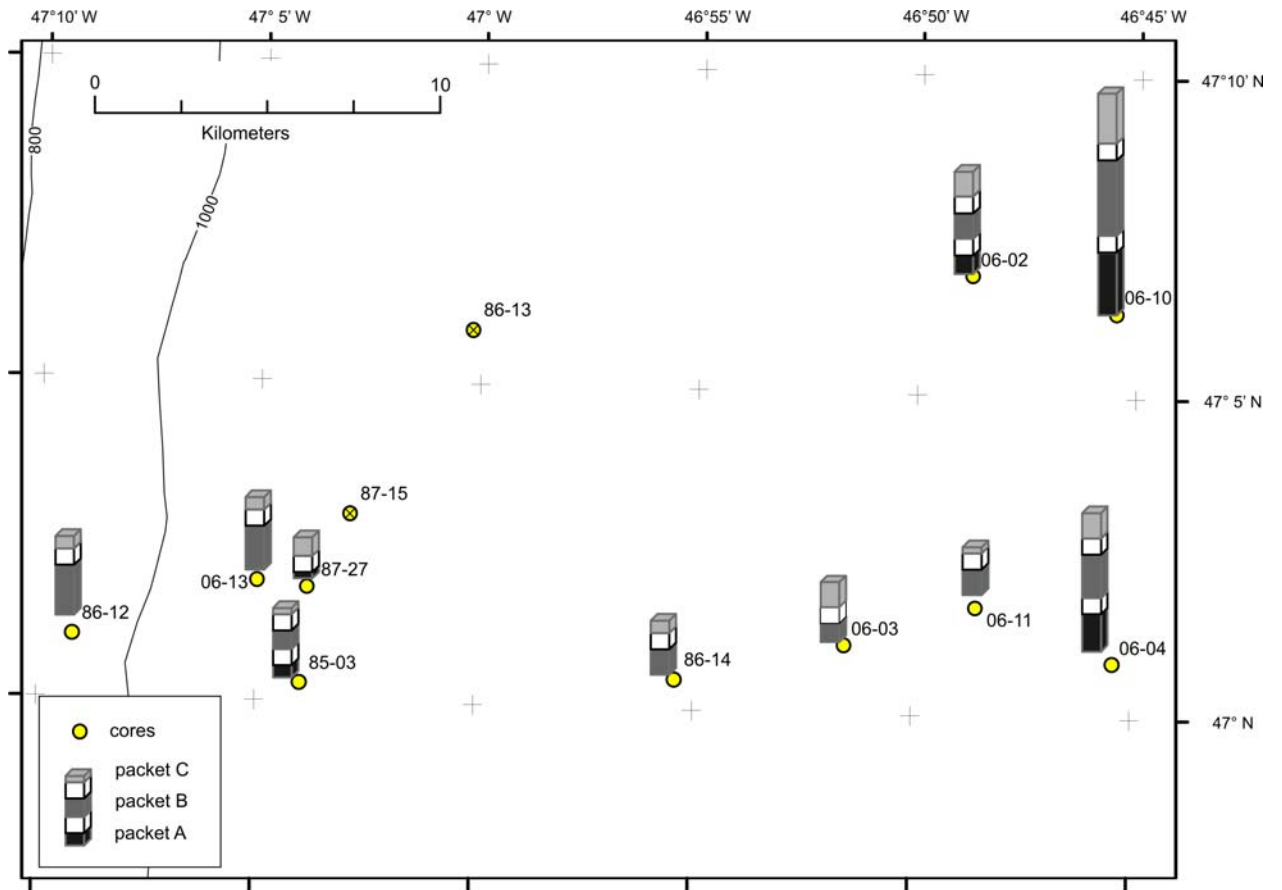


Figure 3.10: Spatial distribution and thickness of sand packets A through C on Kyle Lobe, X indicates no sands.

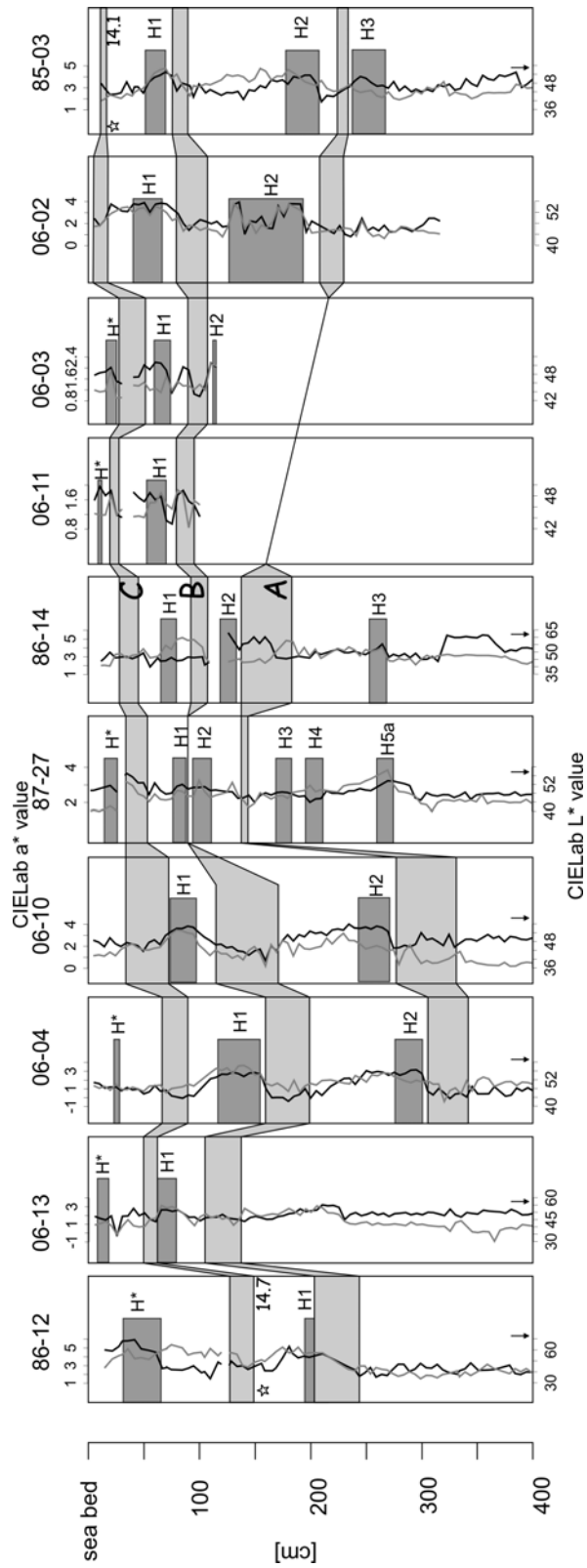


Figure 3.11: Stratigraphic position of sand bed in cores in Flemish Pass. The arrow indicates that the core is longer than displayed.

Sand packet C (Figs. 3.10 and 3.11) is the youngest correlated deposit and was found close to the sea bed in 10 cores; grain size data is available from 8 of the cores (Fig 3.4a). Due to its shallowness in the sequence, this sand packet was usually either found at the base of trigger weight cores or at the top of piston cores, so its whole continuous sequence was only sampled in three cores (Fig. 3.4). In the basin it is approximately 30 cm in thickness; on the lower slope it is significantly thinner. This bed is dominated along the slope by the graded sand facies (F IV, Fig. 3.10, core 86-12); the basal sequences of the packet may show the graded silty mud facies (F V) locally. As it reaches the floor of the basin, it thickens, and the uniform sorted sand facies (F I) and the graded sand facies (F IV) characterize the individual beds. At the base of several individual beds the poorly sorted sand facies (F III) is found.

#### **3.4.5 Temporal Distribution of Facies**

Heinrich layers commonly occur at the base or at the top of sand beds characterized by the uniform sorted sand facies (F I) and the poorly sorted sand facies (F III). This was observed in core 96-05, where a radiocarbon date on foraminifera at 79 cm core depth gives an age of 16.6 ka within a sequence characterized by the uniform sorted sand facies (F I). This is just below an interval with a high  $L^*$  value that indicates a Heinrich layer, interpreted as H1 (Figs. 3.3, 3.9). The top sequence of the uppermost sand bed in core 96-06 consists of the poorly sorted sand facies (FIII) with a similar grain size character and a radiocarbon date of 15.0 ka at the base of the bed, and has therefore a

similar sequence as the 96-05 core sequence. Similar observations of F I and F II characterizing the uppermost parts of F IV sequences were made in cores 96-08, 87-13 and 86-14. The duration of deposition of the uniform sorted sand facies (F I) may therefore be several hundreds of years, as some of the sand beds span entire Heinrich layers, e. g. in core 96-06 and 86-14 (Fig. 3.9).

In some sand packets e. g. in the uppermost packet in core 06-10, the uniform sorted sand facies (F I) and the graded sand facies (F IV) can occur stacked (Fig. 3.9). When such a stacking is observed, the sand packets occur either at the top or base of the Heinrich layers, or exceed the Heinrich layer as observed in core 96-06 (Fig. 3.9).

The graded sand facies (F IV) and the graded silty mud facies (F V) are exclusively deposited between Heinrich events and are mostly separated from these Heinrich events by muddy sediment beds more than 5 cm thick, e.g. in core 86-12, 06-03 and 06-02 (Fig. 3.9).

The three sand packets A through C could be indirectly dated using the available radiocarbon dates and the Heinrich layer stratigraphy. Sand A was deposited below H2 with an age of ~ 24 ka (Fig 3.11), sand B was found just below H1 at 16 ka (Fig 3.11) and sand C just below the youngest H-event found in Flemish Pass: based on radiocarbon dates this Heinrich event most likely correlates to the Younger Dryas cooling period (H\* in Fig 3.11).

## 3.5. Discussion

### 3.5.1. Characterization of Facies

The six different facies described from Flemish Pass show distinct sedimentary and petrologic character that can be used to characterize the depositional mode of the beds (Table 3.2). Most of the sand packets in Flemish Pass include more than one facies, with possible erosional contacts between individual beds (Fig 3.4). Six attributes were used to characterize the facies and relate them to specific sedimentary characters directly related to their origin: not all the beds could be linked definitively to one of the facies.

(1) The geographic position in Flemish Pass is the first indicator for inferring the depositional origin: sands deposited to the west of the bathymetric axis of Flemish Pass (BAFP in Fig. 3.2) show a lobe-like distribution and fine basinwards (Fig. 3.10) away from the few channels on the Grand Banks slope (e. g. Kyle channel system, Fig. 3.2). The lack of sandy sources on Flemish Cap or of channels along the Flemish Cap slope and the presence of sediment wave fields suggest that sands to the east of the BAFP are more likely deposited by reworking oceanic currents.

(2) The stratigraphic position of the sand facies in the basin indicate a greater likelihood of the graded sand facies (F IV) during stadial climatic stages (Fig. 3.9, e. g. cores 06-02 and 06-03), whereas during interstadials the sands are more likely characterized by the uniform sorted sand facies (F I) and the poorly sorted sand facies (F III) (Figure 3.9, e. g. cores 96-05, 96-06). Some sand packets within the basin show this trend more clearly (Fig. 3.10), whereas

other sand packets may have lost their initial depositional character e. g. due to winnowing (e. g. Fig. 3.4b, core 06-11). Several beds characterized by the graded sand facies (F IV) to the west of the BAFP (Fig. 3.2) were deposited during the LGM (e. g. Fig. 3.9, core 06-03 and Fig 3.12). To the east of the BAFP, the sand beds are mostly found within or towards the end of Heinrich events and were therefore likely deposited during warmer climatic stages (interstadials).

(3) The petrology data from specific cores may also be used to differentiate between depositional modes of the different facies in Flemish Pass. The distinction is based on the character of the two sources influencing Flemish Pass: sand beds from the Grand Banks side are characterized by shell fragments, quartz rich sands (more than 75%) and low lithic carbonate content (<7%) (Table 3.1, core 85044-003). Light colored heavy minerals that were concentrated in these sands by reworking on the Grand Banks (Slatt, 1977), characterize these beds. This is in contrast to the sands to the east of the BAFP (Fig 3.2), where sands contain various types of volcanic ash transported to the area by icebergs or sea ice in the Labrador Current (Table 3.1, cores 96018-007 and 008) (Piper et al., 1990). Additionally, foraminifers are much more abundant in the sands east of the BAFP.

(4) Some of the sand beds within the sand packets east of the BAFP (Fig. 3.2) show durations of deposition exceeding that of Heinrich events (Fig 3.9, core 96-06), by hundreds to a thousand years (Hemming, 2004), indicating long stable current systems during their deposition.

(5) Small scale primary sedimentary structures have been found only from cores to the west of the BAFP. Small scale cross-bedding and coarsening and fining trends are locally observed (Fig. 3.4). Locally, the base of the beds has cut into the underlying muddy sequences (e. g. the cores above the basin floor, core 06-13, 86-14, Fig 3.4). Sand beds east of the BAFP lack basal erosion and have less frequently graded beds. If fining or grading is observed, the sand fines or coarsens within less than 2 phi.

(6) The facies defined on the basis of grain size character show patterns similar to the above attributes. East of the BAFP uniform sorted sand facies (F I) and poorly sorted sand facies (F III) predominate, whereas west of the BAFP the beds were generally less well sorted with various coarsening and fining trends (graded sand facies (F IV) and graded silty mud facies (F V)). Some of the beds to the west of the BAFP also showed the uniform sorted sand facies and the poorly sorted sand facies (Figs. 3.4 and 3.9).

### **3.5.2 Facies Interpretation**

Several lines of evidence were used to interpret the uniform sorted sand facies (F I) and the poorly sorted sand facies (F III), which show an overall similar sedimentological character (Table 3.2). The most prominent characteristics are the high component of granules, which may be interpreted as a gravel lag. The high degree of sorting, which has previously been used to interpret deposits as contourite (Lovell and Stow, 1981; Toucanne et al., 2007) in combination with the lack of drop stones (Knutz et al., 2002) and the presence of foraminifera support an interpretation as a contourite (core 96-05 at 70 cm, and core 96-08 at 530 cm



in Table 3.1 and Fig. 3.9). The petrology samples show the lithologies indicative for contourites at these depth intervals and in the grain size maps show F I facies within or close to H-layers. These sediment characteristics suggest that the uniform sorted sand facies is likely a contourite sand and the poorly sorted sand facies, with very similar characteristics, is likely a winnowed sequence or a pre-contourite stage. A pre-contourite stage is defined as a short period of time, when winnowed sand starts to create sedimentary characteristics similar to contourite deposits. These characteristics are less well developed than in a contourite deposit due to the shorter time span of formation. After this short time span, the oceanic circulation changes to a new pattern. Some of these sands may have been transported into the basin as turbidites and then reworked, or the sands may have been winnowed from ice rafted sediment in hemipelagic facies. Several facies classified as the poorly sorted sand facies (F III) may have originally been turbidite sands that were winnowed by sea bed currents. This is especially true for the sands deposited at the end of stadials and in proximity to Heinrich events (Fig. 3.9. core 06-10).

The graded sand facies (F IV) is characterized by fining upwards sequences, but locally basal inverse grading is observed (Table 3.2). Some beds have further preserved faint cross bedding and show basal erosion with granules along the base (Fig. 3.4). Similar sedimentary properties are characteristic for the Bouma sequence and indicate a turbidite flow origin (Bouma, 1962; Middleton and Hampton, 1973; Gladstone and Sparks, 2002).

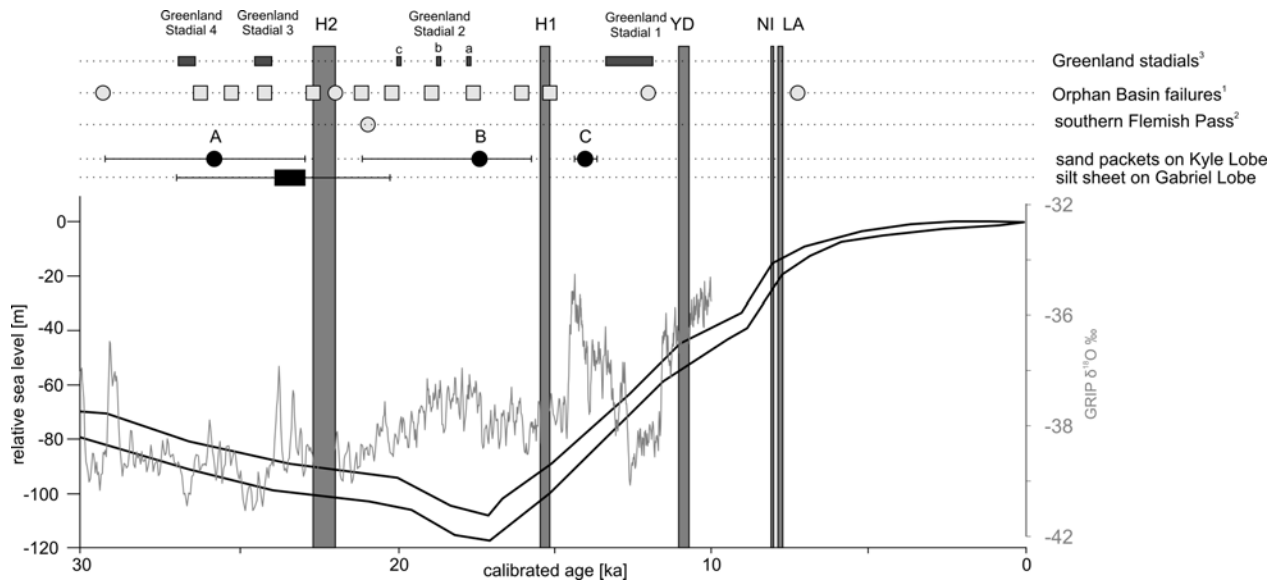


Figure 3.12: Summary figure showing the relationship of the sand beds over time in relationship to the global sea level curve (Lambeck and Bard, 2000) and to the earthquake record inferred from MTD failures from Orphan Basin : LA= Lake Agassiz melt water, NI= Noble Inlet melt water, YD= Younger Dryas cooling period, and southern Flemish Pass. <sup>1</sup>Orphan Basin failures from Tripsanas and Piper (2007), <sup>2</sup> southern Flemish Pass failures from Piper and Campbell (2005), <sup>3</sup>stadials and interstadials of the GRIP ice core from Björck et al. (1998) and Andersen et al. (2006), circles indicate sand beds deposited as turbidite deposits, squares are likely jökulhlaups deposits.

The graded silty mud facies (F V) shows several characteristics indicating deposition as muddy turbidites: the beds show a high mud content, and are interlayered by poorly sorted silt beds on a 2 cm scale creating faint laminae. Each bed shows fining sequences internally and sets comprised of different beds fine overall. These are typical characteristics for muddy turbidites (Piper, 1978; Stow and Piper, 1984). Therefore, Facies F IV and F V are both facies deposited from turbidity currents with a different grain size range: the graded sand facies (F IV) is a sandy and coarse silty turbidite whereas the graded silty mud facies (F V) is a fine silty to muddy turbidite deposit (Table 3.2).

The muddy facies (F VI) is a clayey facies with varying degrees of silt. Locally, sand, pebbles and cobbles may be within this fine sequence: these are IRD transported by icebergs with the Labrador Current to Flemish Pass. The muds can have various colorations. No sedimentary structures are observed. These characteristics are typical for hemipelagic sedimentation.

The thick sheet-like body on Gabriel Lobe (Fig 3.2) represents the only bed from which the uniform sorted silt facies (F II) was described; its timing indicates an age of 25 ka. The geometry of this sheet shows a lobe-like form with a source in Gabriel channel. The geometry and the grain size character in combination with the lack of correlative beds to the east of the BAFP rules out the possibility of a contourite. The thickness and widespread distribution also militates against a conventional turbidite deposit. It covers an estimated area of 240 km<sup>2</sup> and has an approximate volume of up to 2.5 km<sup>3</sup>, similar to single correlatable turbidite deposits in the ancient record which are generally a few km<sup>3</sup>

in volume (Talling et al., 2007). In Flemish Pass, the timing of the sand bed might indicate an origin as a jökulhlaup from the Grand Banks (Fig. 3.12), as jökulhlaups occur at this time in Orphan Basin (Tripsanas and Piper, 2008, in revision). The sedimentary sequence of the bed shows poorly developed coarsening and fining of an overall rather uniform silt bed. The depositional sequence shows elements of the hyperpycnal flow sequence (Mulder et al., 2003), e. g. the bell-shaped grain size distribution, a high percentage of fines and basal erosional contacts.

### **3.5.3 Distribution of Sandy Facies in Flemish Pass**

The characteristics of contourites in Flemish Pass, illustrated in the grain size maps include: (1) grain size distribution (Fig. 3.5), (2) stable grain size distribution over time spans exceeding Heinrich events (Fig. 3.9) and (3) rapid onset and decline of the sandy contourite system.

The occurrence of sandy turbidite and contourite facies show a strong correlation to stadials and interstadials respectively: the turbidites were deposited during stadials, the contourites during interstadials (Fig. 3.9). The remaining facies inferred from the grain size data have a less well defined temporal distribution: the stratigraphic position of winnowed sequences indicates that they may occur during transitions between stadials and interstadials (Fig. 3.12).

The different sandy facies have a specific aerial distribution within Flemish Pass: generally, turbidites are confined to the Grand Banks slope whereas contourites are mostly found along the Flemish Cap slope (Fig 3.2). Locally,

contourites may be present from cores on the lower Grand Banks slope (Facies F1 in cores 86-14 and 87-27 in Figure 3.4a, b).

The temporal and spatial distribution of contourites in Flemish Pass may help understand the history of oceanic circulation during the Pleistocene and the Holocene in Flemish Pass, but would need data sets integrating proxies for deep-water current variations such as foraminifera distributions.

Some of the turbidites in Flemish Pass show lateral fining from sand to coarse silt (Fig. 3.4), as described from the facies sequences for turbidites (Bouma, 1962; Walker, 1967). The turbidite beds in Flemish Pass show a limited km-scale runout distance and create a small lobe-like feature proximal to the source channel system. This differs strongly from other turbidite systems with a similar setting (Piper and Normark, 2001), where turbidites show long runout distances (Nakajima, 2006) possibly due to basal hydroplaning (Mohrig et al., 1999). The basin floor gradient in Flemish Pass is below  $0.01^\circ$  and therefore the flow energy may be insufficient to maintain the flow. When long runout distances are observed the critical slope angle is usually above  $0.1^\circ$  (Piper and Normark, 2001); the sands in Flemish Pass lack hemipelagic interbeds, which some authors suggest are needed for hydroplaning (Niedoroda et al., 2006). The low mud content may also be insufficient to support the flow over large distances (Ilstad et al., 2004).

### 3.5.4 Initiation of Turbidity Currents in Flemish Pass

Several initiating processes may have caused the turbidite beds observed west of the BAFP. Earthquake triggering of failures is the classic initiation process for turbidity currents (Piper et al., 1999). A paleo-seismic record has been inferred just north of Flemish Pass from the southern margin of Orphan Basin (Fig 3.1) based on well dated widespread slumps and resulting sandy turbidites in Orphan Basin (Tripsanas and Piper, 2007). Their data show evidence of large failures in the early Holocene around 7 ka, around 14 ka and around the time of H2 at about 22 ka (Fig 3.12). The 22 ka paleo-seismicity correlates to the thick silt sheet of facies F II, but sand packets A, B and C show no correlation with earthquakes in southern Orphan Basin. In central Flemish Pass, no slope failures are recognized in the last 30 ka (see Chapter 4), but in the southern part of the Pass, a failure on the Flemish Cap slope lies stratigraphically between the LGM and H2 (Piper and Campbell, 2005) and thus could correlate to sand packet B in central Flemish Pass (Fig 3.12). Overall, there is no strong evidence that large earthquakes were responsible for the multiple turbidite beds in packets A through C.

Catastrophic discharge of meltwater in jökulhlaups has been recognized as a method of initiating turbidity currents, although most well known examples involve discharge off ice streams at the shelf break (Piper et al., 2007; Tripsanas and Piper, submitted). Tripsanas and Piper (2008, in revision) have demonstrated the presence of meltwater discharge in Orphan Basin at the time of H2. Similar meltwater discharge on the Grand Banks might have been

responsible for the unique thick massive silt sheet in Flemish Pass on the Gabriel Lobe that dates from this time (Fig. 3.12). In general, however, the lack of prominent ice streams and the limited extent of ice on the Grand Banks make ice-margin sand discharge unlikely as an initiating process for turbidity currents in Flemish Pass in the last 30 ka.

Therefore, processes other than earthquake triggering of slumps and discharge of subglacial meltwater are needed to initiate the turbidites in the packets A through C. There is no evidence for correlation with enhanced iceberg scouring during Heinrich events. Possible initiating processes may be related to the variation of the Labrador Current during this time: the stronger Labrador current during glacial stages may have reworked sands on the outer shelf (King et al., 2001) and distributed them into canyon heads upslope from the Kyle Lobe channel system (see Chapter 4) which may have over-steepened and failed, creating turbidity currents. Similarly, storm events may have also reworked these surficial sands and lead to accumulation in canyon heads, especially as several studies have shown the increased storminess in the North Atlantic during the Pleistocene (Stauffer, 2000). More detailed work is needed to understand more thoroughly the processes initiating sandy turbidites on the eastern Grand Banks slope, especially by improving the age control of the sand beds and the understanding of the strength of the Labrador Current over this time span.

### 3.6 Conclusions

In Flemish Pass, contourites can be distinguished from turbidites based on the sedimentary characteristics of the sand beds, including the spatial and

temporal distribution, the grain size character and petrology data of the beds.

Grain size maps, created by stacking of grain size data on a 2 cm interval using Golden Software Surfer are a robust method for distinguishing between different contourite and turbidite facies.

The turbidites are deposited west of the bathymetric axis in Flemish Pass (BAFP) and are linked to stadials. Several beds show basinward fining. It was shown that these turbidites were not initiated by earthquakes, slumps or meltwater discharge; therefore possible initiating processes may include storm surges and short-term variations in the Labrador Current initiating small failures on the upper slope. Contourites are deposited mostly during interstadials east of the BAFP and their activity is directly related to the variation of the Labrador Current.



## Chapter 4. CONCLUSIONS

A new seismic stratigraphy based on radiocarbon dates, Heinrich events, CIELab color L\* and a\* plots, the North Atlantic Ash Zone II and an oxygen isotope curve was established for central and northern Flemish Pass, which was used to understand the types, volumes and processes of sediment flux into the basin over the last 170 ka. The correlation of events to Orphan Basin, an open basin north of Flemish Pass, was used to understand the influence of the ice sheet on a regional scale. The seismic stratigraphy was defined in a new type section on Kyle Lobe and was correlated throughout the basin to Sackville Spur, where it was correlated to a core with an oxygen isotope curve. Upslope, the resolution of the stratigraphy was limited by iceberg scouring at 450 m present water depth. The high resolution multi-dated stratigraphy had a resolution of 5 ka in the younger sequence and 10 ka during OIS 6.

This accurate stratigraphy improved the temporal understanding of MTDs, turbidites and contourites in the basin and their relationship to glaciation over the last 170 ka. Ice sheets terminated during OIS 6 and likely OIS 4 along the margin (Fig. 4.1), where they created till tongues and related moraine ridges on Sackville Spur. During stages when ice reached the margin, the highest sedimentation rates are observed, which further supports the presence of ice at the margin during OIS 6 and 4 with high sedimentation rates and low sedimentation rates during the last glaciation (OIS 2).

During these times, MTDs from both sides of the basin are found widespread on the basin floor. Their seismic character was used to define three

types of MTDs in Flemish Pass. Overall, the thickness and extent of MTDs decreases over time: during OIS large thick (more than 20 ms) MTDs are widespread, during OIS 4 only small flows characterize the basin floor and are generally 1-5 ms in thickness. During OIS 2 no MTDs are found in the section, indicating that no sediment failures and related initiating processes were active during this time. This temporal distribution of the MTDs indicates that the MTDs are only initiated during glacial stages, when the ice sheet terminated at the shelf break. The more extensive the ice sheet is during times of shelf-crossing ice, the more MTD activity is found in Flemish Pass. The ice sheet, terminating during OIS 4 on the slopes along Flemish Pass, had a less severe impact on the area, than the OIS 6 ice sheet, resulting in smaller sediment failures with overall less volume than the OIS 6 sediment failures. Additionally, sediment failures along Flemish Cap were only present during OIS 6, also indicating that this ice sheet resided longer along the margin than the OIS 4 ice sheet, and may have also been more fluctuating, with several calving events, for example during the Greenland ice core interstadials, when icebergs and plumes may have crossed Flemish Pass for initiating the observed sediment failures on Flemish Cap.

The seismic character of the four key reflections in Flemish Pass is a regionally distributed, strong double reflection signal. These horizons were never eroded by MTDs and were always bound by well stratified sequences. These layers were therefore more likely deposited during quiescent times, e. g. during interglacials/interstadials, when a higher sea level and the absence of ice allowed basin-wide hemipelagic sedimentation.

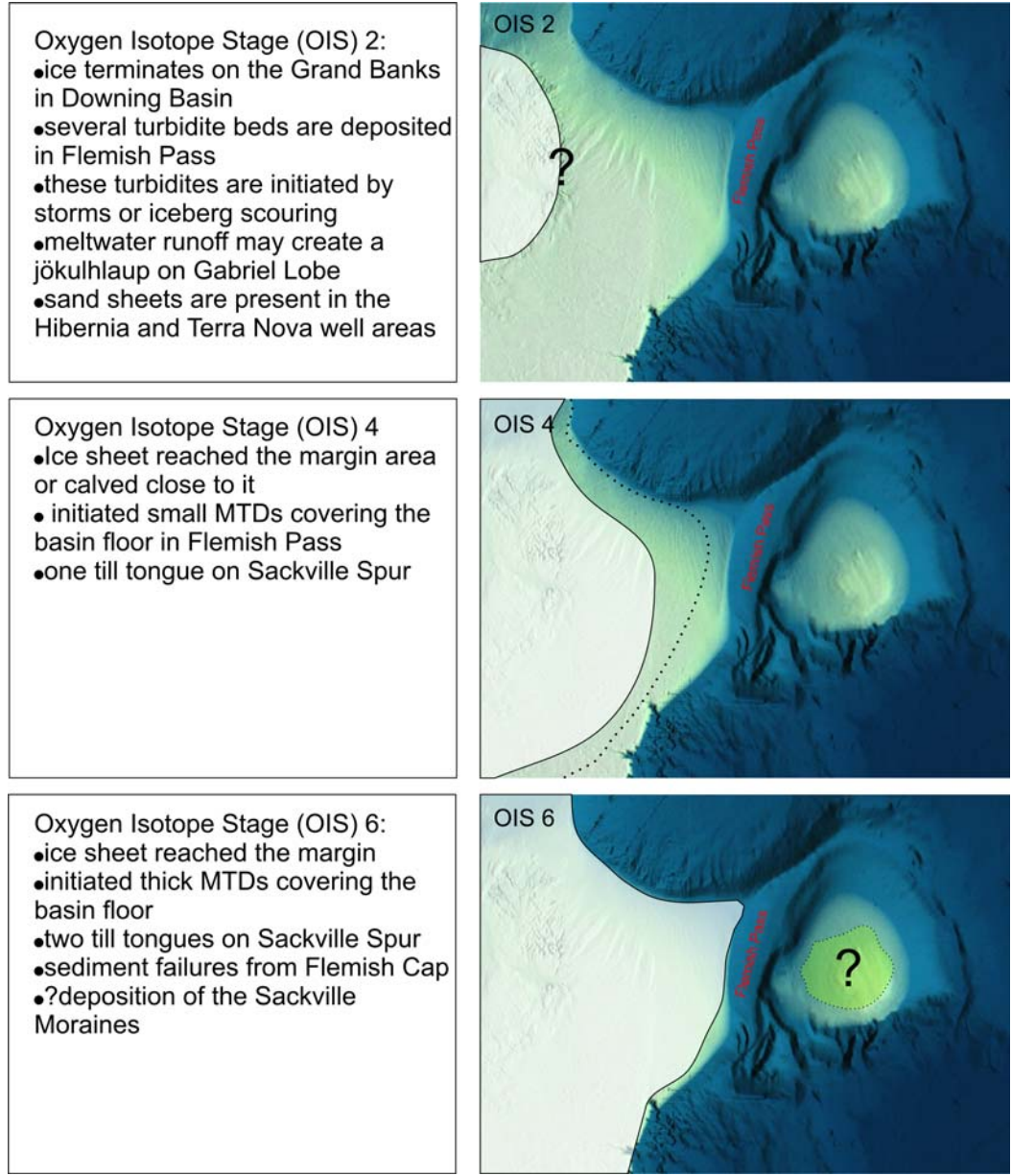


Figure 4.1: Ice sheet configuration on the easternmost Grand Banks margin adjacent to Flemish Pass

Sand beds are limited to the area of Kyle Lobe in western central Flemish Pass and Southern Baccalieu Lobe. Two depositional processes created these deposits: turbidites and contourites. Different specific characteristics of the beds, as temporal and spatial distribution, their grain size character and petrology of the beds could be used to differentiate between the two processes. A newly developed 3-D display, termed 'grain size maps' simplified the distinction between the depositional mode by showing more clearly grain size trends in the grain size data, some of them are clearly indicative for the depositional mode. Generally, turbidites are found along the Grand Banks slope whereas the sands along the Flemish Cap slope are characteristically deposited by contour currents.

The temporal distribution of contourites and turbidites shows a correlation of turbidites to Greenland stadial conditions, when the Labrador Current likely strengthens and the zone of mixing with the North Atlantic current shifts southwards. During warmer, Greenland interstadial climates, the oceanic current mixing zone shifts northwards creating an eddy around Flemish Cap. This circulation pattern initiates contourite activity along the eastern part of the basin (east of the bathymetric axis Flemish Pass). This temporal link of turbidites and contourites to Greenland stadial/interstadial climatic stages was established for the last 30 ka (dated by Heinrich event H3) in Flemish Pass.

Both MTDs and turbidites are therefore more frequently initiated during glacial/stadial times. The turbidite activity is not necessarily related to ice sheet processes, but would likely show an enhanced activity in times when the ice

sheet supplied sediment to the areas upslope of Flemish Pass; MTDs are only initiated during times, when ice sheets terminated at the continental margin.

Generally, sediment failures occur, when the downslope gravitational forces exceed the frictional resistance of the sediment. The initiating processes vary over time and space. The rate of sediment failure is mainly governed by gradual processes pre-conditioning sediment failure, e. g. sediment accumulation. This process may be disrupted by instantaneous events as earthquakes or erosional undercutting. No ultimate link between deposit and initiating process can be drawn because the different initiating processes do not create a specific depositional character. This initiating concept can be used to group possible MTD and turbidite triggers in Flemish Pass into two groups: sediment failure due to pre-conditioning and sediment failure by an unforeseen trigger.

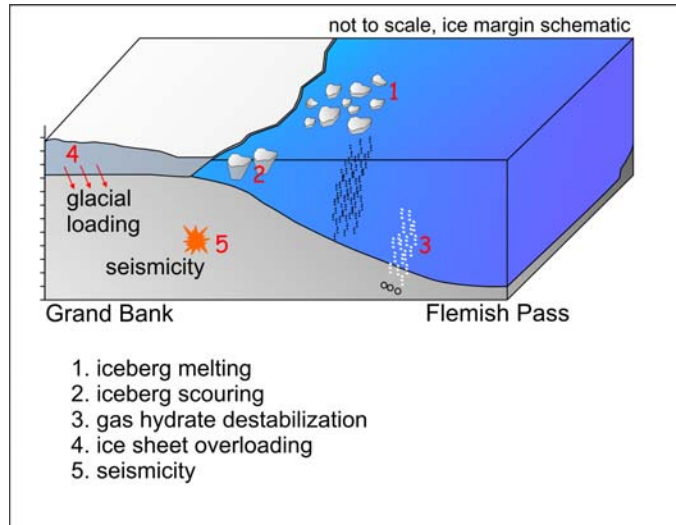
Preconditioning triggers include (i) iceberg melting and IRD creating overloaded sequences along the shelf break, (ii) glacial meltwater runoff (supra- and subglacial) creating oversteepening and sediment overloading, (iii) decomposition of gas hydrates and related sediment instability and (iv) sediment failure along weakness layers due to liquefaction. Unpredictable triggers include (I) cyclic sediment loading by storm generated waves or by seismicity, (II) erosional undercutting of sediment and (III) bulldozing by ice sheets and large icebergs. These processes may either create widespread failures which affect wide slope areas, or they may create point-source failures by oversteepening

canyon heads and channel flanks and initiating flows confined to channel systems (Fig. 4.2).

The sedimentation record off the northeast Grand Banks margin differs greatly from the Scotian margin, where ice was present at the shelf break during OIS 2. The hemipelagic sedimentation rates off the northeast Grand Banks margin were an order of magnitude lower than off the Scotian shelf, where sediment accumulated at 1m/ka during OIS 2 (Piper, 2005). Since OIS 4, when the Grand Banks ice sheet reached Flemish Pass for the last time, no MTDs were deposited and fewer turbidites than on the Scotian margin, where locally up to 25 turbidite beds have been described since 14 ka (Piper and Hundert, 2002; Benetti, 2006).

When looking at the sedimentation rates and its relationship to glacial ice sheets, there is an obvious link on the Grand Banks margin between high sedimentation rates and the presence of ice at the shelf break. As this study was restricted to Flemish Pass, this case can only be made for the outer northeast Grand Banks margin, but this generalization may be transferred to other areas along the Canadian margin.

During glacial stages, when ice is present at the shelf break, the hemipelagic sedimentation rates increase significantly and the basin is characterized by thick bedded MTDs and numerous turbidites; during glacial stages with no ice on the outer margin, as in OIS 2, the sedimentation rates remain low and few turbidites are deposited in the basin.



Initiation processes along eastern-most Grand Banks continental margin

Pre-conditioning		Trigger
<ul style="list-style-type: none"> <li>increase downslope gravitational forces</li> <li>• sediment loading</li> <li>• increased gradient</li> <li>- progradation</li> <li>- undercutting</li> </ul>	<ul style="list-style-type: none"> <li>decreased frictional resistance</li> <li>• excess pore pressure</li> <li>- rapid sedimentation</li> <li>- gas hydrates</li> <li>• "weak layer"</li> <li>- liquified silt layers</li> </ul>	<ul style="list-style-type: none"> <li>cyclic loading by earthquakes</li> <li>erosional undercutting</li> <li>bulldozing by ice sheets</li> </ul>

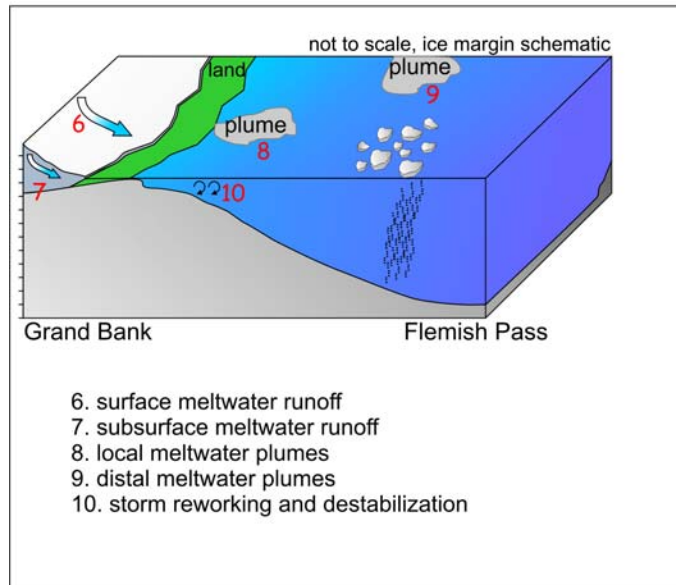


Figure 4.2: Initiating processes in Flemish Pass.

Further work will be needed in Flemish Pass to improve the understanding of basin morphology and sediment deposition in Flemish Pass by surveying the basin using multibeam swath bathymetry and by running a tighter grid of seismic airgun and Hunttec data, supported by additional coring especially in the northern part of the basin and on Flemish Cap. Additionally, more work will be needed in southern Flemish Pass where thick MTDs characterize the seabed. These thick MTDs did not allow a simple extension of the established regional seismic stratigraphy southwards with present data coverage. Similar work will be needed on the outer Grand Banks, where only poor stratigraphic control is available. The regional reflection FP 75 may be extendable onto the Grand Banks in the Sackville Spur area, where it was traced below till tongues to 450 m water depths. The understanding of the age of the Sackville moraines and its character and relationship to the thick sand deposits in the Terra Nova and Hibernia well areas may help to understand more clearly the ice sheet fluctuations of the Grand Banks ice sheet during OIS 4 and its extent during OIS 2 on the outer Banks.



## References

- Aksu, A.E., Mudie, P.J., de Vernal, A. and Gillespie, A., 1992. Ocean-atmosphere responses to climatic change in the Labrador Sea: Pleistocene plankton and pollen records. *Paleogeography, Paleoclimatology, Paleoecology*, 92(1-2): 121-137.
- Anastasakis, G. and Pe-Piper, G., 2006. An 18 m thick volcanoclastic interval in Pantelleria Trough, Sicily Channel, deposited from a large gravitative flow during the Green Tuff eruption. *Marine Geology*, 231(1-4): 201-219.
- Andersen, K.K., Svensson, A., Johnson, S.J., Rasmussen, S., Bigler, M., Röthlisberger, R., Siggaard-Andersen, M.-L., Steffensen, J.P., Dahl-Jensen, D., Vinther, B.M. and Clausen, H.B., 2006. The Greenland Ice Core Chronology 2005, 15-42 ka. Part 1: constructing the time scale. *Quaternary Science Reviews*, 25(24-25): 3246-3257.
- Andrews, J.T., 1998. Abrupt changes (Heinrich events) in late Quaternary North Atlantic marine environments: a history and review of data and concepts. *Journal of Quaternary Science*, 13(1): 3-16.
- Andrews, J.T. and Barber, D.C., 2002. Dansgaard–Oeschger events: is there a signal off the Hudson Strait Ice Stream? *Quaternary Science Reviews*, 21(1-3): 443-454.
- Andrews, J.T. and MacLean, B., 2003. Hudson Strait ice streams: a review of stratigraphy, chronology and links with North Atlantic Heinrich events. *Boreas*, 32(1): 4-17.
- Andrews, J.T., Matthews, R.K., Osterman, L.E., Miller, G.H., Hillaire-Marcel, C. and Williams, K.M., 1987. Deglaciation and meltwater events in Hudson Strait and the eastern Canadian Arctic. *Geo-Marine Letters*, 7(1): 23-30.
- Armishaw, J.E., Holmes, R.W. and Stow, D.A.V., 1998. Morphology and sedimentation on the Hebrides Slope and Barra Fan, NW UK continental margin. In: M.S. Stoker, D. Evans and A. Cramp (Editors), *Geological processes on continental margins: mass-wasting and stability*. Geological Society, London, pp. 81-104.

- Austin, W.E.N., Wilson, L.J. and Hunt, J.B., 2004. The age and chronostratigraphical significance of North Atlantic Ash Zone II. *Journal of Quaternary Science*, 19(2): 137-146.
- Baltzer, A., Holmes, R. and Evans, D., 1998. Debris flows on the Sula Sgeir Fan, NW of Scotland. In: M.S. Stoker, D. Evans and A. Cramp (Editors), *Geological processes on continental margins: sedimentation, mass-wasting and stability*. Geological Society, London, pp. 105-115.
- Benetti, S., 2006. Late Quaternary sedimentary processes along the western North Atlantic margin. Ph. D. Thesis, University of Southampton, Southampton, 188 pp.
- Björck, S., Walker, M.J.C., Cwynar, L.C., Johnsen, S., Knudsen, K.-L., Lowe, J.J., Wohlfarth, B. and INTIMATE Members, 1998. An event proposal for the Last Termination in the North Atlantic region based on the Greenland ice core record: a proposal by the INTIMATE group. *Journal of Quaternary Science*, 13(4): 283-292.
- Bouma, A.H., 1962. *Sedimentology of some flysch deposits*. Elsevier Publishing Company, Amsterdam, 168 pp.
- Bryn, P., Berg, K., Forsberg, C.F., Solheim, A. and Kvalstad, T.J., 2005a. Explaining the Storegga Slide. *Marine and Petroleum Geology*, 22(1-2): 11-19.
- Bryn, P., Berg, K., Stoker, M.S., Haflidason, H. and Solheim, A., 2005b. Contourites and their relevance for mass wasting along the Mid-Norwegian Margin. *Marine and Petroleum Geology*, 22(1-2): 85-96.
- Campbell, D.C., Piper, D.J.W., Douglas, E.V. and Migeon, S., 2002. *Surficial Geology of Flemish Pass: Assessment of hazards and constraints to development*. Open File 1454, Geological Survey of Canada, Ottawa.
- Canals, M., Casamor, J.L., Urgeles, R., Lastras, G., Calafat, A.M., Masson, D.G., Berné, S. and Alonso, B., 2000. The Ebro continental margin, western Mediterranean Sea: Interplay between canyon-channel systems and mass wasting processes, GCSSEPM Foundation 20th Annual Research Conference: Deep Water reservoirs of the World, Houston, TX, pp. 152-174.

- Clark, J.I. and Landva, J., 1988. Geotechnical aspects of seabed pits in the Grand Banks area. *Canadian Geotechnical Journal*, 25(3): 448-454.
- Colbourne, E.B. and Foote, K.D., 2000. Variability of the stratification and circulation on the Flemish Cap during the decades of the 1950s-1990s. *Journal of Northwest Atlantic Fishery Science*, 26: 103-122.
- Cronin, B., Owen, D., Hartley, A. and Kneller, B., 1998. Slumps, debris flows and sandy deep water channel systems: implications for the application of sequence stratigraphy to deep water clastic sediments. *Journal of the Geological Society of London*, 155(3): 429-432.
- Cuny, J., Rhines, P.B., Niiler, P.P. and Bacon, S., 2002. Labrador Sea boundary currents and the fate of the Irminger Sea Water. *Journal of physical Oceanography*, 32(2): 627-647.
- Domack, E.W., Jacobson, E.A., Shipp, S. and Anderson, J.B., 1999. Late Pleistocene–Holocene retreat of the West Antarctic Ice-Sheet system in the Ross Sea: Part 2—Sedimentologic and stratigraphic signature. *Geological Society of America Bulletin*, 111(10): 1517-1536.
- Enachescu, M.E., 1987. Tectonic and structural framework of the northeast Newfoundland continental margin. In: C. Beaumont and A.J. Tankard (Editors), *Sedimentary Basins and Basin-forming Mechanisms*. Canadian Society of Petroleum Geologists, Memoir 12, pp. 117-146.
- Fader, G.B.J. and King, L.H., 1981. A reconnaissance study of the surficial geology of the Grand Banks of Newfoundland. Current Research Paper 81-1A, Geological Survey of Canada, Ottawa.
- Fader, G.B.J. and Miller, R.O., 1986. A reconnaissance study of the surficial and shallow bedrock geology of the southeastern Grand Banks of Newfoundland. Current Research; Paper 86-1B, Geological Survey of Canada, Ottawa.
- Folk, R.L., 1966. A review of grain size parameters. *Sedimentology*, 6(2): 73-93.
- Foster, D.G. and Robinson, A.G., 1993. Geological history of Flemish Pass Basin, offshore Newfoundland. *AAPG Bulletin*, 77(4): 588-609.

- Galloway, W.E., 1998. Siliciclastic slope and base-of-slope depositional systems: component facies, stratigraphic architecture, and classification. *AAPG Bulletin*, 82(4): 569-595.
- Gauley, B.-J.L., 2001. Lithostratigraphy and sediment failure on the central Scotian slope. M. Sc. Thesis, Dalhousie University, Halifax, 214 pp.
- Gladstone, C. and Sparks, R.S.J., 2002. The significance of grain-size breaks in turbidites and pyroclastic density current deposits. *Journal of Sedimentary Research*, 72(1): 182-191.
- Gonthier, E., Faugères, J.-C. and Stow, D.A.V., 1984. Contourite facies of the Faro Drift, Gulf of Cadiz. In: D.A.V. Stow and D.J.W. Piper (Editors), *Fine grained sediments: deep water processes and facies*. Geological Society, London, pp. 275-292.
- Grant, A.C., 1972. The continental margin off Labrador and eastern Newfoundland - morphology and geology. *Canadian Journal of Earth Sciences*, 9: 1394-1430.
- Grant, A.C. and McAlpine, K.D., 1990. The continental margin around Newfoundland; Chapter 6. In: G.L. Williams (Editor), *Geology of the Continental Margin of eastern Canada*. Geological Survey of Canada, Ottawa, pp. 241-292.
- Hafliðason, H., Eiriksson, J. and van Kreveld, S., 2000. The tephrochronology of Iceland and the North Atlantic region during the Middle and Late Quaternary: a review. *Journal of Quaternary Science*, 15(1): 3-22.
- Heinrich, H., 1988. Origin and consequences of cyclic ice rafting in the Northeast Atlantic ocean during the past 130,000 years. *Quaternary Research*, 29: 142-152.
- Hemming, S.R., 2004. Heinrich Events: massive late Pleistocene detritus layers of the North Atlantic and their global climate imprint. *Review of Geophysics*, 42(RG 1005): 1-43.
- Hesse, R., Khodabakhsh, S., Klauck, I. and Ryan, W.B.F., 1997. Asymmetrical turbid surface-plume deposition near ice-outlets of the Pleistocene

- Laurentide ice sheet in the Labrador Sea. *Geo-Marine Letters*, 17(3): 179-187.
- Hesse, R., Klauck, I., Ryan, W.B.F., Edwards, M.B. and Piper, D.J.W., 1996. Imaging Laurentide ice sheet drainage into the deep sea: impact on sediments and bottom water. *GSA Today*, 6(9): 3-9.
- Hillaire-Marcel, C. and Bilodeau, G., 2000. Instabilities in the Labrador Sea water mass structure during the last climatic cycle. *Canadian Journal of Earth Sciences*, 37(5): 795-809.
- Hiscott, R.N., Aksu, A.E., Mudie, P.J. and Parsons, D.F., 2001. A 340,000 year record of ice rafting, palaeoclimatic fluctuations, and shelf-crossing glacial advances in the southwestern Labrador Sea. *Global and Planetary Change*, 28(1-4): 227-240.
- Hughen, K.A., Baillie, M.G.L., Bard, E., Beck, J.W., Bertrand, C.J.H., Blackwell, P.G., Buck, C.E., Burr, G.S., Cutler, K.B., Damon, P.E., Edwards, R.L., Fairbanks, R.G., Friedrich, M., Guilderson, T.P., Kromer, B., McCormac, F.G., Manning, S., Bronk Ramsey, C., Reimer, P.J., Reimer, R.W., Remmele, S., Southon, J.R., Stuvier, M., Talamo, S., Taylor, F.W., van der Plicht, J. and Weyhenmeyer, C.E., 2004. Marine04 Marine radiocarbon age calibration, 0-26 CAL kyr BP. *Radiocarbon*, 46(3): 1059-1086.
- Husebye, E.S. and Mäntyniemi, P., 2005. The Kaliningrad, West Russia earthquakes on the 21st of September 2004—Surprise events in a very low-seismicity area. *Physics of the Earth and Planetary Interiors*, 153(4): 227-236.
- Ilstad, T., Elverhøi, A., Issler, D. and Marr, J.G., 2004. Subaqueous debris flow behaviour and its dependence on the sand/clay ratio: laboratory study using particle tracking. *Marine Geology*, 213(1-4): 415-438.
- Jacobs, C.L., 1988. Sedimentary processes along Flemish Pass, offshore eastern Canada: a GLORIA and high resolution seismic reconnaissance. *Canadian Journal of Earth Sciences*, 26: 2177-2185.
- Jenner, K.A., Piper, D.J.W., Campbell, D.C. and Mosher, D.C., 2007. Lithofacies and origin of late Quaternary mass transport deposits in submarine canyons, central Scotian Slope, Canada. *Sedimentology*, 54(1): 19-38.

- Keen, C.E., Boutilier, R., de Voogd, B., Mudford, B. and Enachescu, M.E., 1987. Crustal geometry and extensional models for the Grand Banks, eastern Canada: constraints from deep seismic reflection data. In: C. Beaumont and A.J. Tankard (Editors), *Sedimentary Basins and Basin-forming Mechanisms*. Canadian Society of Petroleum Geologists, Memoir 12, pp. 101-115.
- Kennard, L., Schafer, C. and Carter, L., 1990. Late Cenozoic evolution of Sackville Spur: a sediment drift on the Newfoundland continental slope. *Canadian Journal of Earth Sciences*, 27(11): 863-878.
- Kennett, J.P., Cannariato, K.G., Hendy, I.L. and Behl, R.J., 2003. Methane hydrates in Quaternary climate change: the clathrate gun hypothesis, Special Publication 54. American Geophysical Union, Washington, 215 pp.
- King, E.L., Fader, G.B.J. and Sonnichsen, G.V., 2001. Quaternary Geology of the Northeast Newfoundland Shelf: Contrasts in Late Wisconsinan glacial regimes, Geological Association of Canada (GAC/MAC) Annual Meeting, St. John's.
- King, E.L., Hafliðason, H., Sejrup, H.P. and Løvlie, R., 1998. Glacigenic debris flows on the North Sea Trough Mouth Fan during ice stream maxima. *Marine Geology*, 152(1-3): 217-246.
- King, E.L., Sejrup, H.P., Hafliðason, H., Elverhøi, A. and Aarseth, I., 1996. Quaternary seismic stratigraphy of the North Sea Fan: glacially-fed gravity flow aprons, hemipelagic sediments, and large submarine slides. *Marine Geology*, 130(3-4): 293-315.
- King, E.L. and Sonnichsen, G.V., 1999. Characterization of near-surface seismostratigraphy and features of Northeastern Grand Bank: sea level fluctuations, glaciation and slope stability. Open File 3886, Geological Survey of Canada, Ottawa.
- King, E.L., Tripsanas, E.K. and Shaw, J., 2007. Possible late glacial catastrophic discharges related to ice streams: evidence from a shelf crossing trough on the Northeast Newfoundland shelf, Geological Association of Canada, Ottawa.

- King, L.H., 1976. Relict iceberg furrows on the Laurentian Channel and western Grand Banks. *Canadian Journal of Earth Sciences*, 13: 1082-1092.
- King, L.H., 1993. Till in the marine environment. *Journal of Quaternary Science*, 8(4): 347-358.
- King, L.H. and Fader, G.B.J., 1986. Wisconsin glaciation of the Atlantic Continental Shelf of southeast Canada. Bulletin 363, Geological Survey of Canada, Ottawa.
- King, L.H., Fader, G.B.J., Poole, W.H. and Wanless, R.K., 1985. Geological setting and age of the Flemish Cap grandiotite, east of the Grand Banks of Newfoundland. *Canadian Journal of Earth Sciences*, 22(9): 1286-1298.
- King, L.H., Rokoengen, K., Fader, G.B.J. and Gunleiksrud, T., 1991. Till-tongue stratigraphy. *Geological Society of America Bulletin*, 103(5): 637-659.
- Knutz, P.C., Jones, J.W., Howe, J.A., van Weering, T.J.C. and Stow, D.A.V., 2002. Wave-form contourite drift on the Barra Fan, NW UK continental margin. In: A.R. Viana (Editor), *Deep-water contourite systems: modern drifts and ancient series, seismic and sedimentary characteristics*. The Geological Society, London, pp. 85-97.
- Laberg, J.S. and Vorren, T.O., 1995. Late Weichselian submarine debris flow deposits on the Bear Island Trough Mouth Fan. *Marine Geology*, 127(1-4): 45-72.
- Lambeck, K. and Bard, E., 2000. Sea level change along the French Mediterranean coast for the past 30 000 years. *Earth and Planetary Science Letters*, 175(3-4): 203-222.
- Lambeck, K. and Chappell, J., 2001. Sea level change through the last glacial cycle. *Science*, 292: 679-686.
- Lambeck, K., Esat, T.M. and Potter, E.-K., 2002a. Links between climate and sea levels for the past three million years. *Nature*, 419: 199-206.

- Lambeck, K., Yokoyama, Y. and Purcell, T., 2002b. Into and out of the Last Glacial Maximum: sea-level change during Oxygen Isotope Stages 3 and 2. *Quaternary Science Reviews*, 21(1-3): 343-360.
- Lemmen, D.S., 1990. Glaciomarine sedimentation in Disraeli Fiord, high arctic Canada. *Marine Geology*, 94(1-2): 9-22.
- Lewis, C.F.M. and Parrott, D.R., 1987. Iceberg scouring rate studies, Grand Banks of Newfoundland. Current Research Paper 87-1A, Geological Survey of Canada, Ottawa.
- Lønne, I., 1997. Facies characteristics of a proglacial turbiditic sand-lobe at Svalbard. *Sedimentary Geology*, 109(1-2): 13-35.
- Lovell, J.P.B. and Stow, D.A.V., 1981. Identification of ancient sandy contourites. *Geology*, 9(8): 347-349.
- Maslin, M., Owen, M., Day, S. and Long, D., 2004. Linking continental-slope failures and climate change: Testing the clathrate gun hypothesis. *Geology*, 32(1): 53-56.
- Middleton, G. and Hampton, M.A., 1973. Sediment gravity flows: mechanics of flow and deposition. In: A.H. Bouma (Editor), *Turbidites and deep water sedimentation*. Pacific Section S. E. P. M., Los Angeles, pp. 1-38.
- Mohrig, D., Elverhøi, A. and Parker, G., 1999. Experiments on the relative mobility of muddy subaqueous and subaerial debris flows, and their capacity to remobilize antecedent deposits. *Marine Geology*, 154(1-4): 117-129.
- Monahan, D. and Macnab, R.F., 1974. Macro-and meso-morphology of Flemish Cap, Flemish Pass and the northeastern Grand Banks. In: W.J.M. van der Linden and J.A. Wade (Editors), *Offshore Geology of eastern Canada, Volume 2 - Regional Geology*. Geological Survey of Canada, Ottawa, pp. 207-216.
- Mosher, D.C., Moran, K. and Hiscott, R.N., 1994. Late Quaternary sediment, sediment mass flow processes and slope stability on the Scotian slope, Canada. *Sedimentology*, 41(5): 1039-1061.



- Mosher, D.C., Piper, D.J.W., Campbell, D.C. and Jenner, K.A., 2004. Near-surface geology and sediment-failure geohazards of the central Scotian Slope. *AAPG Bulletin*, 88(6): 703-723.
- Mosher, D.C., Piper, D.J.W., Vilks, G.V., Aksu, A.E. and Fader, G.B.J., 1989. Evidence for Wisconsinan glaciation in the Verill canyon area, Scotian slope. *Quaternary Research*, 31(1): 27-40.
- Mosher, D.C. and Simpkin, P.G., 1999. Environmental marine geosciences 1: status and trends of marine high-resolution seismic reflection profiling: data acquisition. *Geoscience Canada*, 26(4): 174-188.
- Mulder, T. and Cochonat, P., 1996. Classification of offshore mass movements. *Journal of Sedimentary Research*, 66(1): 43-57.
- Mulder, T., Syvitski, J.P.M., Migeon, S., Faugères, J.-C. and Savoye, B., 2003. Marine hyperpycnal flows: initiation, behavior and related deposits. A review. *Marine and Petroleum Geology*, 20(6-8): 861-882.
- Nakajima, T., 2006. Hyperpycnites deposited 700 km away from river mouths in the central Japan Sea. *Journal of Sedimentary Research*, 76(1): 60-73.
- Niedoroda, A.W., Reed, C., Das, H., Hatchett, L. and Perlet, A.B., 2006. Controls of the behaviour of marine debris flows. *Norwegian Journal of Geology (Norsk Tidsskrift)*, 86(3): 256-274.
- Nisbet, E.G., 1990. Climate change and methane. *Nature*, 347: 23.
- Parrott, D.R., Lewis, C.F.M., Banke, E., Fader, G.B.J. and Sonnichsen, G.V., 1990. Seabed disturbance by a recent (1989) iceberg grounding on the Grand Banks of Newfoundland. Current Research Paper 90-1B, Geological Survey of Canada, Ottawa.
- Pereira, C.P.G., Piper, D.J.W. and Shor, N.A., 1985. Seamarc-I Midrange Sidescan Sonar Survey of Flemish Pass, East of the Grand Banks of Newfoundland. Open File 1161, Geological Survey of Canada, Ottawa.
- Piper, D.J.W., 1978. Turbidite muds and silts on deepsea fans and abyssal plains. In: D.J. Stanley and G. Kelling (Editors), *Sedimentation in*

submarine canyons, fans and trenches. Dowden, Hutchinson & Ross, Inc., Stroudsburg, pp. 163-176.

Piper, D.J.W., 2005. Late Cenozoic evolution of the continental margin of eastern Canada. *Norwegian Journal of Geology (Norsk Tidsskrift)*, 85: 305-318.

Piper, D.J.W. and Brunt, R.A., 2006. High-resolution seismic transects of the upper continental slope off southeastern Canada. Open File 5310, Geological Survey of Canada (Atlantic), Dartmouth.

Piper, D.J.W. and Campbell, D.C., 2005. Quaternary geology of Flemish Pass and its application to geohazard evaluation for hydrocarbon development. In: R.N. Hiscott and A. Pulham (Editors), *Petroleum Resources and Reservoirs of the Grand Banks, Eastern Canadian Margin*. Geological Association of Canada (GAC) Special Paper 43, pp. 29-43.

Piper, D.J.W., Cochonat, P. and Morrison, M.L., 1999. The sequence of events around the epicentre of the 1929 Grand Banks earthquake: initiation of debris flows and turbidity current inferred from sidescan sonar. *Sedimentology*, 46(1): 79-97.

Piper, D.J.W. and DeWolfe, M., 2003. Petrographic evidence from the eastern Canadian margin of shelf-crossing glaciations. *Quaternary International*, 99-100: 99-113.

Piper, D.J.W. and Gould, K., 2004. Late Quaternary geological history of the continental slope, South Whale Subbasin, and implications for hydrocarbon development, southwestern Grand Banks of Newfoundland. Current research D-1, Geological Survey of Canada, Ottawa.

Piper, D.J.W. and Hundert, T., 2002. Provenance of distal Sohm Abyssal Plain sediments: history of supply from the Wisconsinan glaciation in eastern Canada. *Geo-Marine Letters*, 22(2): 75-85.

Piper, D.J.W. and King, E.L., 2008. Cruise report Hudson 2006-048. Open File Report 5426, Geological Survey of Canada (Atlantic), Dartmouth.

Piper, D.J.W. and MacDonald, A., 2001. Timing and position of late Wisconsinan ice margins on the upper slope seaward of Laurentian channel. *Géographie physique et Quaternaire*, 55(2): 131-140.

- Piper, D.J.W., MacDonald, A., Ingram, S., Williams, G.L. and McCall, C., 2005. Late Cenozoic architecture of the St. Pierre Slope. *Canadian Journal of Earth Sciences*, 42(11): 1967-1985.
- Piper, D.J.W., Mosher, D.C. and Newton, S., 2002. Ice-margin seismic stratigraphy of the central Scotian Slope, eastern Canada. *Current Research 2002-E16*, Geological Survey of Canada, Dartmouth.
- Piper, D.J.W., Mudie, P.J., Fader, G.B., Josenhans, H.W., MacLean, B. and Vilks, G., 1990. Quaternary Geology; Chapter 10. In: G.L. Williams (Editor), *Geology of the Continental Margin of eastern Canada*. Geological Survey of Canada, Ottawa, pp. 475-607.
- Piper, D.J.W. and Normark, W.R., 1989. Late Cenozoic sea-level changes and the onset of glaciation: impact on continental slope progradation off eastern Canada. *Marine and Petroleum Geology*, 6(4): 336-347.
- Piper, D.J.W. and Normark, W.R., 2001. Sandy fans—from Amazon to Hueneme and beyond. *AAPG Bulletin*, 85(8): 1407-1438.
- Piper, D.J.W. and Pereira, C.P.G., 1992. Late Quaternary sedimentation in central Flemish Pass. *Canadian Journal of Earth Sciences*, 29: 535-550.
- Piper, D.J.W., Pirmez, C., Manley, P.L., Long, D., Flood, R.D., Normark, W.R. and Showers, W., 1997. 6. Mass transport deposits of the Amazon fan. In: R.D. Flood, D.J.W. Piper, A. Klaus and L.C. Peterson (Editors), *Proceedings of the Ocean Drilling Program, Scientific Results*, College Station, TX, pp. 109-146.
- Piper, D.J.W., Shaw, J. and Skene, K.I., 2007. Stratigraphic and sedimentological evidence for late Wisconsinan sub-glacial outburst floods to Laurentian Fan. *Paleogeography, Paleoclimatology, Paleoecology*, 246(1): 101-119.
- Piper, D.J.W. and Skene, K.I., 1998. Latest Pleistocene ice-rafting events on the Scotian Margin (eastern Canada) and their relationship to Heinrich events. *Paleoceanography*, 13(2): 205-214.

- Piper, D.J.W. and Sparkes, R., 1986. Shallow sediments instability in the central part of Flemish Pass, east of the Grand Banks of Newfoundland. Open File 1368, Geological Survey of Canada, Ottawa.
- Piper, D.J.W. and Sparkes, R., 1987. Proglacial sediment instability features on the Scotian Slope at 63°W. *Marine Geology*, 76: 15-31.
- Piper, D.J.W., von Huene, R. and Duncan, J.R., 1973. Late Quaternary Sedimentation in the Active Eastern Aleutian Trench. *Geology*, 1(1): 19-22.
- Prior, D.B., Bornhold, B.D. and Johns, M.W., 1984. Depositional characteristics of a submarine debris flow. *Journal of Geology*, 92: 707-727.
- Rashid, H., Hesse, R. and Piper, D.J.W., 2003a. Evidence for an additional Heinrich event between H5 and H6 in the Labrador Sea. *Paleoceanography*, 18(4): 1077-1092.
- Rashid, H., Hesse, R. and Piper, D.J.W., 2003b. Distribution, thickness and origin of Heinrich layer 3 in the Labrador Sea. *Earth and Planetary Science Letters*, 205(3-4): 281-293.
- Rashid, H. and Piper, D.J.W., 2007. The extent of ice on the continental shelf off Hudson Strait during Heinrich events 1-3. *Canadian Journal of Earth Sciences*, 44(11): 1537-1549.
- Rasmussen, S., Lykke-Andersen, H., Kuijpers, A. and Troelstra, S.R., 2003. Post-Miocene sedimentation at the continental rise of Southeast Greenland: the interplay between turbidity and contour currents. *Marine Geology*, 196(1-2): 37-52.
- Ross, C.K., 1981. Drift of satellite tracked bouys on Flemish Cap, 1979-81. *NAFO Scientific Council Studies*, 1: 47-50.
- Sasaki, K., Ormura, A., Murakami, K., Sagawa, N. and Nakamori, T., 2004. Interstadial coral reef terraces and relative sea level changes during marine oxygen isotope stages 3-4, Kikai Island, central Ryukyus, Japan. *Quaternary International*, 120(1): 51-64.

- Shanmugam, G., 1996. High-density turbidity currents: are they sand debris flows? *Journal of Sedimentary Research*, 66(1): 2-10.
- Shaw, J., Piper, D.J.W., Fader, G.B.J., King, E.L., Todd, B.J., Bell, T., Batterson, M.J. and Liverman, D.G.E., 2006. A conceptual model of the deglaciation of Atlantic Canada. *Quaternary Science Reviews*, 25(17-18): 2059-2081.
- Shor, A. and Piper, D.J.W., 1989. A large Late Pleistocene blocky debris flow on the central Scotian slope. *Geo-Marine Letters*, 9: 153-160.
- Skene, K.I. and Piper, D.J.W., 2003. Late Quaternary stratigraphy of Laurentian Fan: a record of events off the eastern Canadian continental margin during the last deglacial period. *Quaternary International*, 99-100: 135-152.
- Slatt, R.M., 1977. Late Quaternary terrigenous and carbonate sedimentation on Grand Bank of Newfoundland. *Geological Society of America Bulletin*, 88(9): 1357-1367.
- Sonnichsen, G.V., King, E.L. and MacLean, B., 1999. CSS Hudson 99-031: A Seabed Survey of Northern Grand Bank and Flemish Pass. Internal Report, Geological Survey of Canada (Atlantic), Dartmouth.
- Spahni, R., Chappellaz, J., Stocker, T.F., Loulergue, L., Hausammann, G., Kawamura, K., Flückiger, J., Schwander, J., Raynaud, D., Masson-Delmotte, V. and Jouzel, J., 2005. Atmospheric methane and nitrous oxide of the Late Pleistocene from Antarctic ice cores. *Science*, 310: 1317-1321.
- Stauffer, B., 2000. Long term climate records from polar ice. *Space Science Reviews*, 94(1-2): 321-336.
- Stea, R.R., Piper, D.J.W., Fader, G.B.J. and Boyd, R., 1998. Wisconsinan glacial and sea-level history of Maritime Canada and the adjacent continental shelf: A correlation of land and sea events. *Geological Society of America Bulletin*, 110(7): 821-845.
- Stein, A.B. and Syvitski, J.P.M., 1997. Glaciation-influenced debris flow deposits: East Greenland slope. In: T.A. Davies et al. (Editors), *Glaciated continental margins: an atlas of acoustic images*. Chapman & Hall, London, Weinheim, New York, Tokyo, Melbourne, Madras, pp. 134-135.

- Stein, M., 1996. Flemish Cap – A review on research activities with focus on oceanographic conditions. NAFO Scientific Council Studies, 25: 1-24.
- Stoner, J.S., Channell, J.E.T. and Hillaire-Marcel, C., 1998. A 200 ka geomagnetic chronostratigraphy for the Labrador Sea: Indirect correlation of the sediment record to SPECMAP. *Earth and Planetary Science Letters*, 159(3-4): 165-181.
- Stow, D.A.V., Faugères, J.-C., Howe, J.A., Pudsey, C.J. and Viana, A.R., 2002. Bottom currents, contourites and deep-sea sediment drifts: current state of the art. In: A.R. Viana (Editor), *Deep-water contourite systems: modern drifts and ancient series, seismic and sedimentary characteristics*. The Geological Society, London, pp. 7-20.
- Stow, D.A.V. and Piper, D.J.W., 1984. Deep-water fine-grained sediments: facies models. In: D.A.V. Stow and D.J.W. Piper (Editors), *Fine grained sediments: deep water processes and facies*. Geological Society, London, pp. 611-646.
- Summerhayes, C.P., Bornhold, B.D. and Emblay, R.W., 1979. Surficial slides and slumps on the continental slope and rise of south west Africa: a reconnaissance study. *Marine Geology*, 31(3-4): 265-277.
- Talling, P.J., Lawrence, A.A. and Wynn, R.B., 2007. New insights into the evolution of large-volume turbidity currents: comparison of turbidite shape and previous modelling results. *Sedimentology*, 54(4): 737-769.
- Taylor, J., Dowdeswell, J.A. and Kenyon, N.H., 2000. Canyons and late Quaternary sedimentation on the North Norwegian margin. *Marine Geology*, 166(1-4): 1-9.
- Toews, M.W., 2003. Late Cenozoic geology of Salar Basin, eastern slope of the Grand Banks of Newfoundland. Open File 1675, Geological Survey of Canada, Ottawa.
- Toews, M.W. and Piper, D.J.W., 2002. Recurrence interval of seismically triggered mass-transport deposition at Orphan Knoll, continental margin off Newfoundland and Labrador. Current Research 2002-E17, Geological Survey of Canada, Dartmouth.

- Toucanne, S., Mulder, T., Schönfeld, J., Hanquiez, V., Gonthier, E., Duprat, J., Cremer, M.D. and Zaragosi, S., 2007. Contourites of the Gulf of Cadiz: A high-resolution record of the paleocirculation of the Mediterranean outflow water during the last 50,000 years. *Paleogeography, Paleoclimatology, Paleoecology*, 246(2-4): 354-366.
- Trincardi, F., Asioli, A., Canu, M., Cattaneo, A. and Correggiari, A., 2003. Submarine slides during relative sea level rise: three late Quaternary examples from the central Mediterranean. Abstract #9110, EGS AGU EUG Joint Assembly, Nice.
- Tripsanas, E.K. and Piper, D.J.W., 2007. Orphan Basin earthquake record unpublished dataset. *Atlantic Geology*.
- Tripsanas, E.K. and Piper, D.J.W., 2008, in revision. Late Quaternary stratigraphy and sedimentology of Orphan Basin: implications for meltwater dispersal in the southern Labrador Sea. *Paleogeography, Paleoclimatology, Paleoecology*.
- Tripsanas, E.K. and Piper, D.J.W., in press. Late Quaternary stratigraphy and sedimentology of Orphan Basin: implications for meltwater dispersal in the southern Labrador Sea. *Paleogeography, Paleoclimatology, Paleoecology*.
- Tripsanas, E.K. and Piper, D.J.W., submitted. Glaciogenic debris-flow deposits of Orphan Basin, offshore eastern Canada: geotechnical and rheological properties, origin and relationship to meltwater discharge. *Journal of Sedimentary Research*.
- Tripsanas, E.K., Piper, D.J.W. and Campbell, D.C., 2007 (in press). Evolution and depositional structure of earthquake-induced mass movements and gravity flows: southwest Orphan Basin, Labrador Sea. *Marine and Petroleum Geology*.
- Tripsanas, E.K., Piper, D.J.W. and Jarrett, K.A., 2007. Logs of piston cores and interpreted ultra-high-resolution seismic profiles, Orphan Basin. Open File 5299, Geological Survey of Canada, Atlantic, Dartmouth.
- Tripsanas, E.K., Piper, D.J.W., Jenner, K.A. and Bryant, W., 2007 in press. Submarine mass-transport facies: new perspectives on flow processes from cores on the eastern North American margin. *Sedimentology*.

- Veiga-Pires, C.C. and Hillaire-Marcel, C., 1999. U and Th isotope constraints on the duration of Heinrich events H0-H4 in the southeastern Labrador Sea. *Paleoceanography*, 14(2): 187-199.
- Waelbroeck, C., Labeyrie, L., Michel, E., Duplessy, J.-C., McManus, J.F., Lambeck, K., Balbon, E. and Labracherie, M., 2002. Sea level and deep water temperature changes derived from benthic foraminifera isotopic records. *Quaternary Science Reviews*, 21(1-3): 295-305.
- Walker, M., 2005. *Quaternary Dating Methods*. Wiley & Sons, Chichester, 286 pp.
- Walker, R.G., 1967. Turbidite sedimentary structures and their relationship to proximal and distal depositional environments. *Journal of Sedimentary Petrology*, 37(1): 25-43.
- Walker, R.G., 1976. Facies models 2. Turbidites and associated coarse clastic deposits. *Geoscience Canada*, 3(1): 25-36.



## **Appendix**

The Appendix, found in the „back pocket“ of the thesis contains a draft version of a Geological Survey of Canada Open File report. This report summarizes the raw and interpreted data from Flemish Pass and can be seen as a data compilation.